Tuning catalyst stability by surface functionalisation

The effect of functionalisation of the support surface on the stability of a Cu/SiO2 catalyst for methanol synthesis

THESIS FOR THE DEGREE OF MASTER OF SCIENCE

TANJA PARMENTIER

INORGANIC CHEMISTRY AND CATALYSIS

UNIVERSITEIT UTRECHT

SUPERVISORS

R. VAN DEN BERG, MSC

&

PROF. DR. IR. K.P. DE JONG

Table of Contents

List of abbreviations

Abbreviation	
APTES	3-aminopropyltriethoxysilane
BET method	Brunauer–Emmett–Teller method
BF	Bright field
BJH method	Barrett-Joyner-Halenda method
DME	Dimethyl ether
DRIFTS	Diffuse Reflectance Infrared Fourier Transform Spectroscopy
EDX analysis	Energy Dispersive X-ray analysis
EXAFS	Extended X-ray Absorption Fine Structure
ICI	Imperial Chemical Industries
ICP analysis	Inductive Coupled Plasma analysis
GC	Gas Chromatography
FID	Flame Ionisation Detector
HAADF	High-angular annular dark field
HMDS	Hexamethyldisilazane
MS	Mass Spectrometry
MTMS	Methyltrimethoxysilane
SMSI	Strong metal-support interaction
TCD	Thermal Conductivity Detector
TEM	Transmission Electron Microscope
TGA	Thermal Gravimetric Analysis
THF	Tetrahydrofuran
TPR	Temperature Programmed Reduction
(R)WGSR	(Reverse) Water gas shift reaction
XRD	X-Ray Diffraction

Abstract

The support material in heterogeneous catalysts plays a pivotal role in stabilising metal nanoparticles which form the active phase in the catalysts. It influences and can suppress the growth of the metal nanoparticles in catalysts. Because of this, the support has influence on the quantity of the active phase in the catalyst. Catalysts will become less efficient when the quantity of active phase available for reaction decreases and when the activity drops below a certain level, the catalyst needs to be replaced. This study focuses on how the growth of metal nanoparticles is influenced by the chemical nature of the support of the catalyst. The study focuses on a methanol synthesis catalyst. The activity of the industrially used methanol synthesis catalyst, a $Cu/ZnO/Al_2O_3$ catalyst, decreases over time due to growth of the copper particles. Since world's demand for methanol is increasing every year, one should keep optimising the methanol synthesis process and look for a more stable catalyst.

A model Cu/SiO_2 methanol synthesis catalyst is used this study. The chemical properties of the support of the model Cu/SiO_2 catalyst were changed by functionalisation or grafting of the support with amino groups, methyl groups, alumina, titania and zinc oxide. The functionalised and grafted catalysts were studied with DRIFTS, N_2 physisorption, ICP, TEM, EDX spectroscopy and the catalyst activity and deactivation in methanol synthesis was tested in a catalytic test of 230 hours. The introduction of amino groups on the support was found to stabilise the copper nanoparticles and suppress the particle growth in the catalyst. Methyl groups changed the deactivation behaviour of the catalyst. Alumina and titania have acidic properties. Grafting with these metal oxides resulted in the dehydration of methanol towards DME. Next to this, titania was also found to migrate on the copper particles reducing active surface area caused by the SMSI properties it exhibits. Grafting with alumina, titania and zinc oxide resulted in stronger deactivating catalysts.

1 Introduction

1.1 General introduction

In the Industrial Revolution during the 19th century, fossil fuels such as natural gas, oil and coal seemed to be the ideal source for energy. The use of these fuels as energy source brought us today's modern and technology adapted society. However, world's fossil fuel resources are limited and the increase in world's population together with the increasing standard of living causes an ever growing demand for these fuels. The price of crude oil rises with this growing demand and decreasing oil resources. This can be seen in the graph in Figure 1.1a.

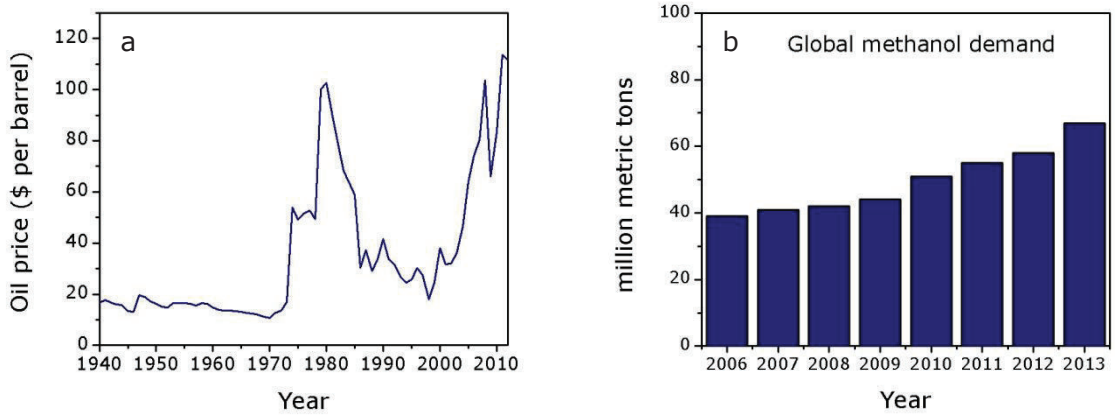

Figure 1.1 [a] Oil price trend from 1940 till 2012, data generated from [1]. [b] Global methanol demand in million metric tons, data generated from [2].

The energy crisis in the 1970s resulted in a peak in the oil price around 1980 and today's raise in price originates from the growing demand and depletion of resources. At a certain moment, oil will become too expensive to be the energy source in our everyday lives. We should therefore look for other sources of energy that are more abundant and next to that we should use the oil that is still left as efficient as possible.

Natural gas, which is often released during oil drilling, is flared because transport and storage of gasses is difficult. However, by using catalysis it is possible to convert the natural gas to liquid fuels such as methanol or hydrocarbons. These liquids can then easily be transported and converted to other products or used as fuels themselves [3]. Catalysts that are used in these conversion processes are based on the more abundant first row transition metals, i.e. iron, cobalt, nickel and copper. By converting natural gas to useful liquids, catalysis plays an important role in making processing crude oil more efficient.

Methanol can be generated out of synthesis gas (a mixture of CO_2/CO/H_2) that is often derived from natural gas. Another more sustainable possibility is generating it out of CO_2 captured from the atmosphere and hydrogen obtained from the splitting of water, as plead for by Nobel laureate George Olah [3–5]. A plant based on the latter method is build in Iceland in 2010 [6]. However, generation out of natural gas is already performed on industrial scale since 1966 and seems to be the more promising method for synthesis gas generation for the future [7]. Methanol can be used itself as fuel or for the production of chemicals such as formaldehyde, dimethyl ether, acetic acid and higher olefins [8]. Essentially all products currently made in the petrochemical industry from oil can be generated out of methanol [4,9]. In Figure 1.1b can be seen that world's demand for methanol is still increasing every year. It is therefore necessary to keep looking for optimisations in the methanol production process. The physical properties of methanol can be seen in Table 1.1.

The catalyst that is used in the generation of methanol out of synthesis gas in the industrial process needs to be replaced by a fresh catalyst after a certain period of time. This replacement is necessary because the activity of the catalyst has decreased over time. The catalyst consists of metal nanoparticles supported on a metal oxide surface in which the metal nanoparticles form the active phase in the catalysts. The deactivation is mainly caused by growth of the metal nanoparticles. One of the roles of the support in the catalyst is to stabilise these metal nanoparticles and limit their growth. Investigations on how the support stabilises the metal particles can provide information that van help increasing the life time of catalysts. Therefore, this study focuses on influence of the chemical nature of the support on the stability of the metal particles.

Table 1.1 Physical properties of methanol (taken from [10])

Boiling point [°C]	Melting point [°C]	Density [g/cm^3]	Flashpoint [°C]
65	-98	0.79	11

1.2 Methanol's history

Ancient Egyptians can be considered as the first discoverers of methanol. They obtained a mixture containing methanol by pyrolysis of wood and used it as a basis for their embalming fluids [11]. Pure methanol was first isolated in 1661 by Sir Robert Boyle. He obtained it by distillation of buxus wood and therefore called it 'spirit of box' [12][13]. Around 1830 Justus Von Liebig as well as Jean-Babtiste Dumas independently succeeded in determining the chemical composition of methanol and introduced the name methyl alcohol. Methanol, still made by distillation of wood, became a popular fuel for lightning, heating and cooking [14].

The industrial revolution in the early 19th century caused an increasing demand in energy. To satisfy this energy demand, wood was largely replaced by the fossil fuel coal as energy source. Methods were developed to isolate hydrogen- and carbon monoxide containing gasses from coal [15]. In 1913, A. Mittasch developed an iron catalyst which could convert those carbon monoxide and hydrogen gasses to methanol, but the selectivity of this process was very poor. Ten years later Mittasch and M. Pier, both working at BASF then, developed an chrome/zinc oxide catalyst that was suitable for the generation of methanol out of hydrogen- and carbon monoxide containing gasses because it had a good selectivity and it was not sensitive for poisoning by sulphur that is present in the feed [16][17]. The catalyst was used in the so called *high pressure process* which was operated at temperatures between 300 and 400˚C and pressures between 250 and 350 bar [18]. This process was soon commercialised.

A new method to gain synthesis gas (a mixture of CO_2/CO/H_2) was developed at BASF in the 1930s. They developed a steam reforming process, in which natural gas is converted into synthesis gas. The gas obtained in this process had an extremely high purity, much higher than synthesis gas obtained from coal. Soon after the discovery of this process, the feedstock for synthesis gas was changed from coal to natural gas. The absence of poisons in the gas made it possible to search for more sensitive and more active catalysts. In 1966, Imperial Chemical Industries (ICI, now Johnson Matthey) developed a *low pressure process* which makes use of a copper-based catalyst that is much more active than the chrome/zinc oxide catalyst used in the *high pressure process* [7]. The low pressure process is operated between temperatures of 220 and 280˚C and pressures of 50 and100 bar. Today, almost all synthesised methanol is made in low pressure processes.

1.3 The methanol production process

A flow diagram of a commercial low-pressure processes can be seen in Figure 1.3, it contains three different processes [19]:

- Synthesis gas preparation
- Methanol synthesis
- Methanol purification

These three processes explained in more detail in this paragraph.

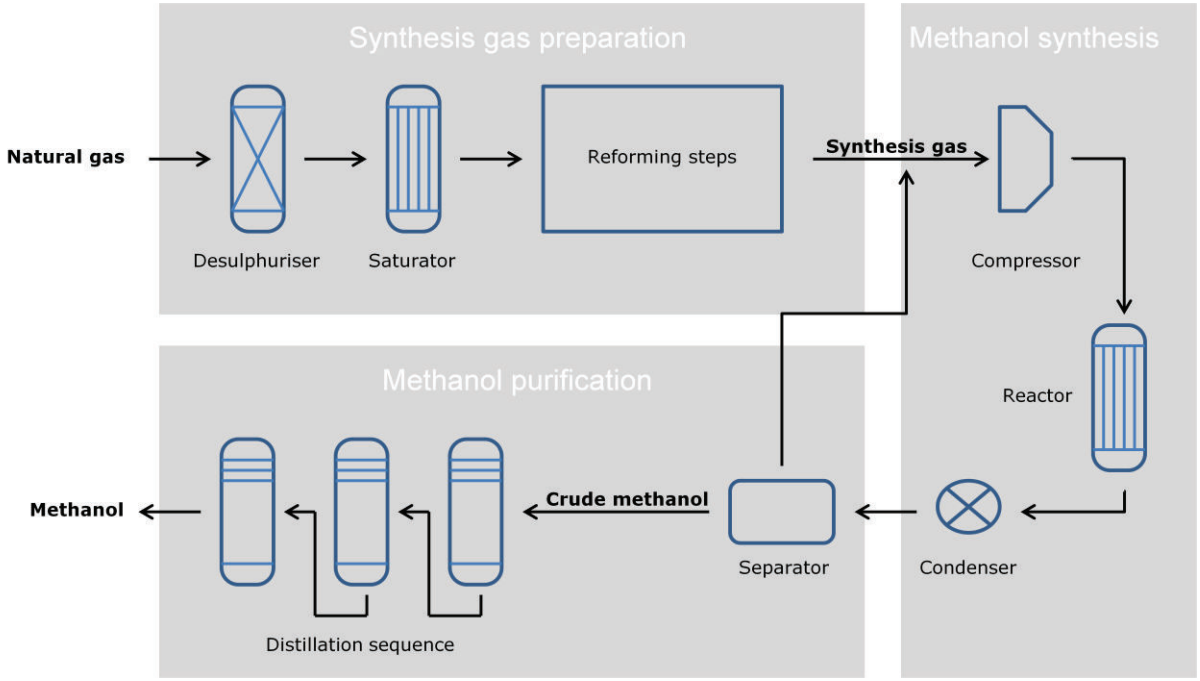

Figure 1.2 Simplified flow diagram of the low-pressure methanol synthesis process (adapted from [18–20])

1.3.1 Synthesis gas preparation

In the first process, the synthesis gas preparation, natural gas is first desulphurised and saturated with steam. That process is followed by reforming steps for which a nickel-based catalyst is used [19]. The following reactions take place during these reforming steps: steam reforming of higher hydrocarbons (1.1), steam reforming of methane (1.2), partial oxidation of methane (1.3) and the water gas shift reaction (1.4) [20].

(1.1) $C_nH_m + nH_2O \rightarrow n\,CO + (n + \frac{m}{2})H_2$

(1.2) $CH_4 + H_2O \rightleftharpoons CO + 3H_2$ $\quad -\Delta H_{rx,298K} = -206\ kJ/mol$

(1.3) $CH_4 + \frac{1}{2}O_2 \rightleftharpoons CO + 2H_2$ $\quad -\Delta H_{rx,298K} = 35\ kJ/mol$

(1.4) $CO + H_2O \rightleftharpoons CO_2 + H_2$ $\quad -\Delta H_{rx,298K} = 40\ kJ/mol$

1.3.2 Methanol synthesis

The prepared synthesis gas is cooled and compressed before it is fed to the methanol reactor [21]. From equation (1.2), (1.3) and (1.4) can be seen the overall methanol synthesis reaction is an exothermal process. Therefore, the methanol reactor needs to be cooled. Two different reactors dominate the market; one is used in the ICI process and the other in the Lurgi process. They are different in their design and in the way they are being cooled as can be seen in Figure 1.3. The ICI process makes use of a adiabatic multi-bed reactor in which

cold feed gas is used to cool reactant gases between the catalyst beds [18]. The Lurgi process uses cold water for cooling, this results in the generation of steam which can be used in the reforming steps in the synthesis gas preparation [20].

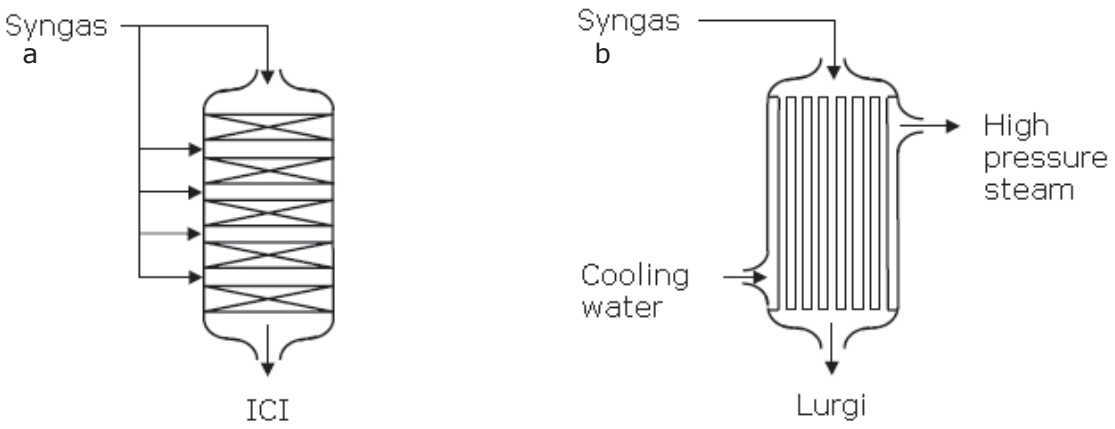

Figure 1.3 [a] The design of the ICI reactor and [b] the Lurgi reactor (taken from [18])

The catalysts beds contain a catalyst that consists of copper, zinc oxide and alumina. In general, the composition of the catalysts ranges between 40-80% copper, 10-30% zinc oxide and 5-10% alumina, depending on their manufacturer [13]. There are four large manufacturers of catalysts for methanol synthesis; *Haldor Topsøe*, *Johnson Matthey*, *Süd Chemie* and *Mitsubishi Gas Chemical* [13].

Three reactions are occurring during methanol synthesis: the hydrogenation of carbon monoxide (1.5), the hydrogenation of carbon dioxide (1.6) and the reverse water-gas shift reaction (RWGSR) (1.7) [22].

(1.5) $CO + 2H_2 \rightleftharpoons CH_3OH$

(1.6) $CO_2 + 3H_2 \rightleftharpoons CH_3OH + H_2O$

(1.7) $CO_2 + H_2 \rightleftharpoons CO + H_2O$

1.3.3 Methanol purification

Methanol conversion is limited by equilibrium; non reacted gas is therefore separated from crude methanol and brought back into the reactor by a gas recycle loop. Crude methanol, which contains only a small amount of by products, is further purified by distillation. The distillation process consists of three columns [23]. Low boiling compounds such as DME and ketones and dissolved gasses are removed in the first column the stabiliser column. Water and ethanol are separated from methanol in the second and the third column.

1.4 Mechanism and thermodynamics

The $Cu/ZnO/Al_2O_3$ catalyst is used in industrial operations since the development of the low pressure process. Although the catalyst and the low pressure process have been used and studied for quite some time, there are still debates going on about it, mainly on the following topics:

- What the main carbon source (CO or CO_2) for methanol is
- The mechanism of the reaction
- The nature of the active site of the catalyst
- The role of zinc oxide in the catalyst

The former two topics will be discussed now, the latter points will be discussed in paragraph 1.5.

1.4.1 The main precursor of methanol

In the 1970's and 80's several studies on the identity of the precursor of methanol were published [13,22]. Based on results of the group of Klier, there was a general assumption that carbon mono-oxide was the main carbon source for methanol [24]. This view changed when inter alia isotope labelling studies pointed out that CO_2 was the main precursor for methanol [25–27]. Nowadays, it is generally assumed that carbon dioxide is the main precursor for methanol that is made with industrially used catalysts and under industrial conditions [22]. The role of carbon monoxide in the process is to remove absorbed oxygen from the surface, forming CO_2 [28].

1.4.2 Reaction mechanism

The water-gas-shift reaction (WGSR) is part of the overall methanol synthesis reaction. It supplies reactants (CO_2 and H_2) for the methanol reaction. Two different mechanisms for the WGSR can be considered [22,29–31]. In the *surface-redox* mechanism, H_2O (g) is completely dissociated in O* and H_2 (g), where * symbolises a free surface site. In the other mechanism, the *formate* mechanism, H_2O* is dissociated in OH* and H*. OH* reacts then with CO_2* to form a formate HCOO*. Surface science studies on Cu(111) surfaces have provided strong evidence for the *surface-redox* mechanism to describe the WGSR [30–32]. The first eight steps in Table 1.2 describe the WGSR as was proposed based on these surface science studies [32].

Table 1.2 Elementary steps in the kinetic model of methanol synthesis

Steps	Surface reactions		
1	H_2O (g) + *	⇌	H_2O*
2	H_2O* + *	⇌	OH* + H*
3	2OH* + *	⇌	H_2O* + O*
4	H_2O* + O*	⇌	O* + H*
5	2H*	⇌	H2 (g) + 2*
6	CO (g) + *	⇌	CO*
7	CO* + O*	⇌	CO_2* + *
8	CO_2*	⇌	CO_2 (g) + *
9	CO_2* + H*	⇌	HCOO* + *
10	HCOO* + H*	⇌	H_2COO* + *
11	H_2COO* + H* + O*	⇌	H_3CO* + O*
12	H_3CO* + H*	⇌	CH_3OH* + *
13	CH_3OH*	⇌	CH_3OH (g) + *

Free surface site is symbolised by * and an adsorbed molecule X is symbolised by X*

Steps 9-13 describe the simplest reaction mechanism for the methanol synthesis reaction. This mechanism is based on the IR spectroscopy, TRP, XPS, EELS and TPD studies in order to identify species present on the copper surface during reaction [30]. Step 11, the hydrogenation of H_2COO to methoxide and oxide was found to be the rate-limiting step. However, one can find other mechanisms for the complete reaction in the literature. For example a more extensive mechanism that is based on DFT calculations proposed by Grabow and Mavrikakis [33].

1.4.3 Reaction thermodynamics

The methanol synthesis reaction consist, as mentioned before, of three different reactions; the hydrogenation reaction of CO (1.8), the hydrogenation reaction of CO2 (1.9) and the reverse WGSR (1.10). The thermodynamics of these equations are given underneath.

(1.8) $CO + 2H_2 \rightleftharpoons CH_3OH$ $\quad -\Delta H_{298\ K,\ 5MPa} = 90.7\ kJ/mol$

(1.9) $CO_2 + 3H_2 \rightleftharpoons CH_3OH + H_2O$ $\quad -\Delta H_{298\ K,\ 5MPa} = 40.9\ kJ/mol$

(1.10) $CO_2 + H_2 \rightleftharpoons CO + H_2O$ $\quad -\Delta H_{298\ K,\ 5MPa} = -49.8\ kJ/mol$

The equilibrium constants of these reactions are defined as follows [34]:

$$k_{f(1.8)} = \left(\frac{fCH_3OH}{fCO\ f2H_2}\right) = \left(\frac{\varphi CH_3OH}{\varphi CO\ \varphi 2H_2}\right)\ \left(\frac{PCH_3OH}{PCO_2\ P2H_2}\right)$$

$$k_{f(1.9)} = \left(\frac{fCH_3OH\ fH_2O}{fCO_2\ f3H_2}\right) = \left(\frac{\varphi CH_3OH\varphi H_2O}{\varphi CO_2\ \varphi 3H_2}\right)\ \left(\frac{PCH_3OH\ PH_2O}{PCO_2\ P3H_2}\right)$$

$$k_{f(1.10)} = \left(\frac{fCO_2\ fH_2}{fCO\ fH_2O}\right) = \left(\frac{\varphi CO_2\ \varphi H_2}{\varphi CO\ \varphi H_2O}\right)\ \left(\frac{PCO_2\ PH_2}{PCO\ PH_2O}\right)$$

Here, f_j is the fugacity, φ_j is the fugacity coefficient and P_j is the partial pressure of component *j*. The involved gases don't behave like ideal gasses under industrial conditions. Therefore it is necessary to use fugacities in the equilibrium constants [22].

The methanol synthesis reaction involves a decrease in entropy since the number of moles decreases and it also involves a decrease in enthalpy so the reaction is exothermic. Therefore, the reaction is thermodynamically favoured at low temperatures and high pressures, as is visualised in Figure 1.4. Industrial methanol synthesis processes are operated at 40 bar and at temperatures between 220 °C and 280 °C [19]. The process is operated between these temperatures because removal of the generated heat is costly.

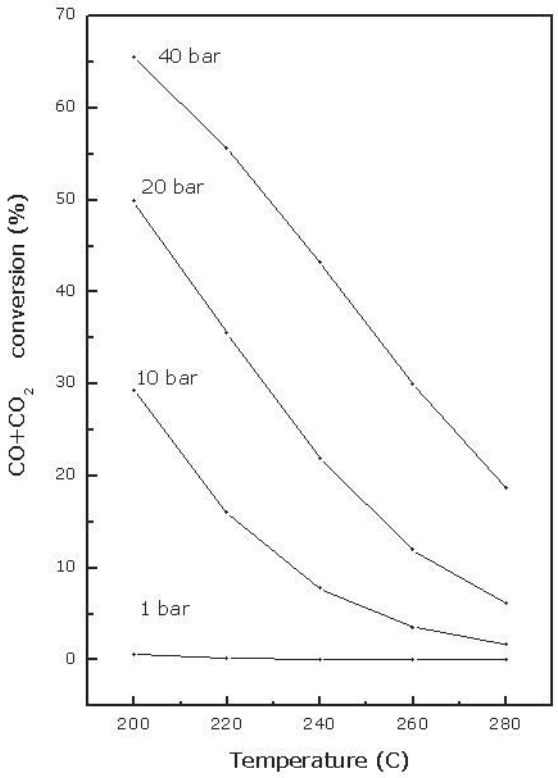

Figure 1.4 Temperature and pressure dependence of the equilibrium conversions of methanol.

1.5 The $Cu/ZnO/Al_2O_3$ methanol synthesis catalyst

1.5.1 Synthesis of the industrial catalyst

The catalyst that is presently used in industrial processes contains copper, zinc oxide and alumina. As said earlier, the ratio between the components depends on the manufacturer of the catalyst. Information on the synthesis of the commercial catalyst is very limited but a general preparation sequence can be found in literature [35]. This procedure can be seen in Figure 1.5.

Figure 1.5 Steps in the preparation of the industrial methanol synthesis catalyst

It is known that the catalyst is synthesised by a co-precipitation method and there is a general assumption that they make use of metal nitrates and alkali metal hydroxides or carbonates [36–39]. Washing and drying of the precipitate is followed by a calcination step in which the precursors are decomposed to mixed oxides and CuO. Calcination temperatures range between 523 to 675 K, depending on the composition of the catalyst [22,37]. This preparation method creates porous aggregates of CuO nanoparticles and ZnO and a low amount of Al_2O_3. These spherical CuO nanoparticles have a size of around 10 nm [36]. A TEM image of the commercially available Haldor Topsøe's MT 151 FENCE^{TM} methanol synthesis catalyst can be seen in Figure 1.6a. After calcination, the catalyst is shaped into pellets. The pelleted MT 151 FENCE^{TM} catalyst can be seen in Figure 1.6b. Before the catalyst can be used, the copper is first reduced in the reactor.

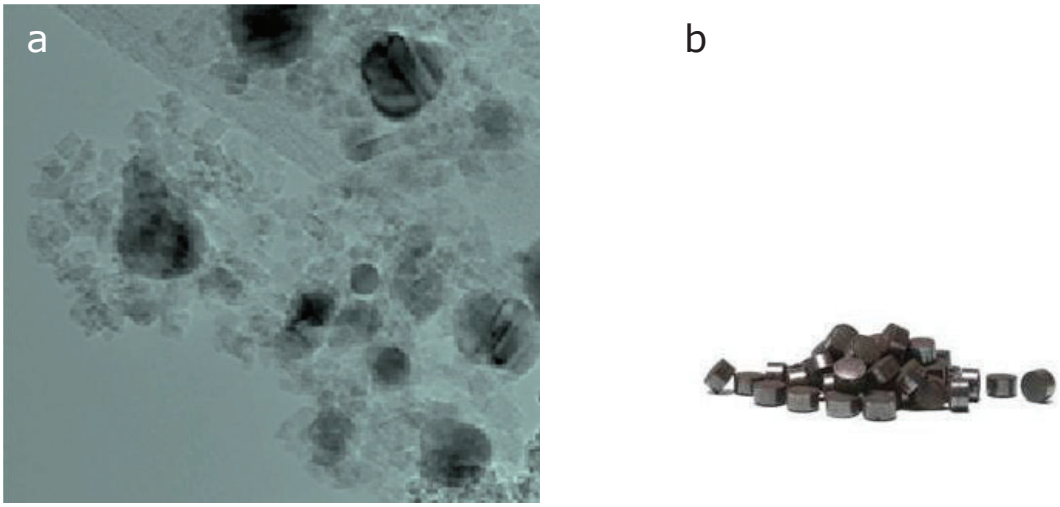

Figure 1.6 [a] TEM image of Haldor Topsøe's MT-151 Fence^{tm} catalyst. Finely dispersed copper crystals (dark) of ~10 nm are surrounded by metal oxide crystals (lighter). (image taken from: [40]) [b] image of pelleted MT-151 FENCE^{TM} catalysts (taken from [41])

The obtained catalyst has a selectivity that is even more than 99%. Impurities in the synthesised methanol involve hydrocarbons, higher alcohols, ethers, esters and ketones but can be only be found in very small amounts [26]. These impurities are, together with water, removed in the distillation process.

1.5.2 The role of zinc and the active site

As mentioned in paragraph 1.4, debates are nowadays still going on concerning the role of zinc oxide and the nature of the active site in the catalyst [42]. Since the use of copper based catalyst in hydrogenation processes it is known that the incorporation of zinc oxide in the catalyst improves the life time and the activity of the

catalyst [37]. It is effective in the removal of sulphur components from the synthesis gas feed. The formation of zinc sulphide will prevent the formation of the more mobile copper sulphide phase [35]. Next to this, zinc oxide acts as a physical barrier between the copper nanoparticles and therefore helps separating the copper particles from each other so that the catalyst keeps its high copper surface area [22,36,42,43]. Small amounts of alumina are incorporated in the catalyst to stabilise the zinc oxide, which is otherwise not as stable as required under reaction conditions [22,37].

Zinc oxide itself is also a methanol catalyst that was used in the high pressure methanol process, however, zinc oxide is not very active in methanol catalysis[7]. Next to the capturing of sulphur and the stabilising effect of zinc oxide, the presence of zinc oxide in catalyst also seems to increase the activity of the catalyst [22,42–44]. Some groups attributed this increase in activity to a synergy between zinc oxide and copper. There are multiple theories on the origin of the copper-zinc synergy suggested such as a hydrogen spillover effect on zinc oxide, the formation of a copper-zinc alloy on the copper surface or a morphology effect [27,36,45–48]. In the hydrogen spillover theory is proposed that hydrogen is split on the copper surface. The split hydrogen is then transported to the zinc oxide surface. It is stored there until it returns to the copper. On the copper surface it can reacts with methoxy and formate species that are present to form methanol. The theory is that the continuous availability of split hydrogen increases the catalyst activity [22,45,49]. Others attribute the increase in activity to the migration of zinc atoms on the copper surface, creating a copper-zinc surface alloy [43,46] The presence of zinc on the copper surface will affect the absorption properties and will therefore enhance the CO_2 hydrogenation. The last theory concerns morphological changes of copper in contact with zinc oxide. Copper particles supported zinc oxide were found to change from spherical non wetting copper particles in oxidising atmosphere to more disk like, wetting copper particles in more reducing atmosphere [47,48,50]. These morphological changes change the surface area of the catalyst and will therefore also affect the activity of the catalyst. Alloy formation on the surface of the support might even increase the wetting behaviour of copper. Such morphological and wetting / non wetting phenomena are not observed for copper supported on silica.

It is generally assumed that the methanol reaction takes place at the copper phase in the catalyst, however the exact identity of the active site still remains unclear. In literature one can find a lot of published work on this study. Some suggest that the active site for CO hydrogenation is different that for CO_2 hydrogenation [46], others claim that the reaction takes place at lattice defects on the copper surface [51] or at steps on the copper surface where zinc is present nearby [36].

1.6 Deactivation

The activity of catalysts will decrease over time during industrial operation. To achieve the same conversion as was achieved by the fresh catalysts it is common to adapt the pressure and temperature of the processes and in this way compensate for the loss in activity. After a certain period of time, the activity of the catalyst drops below a certain level and the catalyst needs to be replaced. This deactivation of catalysts can be caused by several processes like physical damage, fouling, poisoning and particle growth [52–54]. Deactivation of the methanol synthesis catalysts is predominantly caused by particle growth. The processes of particle growth and poisoning will be explained in more detail in the coming paragraphs. To increase the lifetime of a catalyst, that is the time after which the catalyst needs to be replaced in industrial operations, it is important to know the possible mechanisms of particle growth.

1.6.1 Deactivation by particle growth

For optimal performance of a heterogeneous metal based catalyst, the catalyst should contain a high degree of active surface area that is accessible for reactants. Such a high degree of active surface area can be achieved by deposition of small metal nanoparticles on a high surface area support. However, small nanoparticles tend to grow and form larger particles under reaction conditions. This is driven by the fact that the surface contribution to the total free energy of the metal particle is larger for small particles then for bigger ones. This makes small particles prone for free energy reduction through particles growth [55]. A particle with a high total

free energy has a high chemical potential. This relation between the particle's chemical potential and size can be seen from the Gibbs-Thompson relation (1.11) :

(1.11) $\mu(r) = \mu(\infty) + 2\gamma\Omega/r$

where $\mu(r)$ is the chemical potential of a nanoparticle with radius r, $\mu(\infty)$ is the chemical potential of the bulk material, γ is the metal surface energy and Ω is the atomic volume [56]. Particle growth can proceed via two different mechanism namely, migration and coalescence and Ostwald ripening [57,58]. These mechanisms will be discussed in more detail underneath.

1.6.1.1 Migration and coalescence

Migration and coalescence of metal nanoparticles, sometimes also referred as sintering, takes place when metal nanoparticles have a poor interaction with their support. This gives the particles mobility to diffuse over their support and when they come into contact with another nanoparticle they can fuse together. This mechanism is illustrated in Figure 1.7.

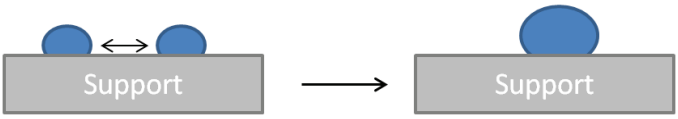

Figure 1.7 Schematic representation of sintering

When the interaction with the support is weak, the temperature from the environment can provide enough energy for Brownian motion of the nanoparticles. Particles can align their crystal planes as they fuse together and this will result in a larger particle with lower total free energy [55].

1.6.1.2 Ostwald ripening

Another mechanism of particle growth is Ostwald ripening, where atoms detach as monomers from small nanoparticles with a high chemical potential and diffuse towards larger particles with a lower chemical potential and attach to these particles. This results in growth of large particles at the expense of smaller ones [59]. All classical models for Ostwald ripening are based on the Gibbs-Kelvin equation (1.12). The equation assumes that the chemical potential of the molecules in the nanoparticle is equivalent to the chemical potential of the vapour phase. One can see from this equation that the vapour pressure around a small particle is higher than around large particles [60].

(1.12) $P(r) = P(0)e^{\frac{2\gamma\Omega}{rRT}}$

Here $P(r)$ is the vapour pressure around a particle with radius r, $P(0)$ is the vapour pressure, R is the gas constant and T is the temperature in Kelvin. The vapour pressure around a particle is correlated to the monomer concentration, there is a higher concentration of metal monomers around a small particle then around a large one. This concentration difference will result in a net flux of metal monomers towards larger particles that can either go over the surface of the support or via the vapour phase. Ideally the metal particles should have the same size and should be homogenously distributed over the support so that there is no difference in chemical potential ($\Delta\mu_{np)}$ between the particles. However, in reality there are often differences in $\Delta\mu_{np}$. This will drive particles with radius (r) smaller than the critical radius (r*) to shrink and one with a larger radius (r) to grow [61].

The process of Ostwald ripening is schematically represented in Figure 1.8. In principle one can divide the process in two equilibria, that is the detachment of monomers from small particles and the attachment of the monomers to the larger particle (**A)** and the second equilibrium is the diffusion of monomers towards larger particles (**B**).

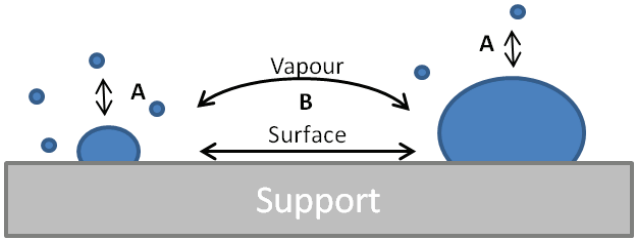

Figure 1.8 Schematic representation of Ostwald Ripening. There are two different equilibriums to be considered, the first, (A) is the detachment and attachment of monomers from the metal particles. This is inter alia influenced by the particle size. The second equilibrium is the diffusion (B) of the monomers towards a particle with a lower chemical potential, this can proceed either via the vapour phase or over the surface.

The ripening progress in influenced by factors like the particle size as follows from the Gibbs-Kelvin equation (1.12), the reaction environment and by the support material [58,59,62]. How these factors affect the ripening process will be discussed. The formation energy of the metal monomers around the nanoparticles is depending on the chemical potential of the particle. That is depended on size of the particles, on the reaction environment and on the support material [63]. The relation with the size of the nanoparticle follows from the Gibbs-Kelvin equation. The reaction environment of a catalyst will influence the surface energy and morphology of the particles and this can also affects the ripening progress [61]. Mass transport during Ostwald ripening takes place via the formation and diffusion of metal monomers. These metal monomers are metal-reactant or metal-reaction intermediate complexes. The detachment of such metal monomers, hence the energy of formation of the monomers, is often more favourable than the detachment of metal atoms itself [61]. Detached single metal atoms will be further referred to as adatoms. Next to the difference in formation energy between metal monomers and adatoms, they will also have a different mobility on the support material. Diebold *et al.* showed that Pd-carbonyl complexes, formed by absorption of CO on palladium are more mobile on a Fe_3O_4(001) surface than Pd adatoms [58]. The last factor that influences the chemical potential of the metalnanoparticles is the support material. The support can influence the particle size, morphology, electronic properties of the metal particles by its chemical properties or its morphology and therefore influences the stability of the metal particles. The interaction that the metal has with the support, the so called metal-support interaction (MSI) plays an important role herein [64]. The support can provide stability to the particles depending on the strength of chemical bonding to the supports surface. For example Campbell *et all.* found that silver nanoparticles are more stable on ceria than on magnesia. This stability difference is attributed to a higher energy of absorption of silver nanoparticles on ceria than on magnesia and the nanoparticles are likely to be more stable at lattice defect of the support [62]. The interaction between the metal and the support is different for each catalytic system. The choice of a good support is therefore crucial for the design of a stable catalyst.

1.6.1.3 Particle growth in the methanol synthesis catalyst

The process of particle growth is related to the melting point of the metal and is thus strongly dependent on the reaction temperature. Hüttig and Tamman temperatures give an indication of the temperature at which respectively atoms at defects and atoms from the bulk become mobile [52]. An overview of Hüttig and Tamman temperatures of several copper and zinc phases are given in Table 1.3.

Table 1.3 Overview of Hüttig and Tamman temperatures of several copper and zinc phases

	Hüttig (˚C)	Tamman (˚C)
Cu[a]	129	397
ZnO[a[	423	887
$CuCl_2$[b]	-5	147
Cu_2Cl_2[b]	-62	79

[a] obtained from [20]. [b] obtained from [52]

Because the Hüttig temperature of copper lies below the reaction temperature, it is expected that copper particle growth will occur via Oswald ripening rather than via migration and coalescence. Diffusion of copper towards larger particles will probably go via copper-reactant (intermediate) complexes since the formation energy of a copper adatom is high. Rasmussen *et al.* suggested, based on DFT calculations, that the copper transport occurs via diffusion of CuCO and Cu_2HCOO species [65].

1.6.2 Deactivation by poisons

The synthesis gas that is used in the methanol process is subjected to a desulphurisation step in which sulphur containing species are removed. This is an essential step in the process because sulphides work as site blocking poisons for copper based catalysts. Sulphides will accumulate on the copper surface and this will decrease the active surface area of the catalyst. The presence of zinc oxide prevents poisoning of copper to some extent by the formation of the more favourable ZnS phase [54]. Chloride species are also strong poisons for methanol catalysts but luckily not often present in the synthesis gas feed. Chloride will cause an increase in mobility for the copper phases as well as the zinc phases. All transitions metals other than copper are known to affect the selectivity of the catalyst. The presence of iron can, for example, result in the formation of waxes and higher paraffin's by Fischer-Tropsch catalysis [54].

Since poisons in the synthesis gas feed are these days well removed and the catalysts can be produced without any poisons present, deactivation of the methanol synthesis catalyst is mainly caused by growth of the copper particles.

1.7 Scope of this thesis

One of the roles of the support of a catalyst is to stabilise the metal nanoparticles and prevent them from growing [61]. This stabilising effect can come from textural properties of the support as well as the chemical properties [66]. The scope of this thesis is to investigate the influence of the chemical properties of the support on the particle growth of a model catalyst for the methanol synthesis reaction. The model catalyst that is used in this study is a Stöber silica supported copper catalyst. The chemical nature of the support is changed by the introductions of amino groups, methyl groups, alumina, titania or zinc oxide to the silica surface. These organic groups and metal oxides are introduced by functionalisation or grafting of the support.

1.8 Research approach

Silica is chosen as the support material in this study because one can make it as such that it contains almost no micropores. This and the very clear morphology of the support make it very suitable for transmission electron microscope (TEM) studies. The silanol groups present on the surface allow the introduction off other chemical groups on the surface. One can modify the surface of silica by reaction with for example alkoxysilanes or metal alkoxides with these silanol groups. Reaction of silanol groups with organic precursor is called functionalisation and with metal based precursors is called grafting. Methods for the functionalisation or grafting of silica are well described in literature.

When one wants to compare the performance and deactivation of the functionalised and grafted catalyst with each other, the functionalisation or grafting layer must be the only varying parameter. This implies that other catalyst parameters, such as particle size, particle distribution and loading must tried to kept the same in each catalysts. Therefore the same weight loading of copper is used for each of the grafted catalysts.

Textural properties of the supports are investigated with N_2-physisorption. Diffuse reflectance infrared spectroscopy (DRIFTS), elemental analysis (ICP-OES) and thermogravimetric analysis (TGA) were used to study the organic functional groups. Copper particles are deposited on the bare, functionalised or grafted supports by incipient wetness impregnation with a copper nitrate solution in water that is followed by calcination in a nitrogen atmosphere. The reduction behaviour of the catalysts is studied with temperature programmed reduction (TPR). Catalysts are reduced *in situ* in the catalytic testing setup, where after they are tested on

activity in the methanol synthesis reaction for ± 230 hours. Catalysts particle sizes are studied before and after reaction with TEM and X-ray diffraction (XRD).

The effect of functionalisation of the silica material with amino groups is discussed in Chapter 1. Chapter 3 covers the functionalisation with methyl groups and Chapter 4 the grafting with different metal oxides.

1.9 References

[1] BP statical review of world energy, 2013.

[2] D. Johnson, Global Methanol Market Review, 2012.

[3] G. a Olah, Towards oil independence through renewable methanol chemistry., Angew. Chem. Int. Ed. Engl. 52 (2013) 104–7.

[4] G. a. Olah, The Role of Catalysis in Replacing Oil by Renewable Methanol Using Carbon dioxide Capture and Recycling (CCR), Catal. Letters. 143 (2013) 983–987.

[5] G. a Olah, Beyond oil and gas: the methanol economy., Angew. Chem. Int. Ed. Engl. 44 (2005) 2636–9.

[6] Iceland starts international carbon recycling, IceNews. (2008).

[7] K.C. Waugh, Methanol Synthesis, Catal. Today. 15 (1992) 51–75.

[8] Mitsubishi Gas Chemical Company, Group guide, (n.d.).

[9] A. Riaz, G. Zahedi, J.J. Klemeš, A review of cleaner production methods for the manufacture of methanol, J. Clean. Prod. 57 (2013) 19–37.

[10] Veiligheidsinformatieblad Methanol, 2001.

[11] Methanol, (n.d.) 1–2.

[12] R. Boyle, The Sceptical Chymist: or Chymico-Physical Doubts & Paradoxes, F. Cadwell, London, 1661.

[13] S. Vukojevic, Copper Colloids and Nanoparticular Cu/ZrO2- based Catalysts for Methanol Synthesis, Ruhr-Universität Bochum, 2009.

[14] T.B. Reed, R.M. Lerner, Methanol : A Versatile Fuel for Immediate Use, Science (80-.). 182 (1973) 1299–1304.

[15] J.E. Sinor Consultants, Methanol: Born in 1923 and Still Going Strong, Sinor Synth. Fuels Rep. 4 (1999) 1–4.

[16] E. Supp, How to Produce Methanol form Coal, Springer-Verlag Berlin Heidelberg, 1990.

[17] A. Mittasch, M. Pier, United States Patent Office, 735823, 1926.

[18] E.K. Poels, D.S. Brands, Methanol Synthesis, (2002) 1–6.

[19] B.K. Aasberg-Petersen, C.S. Nielsen, I. Dybkjær, J. Perregaard, Large Scale Methanol Production from Natural Gas, Haldor Topsøe, n.d.

[20] I. Lovik, Moddeling, Estimation and Optimization of hte Methanol Synthesis with Catalyst Deactivation, NTNU - Norwegian University of Science and Technology, 2001.

[21] T. Arthur, Control structure design for methanol process, NTNU - Norwegian University of Science and Technology, 2010.

[22] J.B. Hansen, P.E.H. Nielsen, Methanol synthesis, in: Handb. Heterog. Catal., 2008: pp. 2920–2948.

[23] B. Carsten, S. Nielsen, Topsøe Methanol Technology for Coal Based Plants, Haldor Topsoe, n.d.

[24] K. Klier, Methanol synthesis, Adv. Catal. 31 (1982) 243.

[25] G.C. Chinchen, P.J. Denny, J.R. Jennings, K.C. Waugh, Synthesis of Methanol, Appl. Catal. 36 (1988) 1–65.

[26] G.C. Chinchen, P.J. Denny, D.G. Parker, M.S. Spencer, D.A. Whan, Mechanism of methanol synthesis from CO2/CO/H2 mixtures over copper/zinc oxide/alumina catalyst: use of 14C-labelled reactants, Appl. Catal. 30 (1987) 333–338.

[27] M.S. Spencer, Role of ZnO in methanol synthesis on copper catalysts, Catal. Letters. 50 (1998) 37–40.

[28] J. Skrzypek, M. Lachowska, M. Grzesik, J. Sloczynski, P. Nowak, Thermodynamics and kinetics of low pressure methanol synthesis, Chem. Eng. J. 58 (1995) 101–108.

[29] P.B. Rasmussen, P.M. Holmblad, T. Askgaard, C. V Ovesen, P. Stoltze, J.K. Norskov, et al., Methanol synthesis on Cu (100) from a binary gas mixture of CO2 and H2, Catal. Letters. 26 (1994) 373–381.

[30] T.S. Askgaard, J.K. Norskov, C. V Ovesen, Stoltze P, A kinetic model methanol synthesis, J. Catal. 156 (1995) 229–242.

[31] C. V Ovesen, P. Stoltze, J.K. Norskov, C.T. Campbell, A Kinetic Model of the Water Gas Shift Reaction, J. Catal. 134 (1992) 445–468.

[32] J. Nakamura, J.M. Campbell, C.T. Campbell, Kinetics and Mechanism of the Water-gas Shift Reaction Catalysed, J. Chem. Soc. Faraday Trans. 86 (1990) 2725–2734.

[33] L.C. Grabow, M. Mavrikakis, Mechanism of Methanol Synthesis on Cu through CO2 and CO Hydrogenation, ACS Catal. 1 (2011) 365–384.

[34] G.H. Graaf, P.J.J.M. Sijtsema, G.E.H. Joostes, Chemical equilibria in methanol synthesis, Chem. Eng. Sci. 41 (1986) 2883–2890.

[35] M.S. Spencer, The role of zinc oxide in Cu / ZnO catalysts for methanol synthesis and the water – gas shift reaction, Top. Catal. 8 (1999) 259–266.

[36] M. Behrens, F. Studt, I. Kasatkin, S. Kühl, M. Hävecker, F. Abild-Pedersen, et al., The active site of methanol synthesis over Cu/ZnO/Al2O3 industrial catalysts., Science (80-.). 336 (2012) 893–7.

[37] M.S. Spencer, The role of zinc oxide in Cu / ZnO catalysts for methanol synthesis and the water – gas shift reaction, Top. Catal. 8 (1999) 259–266.

[38] M. Behrens, Meso- and nano-structuring of industrial Cu/ZnO/(Al2O3) catalysts, J. Catal. 267 (2009) 24–29.

[39] J.C.J. Bart, R.P.A. Sneeden, Copper-zinc oxide-alumina methanol catalysts revisited, Catal. Today. 2 (1987) 1–124.

[40] MK-151 FENCE ™ New methanol synthesis catalyst, Haldor Topsoe A/S, n.d.

[41] Catalyst program, Haldor Topsoe A/S, n.d.

[42] T. Fujitani, J. Nakamura, The effect of ZnO in methanol synthesis catalysts on Cu dispersion and the specific activity, Catal. Letters. 56 (1998) 119–124.

[43] S. Zander, E.L. Kunkes, M.E. Schuster, J. Schumann, G. Weinberg, D. Teschner, et al., The role of the oxide component in the development of copper composite catalysts for methanol synthesis, Angew. Chemie (International Ed.). 52 (2013) 6536–40.

[44] Y. Kanai, T. Watanabe, T. Fujitani, T. Uchijima, J. Nakamura, The synergy between Cu and ZnO in methanol synthesis catalysts, Catal. Letters. 38 (1996) 157–163.

[45] W.C. Conner, J.L. Falconer, Spillover in Heterogeneous Catalysis, Chem. Rev. 95 (1995) 759–788.

[46] J.Ã. Nakamura, Y. Choi, T. Fujitani, On the issue of the active site and the role of ZnO in Cu / ZnO methanol synthesis catalysts, Top. Catal. 22 (2003).

[47] J.-D. Grunwaldt, a. . Molenbroek, N.-Y. Topsøe, H. Topsøe, B.. Clausen, In Situ Investigations of Structural Changes in Cu/ZnO Catalysts, J. Catal. 194 (2000) 452–460.

[48] P.L. Hansen, J.B. Wagner, S. Helveg, J.R. Rostrup-Nielsen, B.S. Clausen, H. Topsøe, Atom-resolved imaging of dynamic shape changes in supported copper nanocrystals., Science (80-.). 295 (2002) 2053–5.

[49] R. Burch, R.J. Chappellt, S.E. Golunski, Synergy between Copper and Zinc Oxide during Methanol Synthesis Transfer of Activating Species, J. Chem. Soc. Faraday Trans. 1. 85 (1989) 3569–3578.

[50] B.S. Clausen, J. Schiotz, L. Grabaek, C. V Ovesen, K.W. Jacobsen, J.K. Norskov, et al., Wetting / non-wetting phenomena during catalysis : evidence from in situ on-line EXAFS studies of Cu-based catalysts, Top. Catal. 1 (1994) 367–376.

[51] I. Kasatkin, P. Kurr, B. Kniep, A. Trunschke, R. Schlögl, Role of lattice strain and defects in copper particles on the activity of Cu/ZnO/Al(2)O(3) catalysts for methanol synthesis., Angew. Chemie. 46 (2007) 7324–7.

[52] J.A. Moulijn, A.E. Van Diepen, F. Kapteijn, Catalyst deactivation: is it predictable? What to do?, Appl. Catal. A Gen. 212 (2001) 3–16.

[53] M. V Twigg, M.S. Spencer, Deactivation of copper metal catalysts for methanol decomposition , methanol steam reforming and methanol synthesis, Top. Catal. 22 (2003) 191–203.

[54] M. V. Twigg, M.S. Spencer, Deactivation of supported copper metal catalysts for hydrogenation reactions, Appl. Catal. A Gen. 212 (2001) 161–174.

[55] M. José-Yacamán, C. Gutierrez, M. Miki, D.-C. Yang, K.N. Piyakis, E. Sacher, Surface diffusion and coalescence of mobile metal nanoparticles, J. Phys. Chem. B. 109 (2005) 9703–9711.

[56] C.T. Campbell, S.C. Parker, D.E. Starr, The Effect of Size-Dependent Nanoparticle Energetics on Catalyst Sintering, Science (80-.). 298 (2002) 811–814.

[57] G. Prieto, J. Zečević, H. Friedrich, K.P. de Jong, P.E. de Jongh, Towards stable catalysts by controlling collective properties of supported metal nanoparticles, Nat. Mater. (2012) 1–6.

[58] G.S. Parkinson, Z. Novotny, G. Argentero, M. Schmid, J. Pavelec, R. Kosak, et al., Carbon monoxide-induced adatom sintering in a Pd-Fe3O4 model catalyst, Nat. Mater. 12 (2013) 724–8.

[59] R. Ouyang, J.-X. Liu, W.-X. Li, Atomistic theory of Ostwald ripening and disintegration of supported metal particles under reaction conditions, J. Am. Chem. Soc. 135 (2013) 1760–71.

[60] V. Burlakov, Ostwald Ripening on Nanoscale, (2007) 1–24.

[61] R. Ouyang, J.-X. Liu, W.-X. Li, Atomistic theory of Ostwald ripening and disintegration of supported metal particles under reaction conditions, J. Am. Chem. Soc. 135 (2013) 1760–71.

[62] J.A. Farmer, C.T. Campbell, Ceria Maintains Smaller Metal Particles by Strong Metal-Support Bonding, Science (80-.). 329 (2010) 933–936.

[63] C.T. Campbell, J.R. V Sellers, Anchored metal nanoparticles : Effects of support and size on their energy , sintering resistance and reactivity, Faraday Discuss. 162 (2013) 9–30.

[64] C.T. Campbell, Catalyst-support interactions: Electronic perturbations, Nat. Chem. 4 (2012) 597–8.

[65] D.B. Rasmussen, T.V.W. Janssens, B. Temel, T. Bligaard, B. Hinnemann, S. Helveg, et al., The energies of formation and mobilities of Cu surface species on Cu and ZnO in methanol and water gas shift atmospheres studied by DFT, J. Catal. 293 (2012) 205–214.

[66] G. Prieto, J.D. Meeldijk, K.P. de Jong, P.E. de Jongh, Interplay between pore size and nanoparticle spatial distribution: Consequences for the stability of CuZn/SiO2 methanol synthesis catalysts, J. Catal. 303 (2013) 31–40.

2 The introduction of amino groups on the catalysts surface and the influence on catalyst performance

2.1 Introduction

The use of amino groups is common in absorbents for the removal of heavy metal ions from aqueous solutions [1]. Nitrogen containing functional groups, such as amino groups, are known to be very effective in purification of aqueous solutions. This is explained by a chelating interaction of two nitrogen containing groups with a metal ion [2]. Introducing nitrogen containing groups on the support surface of a catalyst can result in a different interaction between the support and the metal present in the catalyst. This can affect the catalyst activity as well as the catalyst stability.

The interaction between the support and the metal nanoparticles in a catalyst influences the stability of the metal nanoparticles [3]. A favourable interaction between copper and amino groups can affect the stability of the copper particles and prevent them from sintering. Earlier studies in this research group on Cu/SiO_2 systems strongly suggested that particle growth is these systems occur via Ostwald ripening in which copper monomers diffuse over the surface of the support. More information on this can be found in Appendix A. It is likely that the diffusion of copper monomers over the surface is influence by the presence of amino groups on the surface. Probably these amino groups can interact with the copper monomers, serving as anchoring sites and the presence of these groups can possibly also influence the formation of these monomers. Next to this expected interactions, the amino groups will also raise the basicity of the support, which can also affect the metal support interaction [2].

The anchoring properties of the amino groups may also facilitate the formation of small (~1 nm) copper particles when copper is deposited by incipient wetness impregnation on a functionalised support. Small particles have a higher fraction of low-coordinate copper atoms than larger ones. These atoms have fewer neighbours and will therefore bind absorbants differently. This can affect the activity and the selectivity of the catalyst [4]. As described in paragraph 1.5.2, there are suggestions in literature that methanol reaction takes place at steps on the copper surface. These steps, which consist of low-coordinate copper atoms, should have a higher ability to stabilise reaction intermediates than area's with higher-coordinate copper atoms [5]. It is therefore expected that the formation of small copper particles will affect the activity of the catalyst and that the catalyst with 1 nm particles, made by deposition of copper after functionalisation, is more active than the bare catalyst that contains 2 á 3 nm particles.

Three different amino functionalised catalysts are synthesised, two of them by functionalisation of the support before copper deposition and one by functionalisation after copper deposition. The catalysts that are made by functionalisation before copper deposition are calcined in either N_2 or NO. Different copper particle sizes are expected when calcination takes place under different atmospheres. A in NO calcined copper catalyst will contain larger particles than a in N_2 calcined catalyst [6].

Amino groups will be introduced on the silica spheres by functionalisation with aminopropyltriethoxysilane (APTES). Copper deposition is performed by incipient wetness impregnation of the supports by an aqueous copper nitrite solution. Textural properties of the catalysts are investigated with N_2 physisoption. The organic functional groups are studied with DRIFTS, element analysis and TGA. TPR is used to study the redox behaviour and particle sizes were determined with TEM and XRD. The catalysts were subjected to a catalytic test of $\pm$230 hours to test their catalytic performance in the methanol synthesis reaction.

2.2 Experimental

2.2.1 Synthesis of the Stöber silica support

Silica spheres of 30-40 nm in diameter were made via the Stöber method [7]. A PET bottle is used because silica is tending to grow on the wall of glass. This bottle, containing ethanol (230 mL) was continuously stirred at 250 rpm and heated to 35 ˚C by an oil bath. Ammonia [Merck 25% solution for analysis] (11.25 mL) was added to the ethanol. After that, TEOS [Aldrich, 98%] (17.3 g) was added at ones to the ethanol solution. The mixture was left overnight while stirring at 250 rpm at 35 ˚C. After ± 17 hours the mixture was neutralised by dropwise addition of nitric acid [Merck 65% for analysis] (± 8.7 mL). Ethanol was removed by a rotary evaporator and a white powder was obtained. The powder was dried over night at 120 ˚C, where after it was calcined in air. The calcination took place in three steps, first the support was dried for 2 hours at 200 ˚C to remove the remaining water. The second step took place at 400 ˚C for 1 hour, organics and unreacted ethoxy silicates are removed during this step. The last step takes place at 600 ˚C for 3 hours to remove the micropores in the support. The heating ramp used during the calcination is 100 ˚C/h.

2.2.2 Functionalisation procedure

The functionalisation procedure is based on a method that was described in literature and used in this group before [8,9]. It was performed under an inert nitrogen atmosphere using standard Schlenk techniques. In this way, the presence of water is avoided during reaction. Water will promote self-hydrolysis of the silane precursor and that will lead to a non uniform distribution of the functional groups or patches of functional groups that are clustered together [10]. Prior to the functionalisation, the Stöber silica support (0.8 g) was dried overnight at 120 ˚C under vacuum. (3-aminopropyl)triethoxysiliane (ATPES, 0.5 mL) [Aldrich, 99%] was added to a Schlenk containing dry toluene (50 mL). The column dried toluene was taken from a mBraun MB SPS-80. The APTES solution was added dropwise to the dry silica support, while the latter was stirred continuously at high speed. It was left to stir for 2 hours at room temperature. Stirring was stopped after 2 hours and the mixture was centrifuged for 5 minutes at 5000 rmp. The solvent was decanted and the obtained powder was washed with toluene (2x) [interchemica, 100%] and ethanol [interchemica, 100%] via centrifugation. The obtained powder was dried over night at 60 ˚C. The reaction is visualised in Figure 2.1

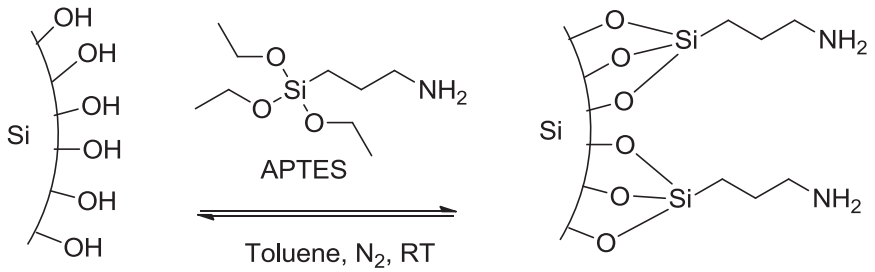

Figure 2.1 Schematic representation of the functionalisation of silica with APTES

2.2.3 Impregnation

Copper was deposited on the support by incipient wetness impregnation with an aqueous copper nitrate solution. The support was dried prior to impregnation under vacuum at a temperature of 120 ºC for 1.5 hours. The pore volume, as determined with N_2 physisorption, was filled with the copper nitrate solution (0.5 M, acidified with HNO_3 to pH~1). The support was dried under vacuum for 12 hours after the impregnation. The copper precursor was decomposed by a thermal treatment at 350 ºC in a pure N_2 (750 mL/min) for 1 hour. A heating ramp of 2ºC/min was used.

2.2.4 N_2 physisorption

Nitrogen physisorption measurements were performed on a Micrometitics Tristar 3000 V6.08 a at liquid nitrogen temperature. Prior to the measurement the samples were first outgassed at 130 ºC in a nitrogen flow for 14 h. The Brunauer-Emmett-Teller (BET) method and the Barret-Joyner-Halenda (BJH) method were used to determine the surface area and the mesopore volume, respectively.

2.2.5 TEM

TEM imaging was performed on a Tecnia 12 (FEI) transmission electron microscope operating at 120 kV. Samples were prepared by crushing followed by sonification in ethanol. A few droplets were supplied on a carbon coated Cu TEM grid (Agar S162 200 Mesh Cu) Cu grid. Images were taken at different magnifications.

Particle sizes were measured using iTEM software. At least 100 particle sizes were measured for each sample.

Figure 2.4a&b are taken with a Titan environmental transmission electron microscope (FEI) working at 300 kV. The sample was crushed and deposited upon an iron grid. This grid was heated inside the microscope by passing an electrical current through it. The sample was reduced *in situ* at 250°C (30°C/min) under 1 mbar of flowing H_2. The sample was then imaged under these conditions.

2.2.6 Catalytic testing

The performance of the catalysts in methanol synthesis was tested in a continuous fixed-bed stainless steel reactor from Autoclave Engineers. The catalyst (0.6-0.9 g, sieve fraction between 0.42-0.63 mm) was reduced *in situ* before catalysis. Reduction was performed by heating the reactor till 250 ˚C with 2 ˚C/min under a 20 (vol.%) H_2/Ar flow, the temperature was maintained for 150 minutes. The reactor was then cooled down to 100 ˚C and flushed for 30 minutes with a synthesis gas mixture of CO, CO_2, H_2 and Ar. CO_2 is present in this mixture to accelerate the deactivation of the catalyst and Ar is used as internal standard for the GC analysis. The synthesis gas ($Ar:CO_2:CO:H_2$=10:7;23:60, vol.%) is supplied from a pressurised gas-mixture cylinder from Linde and is purified in a carbonyl trap before it enters the reactor. The carbonyl trap contains 4.0 g of H-USY zeolite (CVB-780 form Zeolyst Int., 0.5-1.5 mm) and 5 g activated carbon (Norit R3B). After 30 minutes of flushing, the reactor is gradually pressurised to 40 bars in a few hours. Subsequently, the reactor is heated with 2 ˚C min^{-1} to 260 ˚C to start the reaction. The gas that leaves the reactor is depressurised and approximately every two hours injected to a Varian 450 gas chromatograph (GC) for analysis. All reactor outlets are heated at 150 ˚C to avoid product condensation. The GC contains two different channels; the first consists of a HAYESEP Q (0.5Mx1/8") column followed by a MOLSIEVE 13x (15x1/8") column that will lead to a TCD detector. The second channel consists of a CP-SIL 8CB FS capillary column that leads to a FID detector. Argon is used as internal standard for the TCD detector. The product flow is analysed for $\pm$ 230 hours, where after the reaction is stopped.

Catalyst productivities are based on the loss in on CO and CO_2 in comparison to the average CO and CO_2 concentrations before reaction. The methanol yield is based on the loss in CO and CO_2 during the first hours of operation.

After catalytic testing, the samples were passivated by controlled exposure to air. The catalyst were then transferred and stored in a glovebox where it was kept under an inert atmosphere.

2.2.7 ICP analysis

The chemical composition of catalyst is determined by Inductively Coupled Plasma (ICP) analysis at the Mikroanalytisches Laboratorium Kolbe (Mülheim an der Ruhr, Germany). They make use of a ICP-OES Perkin Elmer spectrometer.

2.2.8 TPR

Temperature programmed reduction was performed on a Micromeritric Autochem II ASAP 2920. The samples (~50 mg) were dried first at 120 ºC for 30 min and then cooled down to room temperature. Reduction took place with a flow of 5 vol. % H_2/Ar while increasing the temperature to 600 ºC with 5 ºC/min.

The obtained TPR profiles are normalised on the peak maximum since the loading varies a bit between the samples. The consumed amount of hydrogen was used to calculate the loading of the catalyst, with the assumptions that all the hydrogen was consumed for the reduction of CuO to Cu.

2.2.9 XRD

X-ray diffractrograms were recorded with a Bruker D2 Phaser equipped with a Cu Kα source (λ=1.789 Å). The diffractograms were acquired at a 2Θ range of 20° to 70° with a step size of 0.05° and analysed with DiffracEvaluation V2.0 software, which is based on the Debye-Scherrer-equation.

2.2.10 DRIFTS

DRIFTS spectra were recorded on a Bruker Tensor 27 using a HVC-DRP-3 diffuse reflectance reaction chamber with CaF2 windows and a mercury-cadmium-telluride (MCT) detector. The sample cup holder was 2/3 filled with silicon carbide. This was then covered by a grid on which the sample was placed (~15 mg). The sample was dried *in situ* prior to the measurement by heating to 200 °C with 2 °C/min under a N_2 flow of 10 mL/min. The sample was then allowed to cool down to room temperature still under a continuous gas flow, where after a spectrum was recorded. Diffusion coefficients vary between measurement of different samples, the spectra are therefore set to scale by normalisation on the SiO_2 peak of around 1800 cm^{-1} [11]. In all the recorded spectra is a small peak at ~2300 cm^{-1} visible. Likely this is caused by an error in the detector.

2.3 Results and discussion

2.3.1 Introduction of amino groups on the support

The Stöber silica support was functionalised with amino groups as described in paragraph 2.2.2. Nitrogen physisorption, TGA-MS, elemental analysis and DRIFTS were used to study the extent of functionalisation of the support and these results are discussed below. We refer to non-functionalised Stöber silica support as SS and to amino functionalised Stöber silica as SS-NH_2. Textural properties of these supports were studied with N_2 physisorption, results are shown in Table 2.1.

Table 2.1 Textural properties of Stöber silica and amino functionalised Stöber silica

	$S^{[a]}$ [m^2/g]	$V_{meso}^{[b]}$ [cm^3/g]
SS	101	0.58
SS-NH_2	76	0.53

[a] Surface area. [b] Mesopore volume (2-50 nm pores)

One can see that the functionalisation causes a decrease in the supports surface area and the mesopore volume. Those decreases indicate coverage of amino groups on the spheres [12]. Functionalisation will cause a slight increase in effective diameter of the spheres, this will decrease the mesopore volume and will decrease the effective surface area per gram.

DRIFTS measurements on the functionalised support also indicated the presence of amino groups on the support. These results can be seen in Figure 2.2.

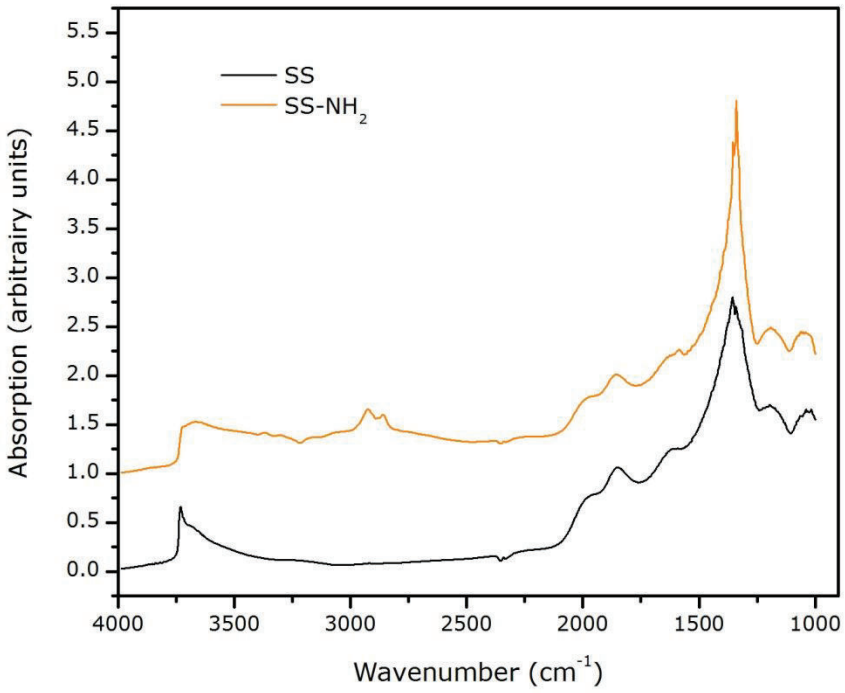

Figure 2.2 Infrared spectra of the support (SS) and the amino functionalised support (SS-NH_2)

The spectra of SS and SS-NH_2 show bands below 2000 cm^{-1} which are characteristic for silica materials. These bands are caused by stretching modes of Si-O-Si and dangling modes of Si-O [13]. Groups on the surface of silica, the silanol groups, can be found around 3700 cm^{-1}. The peak position and profile is somewhat different based on the nature of the silanol groups. Typical silanol groups that can be found are shown in Figure 2.3 [14]. Isolated and free geminal groups are further referred as free silanol and vicinal and hydrogen bonded geminal silanol groups are referred as hydrogen bonded silanol.

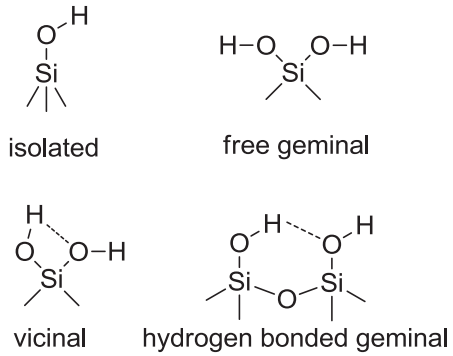

Figure 2.3 Possible silanol groups on a silica surface

The IR spectrum of Stöber silica exhibits a sharp absorption band at 3745 cm^{-1} that is a characteristic for the OH stretching vibration in a free silanol group [15,16]. Hydrogen bonded silanols give a broad peak at 3615 cm^{-1}. When the amino functionalised support is compared to the bare support, one can see that the free silanol peak has disappeared and a broad peak of hydrogen bonded silanol is clearly visible. The spectra of the functionalised support contains the symmetric N-H stretch vibration (ν NHs) of free amino groups at 3380 cm^{-1} and the asymmetric N-H stretch vibration (ν NHas) at 3320 cm^{-1}. C-H vibrations from the propyl chain can be seen at 2940 cm^{-1} and 2875 cm^{-1}, those bands consist of overlapping absorptions [16]. From those results we

can assume that APTES has reacted with the free silanol groups on the supports surface forming propyl amine chains, however, the functionalised support contains unreacted hydrogen bonded silanol groups.

The amount of propylamine groups grafted on the surface was investigated with ICP and TGA, those results are summarised in Table 2.2. The elementary composition of a theoretical monolayer is calculated with the Kiselev-Zhuravlev constant (4.6 OH/nm^2) [17] and the assumption that 1 APTES molecule reacts with 3 surface silanol groups, as visualised in Figure 2.1.

Table 2.2 Elementary composition of the amino functionalised support

Element [wt %]	Theoretical monolayer [a]	ICP	TGA
C	0.9	1.4	1.3
N	0.4	0.4	0.5

[a] number based on the Kiselev-Zhuravlev constant (4.6 OH/nm^2) [17] and the assumption that one APTES molecule reacts with 3 free silanol groups

The weight percentages C and N from ICP and TGA are slightly higher than the theoretical values. It could well be that a part of the APTES molecules has a different degree of binding than we assumed. However, since these values are higher than the value of theoretical monolayer coverage, these results indicate that all the silanol groups have reacted This is contradictory to the DRIFTS results, were the presence of unreacted hydrogen bonded silanol groups is seen. Possible explanations for this could be that APTES bind to the support in a different degree than assumed or that there are patches present of the self-hydrolysed amino precursor.

After functionalisation of the support, copper was deposited on the support by incipient wetness impregnation as described in paragraph 2.2.3.

2.3.2 The influence of the amino groups on catalyst properties

2.3.2.1 The copper particle size

The amino functionalised support is impregnated with an aqueous copper nitrate solution followed by calcination in N_2 or NO. We refer to these samples as SS-NH_2-Cu(N_2) and SS-NH_2-Cu(NO). As described in paragraph 2.1, we expected that the presence of the amino groups would facilitate the formation of very small copper particles when calcination in N_2 is used. Particle sizes in the catalysts could not be determined by XRD because the particle size is probably below the detection limit of XRD. TEM was also used to investigate the material, initially there were no particles visible on the support as can be seen in Figure 2.4a. This catalyst is reduced *in situ* at 250 °C with 1 mbar H_2. After an intense beam treatment there were particles visible, this can be seen in Figure 2.4b. This demonstrates that there is copper present in first instance but can't be visualised with TEM. A possible explanation for this is that the copper is deposited as subnanometer particles or that the copper is present in single atomic species. Another possibility could be that the copper is not reduced yet by the *in situ* reduction and that after the intense beam treatment the copper is fully reduced and became visible.

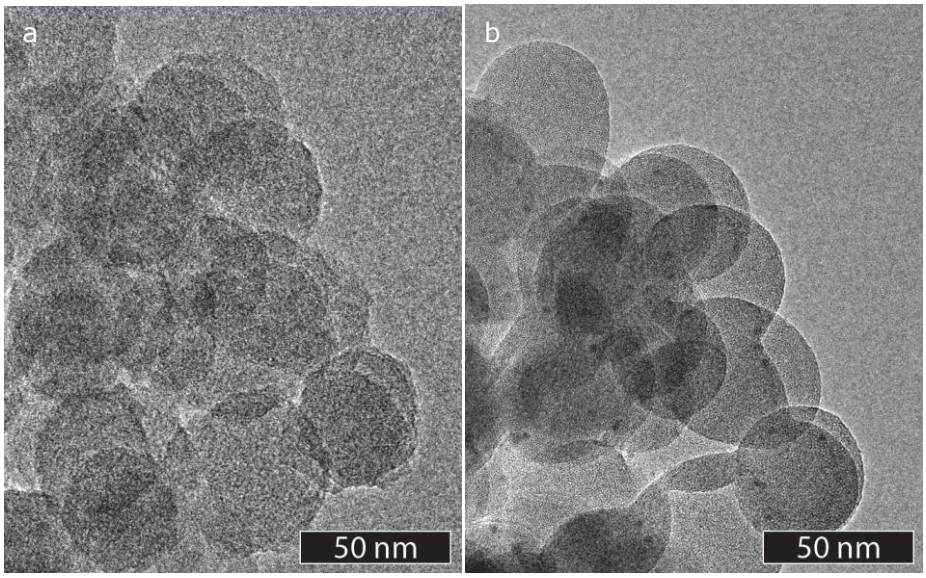

Figure 2.4 [a] The initial SS-NH_2-Cu(N_2) (0.25) sample and [b] the sample after intense beam treatment.

The copper particle size is depended on the atmosphere in which the catalyst is calcined. Earlier studies in this group by inter alia P. Munnik, described the formation of larger copper particles when the catalyst is calcined in NO rather than in N_2 [6]. The copper precursor decomposes via a different copper phase depending on the calcination atmosphere. The difference in size is explained by a different mobility of the copper phases over the support.

The particles size in the in NO calcined catalyst could not be determined with XRD. TEM showed the formation of 2 á 3 nm particles as can be seen in Figure 2.7. A non-functionalised Cu/SiO_2 catalyst that is calcined in NO normally contains 6 á 7 nm copper particles. According to these TEM studies, the presence of amino groups on the support results in the formation of smaller particles. It is likely that the amino groups on the support limit the mobility of the copper phase that is formed in a NO atmosphere than compared a non-functionalised silica supported copper catalyst.

2.3.2.2 The reduction temperature of copper

The influence of the amino groups on the electronic properties of the copper particles was studied with TPR. The TPR profiles for several catalysts can be seen in Figure 2.5. Here SS-Cu is the spectrum of a copper on silica gel catalyst, SS-Cu-NH_2 is a catalyst that is functionalised with amino groups after copper deposition, SS-NH_2-Cu(N_2) and SS-NH_2-Cu(NO) are catalyst that are also described in paragaph 2.3.2.1, they are made by impregnation of a amino functionalised support followed by calcination by either N_2 or NO.

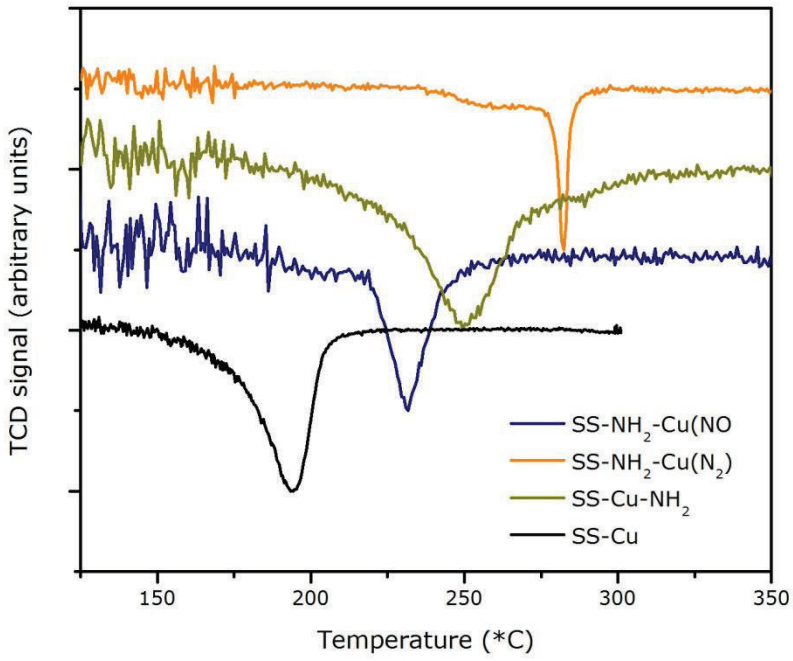

Figure 2.5 TPR results of several amino functionalised catalysts and bare catalyst. The profiles are normalised since the loading varies between the samples

When we compare the SS-Cu and SS-Cu-NH_2 catalyst with each other, one can see that the amino functionalisation causes a change in redox behaviour. The reduction temperature is shifted to higher temperatures. A shift to higher reduction temperatures is observed for all the amino functionalised catalysts. Note that the loading of these catalysts varies. In literature is described that the difference in loading will result in a different hydrogen consumption but will not change the reduction temperature [18]. The peak shifts are therefore attributed to the presence of amino groups, this indicates a difference in catalytic performance of those catalysts compared to the non functionalised catalyst.

Next to the increased reduction temperature for amino functionalised catalyst, there is also a particle size effect visible in **Error! Reference source not found.**. In Table 2.3 one can find the copper particle size as determined by TEM of the different catalysts. The SS-NH2-Cu(N_2) catalysts is likely to have subnanometer copper particles and has the highest reduction temperature. The SS-Cu-NH_2 catalyst has 2 nm copper particles on average and has the second highest reduction temperature. Finally, the SS-NH_2-Cu(NO) catalyst contains of 2.6 nm particles on average and has the lowest reduction temperature of the amino functionalised catalysts. The reduction temperature tends to increase when the particle size decreases in the functionalised catalysts.

2.3.3 The catalytic performance of the catalyst

The difference in reduction temperature of the amino functionalised catalysts compared to a non-functionalised catalyst can indicates a difference in catalytic behaviour. The catalytic performance for methanol synthesis of several amino functionalised catalysts is tested in a deactivation test of $\pm$230 hours. First the activity of the amino functionalised catalysts will be discussed and then the deactivation of these catalysts.

2.3.3.1 Activity of a catalyst with small copper particles

In the introduction is explained that we expect small copper particles to be more active than larger ones because they contain more steps and edges. The results from the catalytic test showed otherwise. These can be seen in Table 1.2. The SS-NH_2-Cu(N_2) has initial methanol productivity of 49 mol kg_{Cu}^{-1} h^{-1}, that is lower than

the SS-NH_2-Cu(NO) catalyst with 2 á 3 nm copper particles. It suggests that subnanometer particles are less active in catalysis than larger ones. However, the particle size in the SS-NH_2-Cu(N_2) could not be determined. It is possible that the copper is present in atomic species that don't have much catalytic activity. Therefore the particle size in this catalyst needs to be determined to be able to draw conclusions on the dependence of activity on particle size. EXAFS could be a possible technique to estimate the particle size in this catalyst.

Table 2.3 Catalytic properties of several catalysts

Catalyst	Cu[a] [wt%]	Cu[b] ICP [wt %]	Cu[c] TPR [wt %]	d Cu[d] TEM [nm]	Methanol yield[f] [mol kg_{Cu}^{-1} h^{-1}]	$k_{D,2}$[g] [10^{-3} h^{-1}]
SS-Cu	0.8	-	-	1.9	70	19.8±0.4
SS-NH_2-Cu(N_2)	0.8	0.79	0.49	-	49	-
SS-NH_2-Cu(NO)	0.8	-	0.83	2.6	68	1.1 ±0.3
SS-Cu	1.8	-	-	2.0	58	15.4±0.7
SS-Cu-NH_2	1.8	-	2.7	2.0	22	-

[a] based on amount of impregnation. [b] from ICP results [c] based on hydrogen consumption during TPR measurements [d] mean diameter of non reduced copper particles by TEM. [e] diameter of copper oxide particles determined by XRD. [f] initial productivity of the catalysts. [g] deactivation constant defined by fitting a second order general power law equation.

The catalysts that is functionalised after the deposition of copper (SS-Cu-NH_2) has a lower activity then the non-functionalised catalyst. This is probably caused by coverage of the copper particles by amino groups. This will be further discussed in paragraph 2.3.3.3.

2.3.3.2 Catalyst deactivation

The deactivation of the catalyst during its time on stream is also studied. The data obtained from the deactivation test is therefore plotted as the productivity normalised by the initial productivity versus the time-on-stream (TOS) in Figure 2.6.

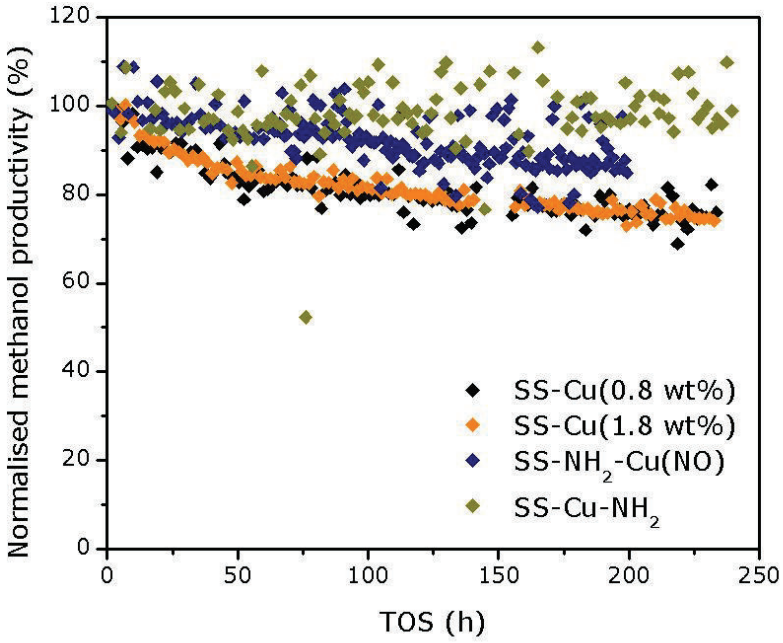

Figure 2.6 Results from deactivation tests of several catalysts plotted as normalised methanol productivity versus the time on stream. Scattering in the data is of the SS-Cu-NH_2 catalyst is caused by the low activity of the catalyst.

Deactivation constants are determined from these deactivation curves by fitting the productivity as a function of time on stream to a general power law equation (2.1):

(2.1) $$\frac{da}{dt} = -k_D \times (a - a_s)^n$$

were t is the time-on-stream, a denotes the normalised catalytic activity, a_s is the normalised activity at $t = \infty$, k_D is the deactivation rate constant and n is a exponent that can range from 1 to 10. The GPLE can be converted to the linear equation (2.2) by integration, normalisation and solving the equation for $(a\text{-}as)^{-n+1)}$.

(2.2) $$(a - as)^{-n+1} = (n-1)k_D \times t + 1$$

In literature is described that n can be taken as 1 or 2 for catalytic systems that deactivate by particle growth [19]. The deactivation constants in Table 2.3 are defined by taking second order deactivation (n=2), this was found to give a better linear fit than first order deactivation (n=1). The linear fits can be found in Figure B 1 in appendix B and the deactivation constants are summarised in Table 2.3.

2.3.3.3 The stabilising effect of the amino groups

In Figure 2.6 is visible that both non-functionalised catalysts, SS-Cu(0.8 wt%) (black) and SS-Cu(1.8 wt%) (orange), shows the deactivation behaviour of copper particles of 2 á 3 nm supported on Stöber silica spheres. Their deactivation constant has the same order of magnitude, 19.8 h^{-1} and 15.7 x 10^{-3} h^{-1} respectively. On the other hand, SS-NH_2-Cu(NO), the catalyst with 2 á 3 nm copper particles and amino groups on the supports surface exhibits a different deactivation behaviour. In the figure one can see that the deactivation curve has a different shape than the curves of the SS-Cu catalysts, the catalyst retains a higher activity during the test. The deactivation constant of this catalyst is much smaller (1.1 x 10^{-3} h^{-1}) than of the non-functionalised catalysts whereas the initial methanol productivity is comparable.

Those results are in accordance with copper particle size studies of the fresh and the spent catalyst Figure 2.7. During the catalytic test of ±230 hours the copper particles in the amino functionalised catalyst have not grown a lot whereas the particles in a non-functionalised catalysts did significantly.

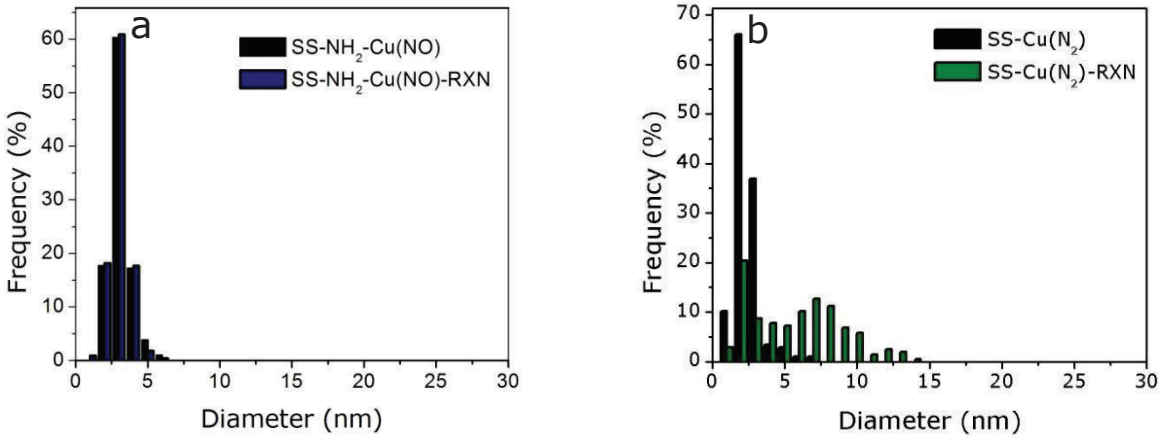

Figure 2.7 [a] Copper particle sizes determined by TEM of the SS-NH_2-Cu(NO) catalyst before and after reaction and [b] copper particles sizes of the SS-Cu(N_2)(1.8 wt%) of before and after reaction.

As described in the introduction, it is assumed that particle growth in these catalysts occurs via Ostwald ripening. This process is explained in detail in paragraph 1.6.1.2. One can consider two different equilibriums in Ostwald ripening, that is the detachment of monomers from small particles and the attachment of the monomers to the larger particle (**A)** and the second equilibrium is the diffusion of monomers towards larger particles (**B**). This process is influenced by a lot of factors including the nature and structure of the supports surface. Based on above results we hypothesise that the formation of copper monomers **(A)** is accelerated by the presence of amino groups. The favourable interaction between copper monomers and amino groups can lower the energy barrier for monomer detachment. However, it is also likely that the amino groups can act as anchoring sites, this will suppress the diffusion of the monomers towards the larger particles **(B)** and will therefore suppress the growth of particles.

The amino functionalised catalysts described above were made by depositing copper after functionalisation. The SS-Cu-NH_2 catalyst is made by first depositing copper and then functionalisation of the catalyst surface. This catalyst was also subjected to a catalytic test but a deactivation constant could not be determined because its deactivation curve contains a lot of scatter (Figure 2.6 (green)). The scatter can be explained by the low productivity of the catalyst. A small integration difference of the GC data will give a significant change in productivity. Since this catalyst is made by functionalisation after copper deposition, it is likely that the low productivity is caused by coverage of the copper surface by amino groups as is probably also the case for methylated catalysts as described in 3.3.2.2.

2.3.3.4 Stability of the amino groups during reaction

The amino groups are organic groups, it could be well possible that these groups decompose during methanol reaction which is at 260 ˚C, 40 bar pressure and involves water generated in the reverse water gas shift reaction. TGA measurements on the functionalised support material pointed out that the amino groups are stable up to ~275 ˚C in oxygen. This graph can be found in the appendix Figure C 2.

In literature it is reported that that decomposition of the amino groups starts at 300 ˚C with a maximum at 500 ˚C [16]. DRIFTS was used to investigate the stability of the amino groups under methanol synthesis reaction conditions. Spectra of the amino functionalised catalyst before and after 230 hours of reaction are shown in Figure 2.8.

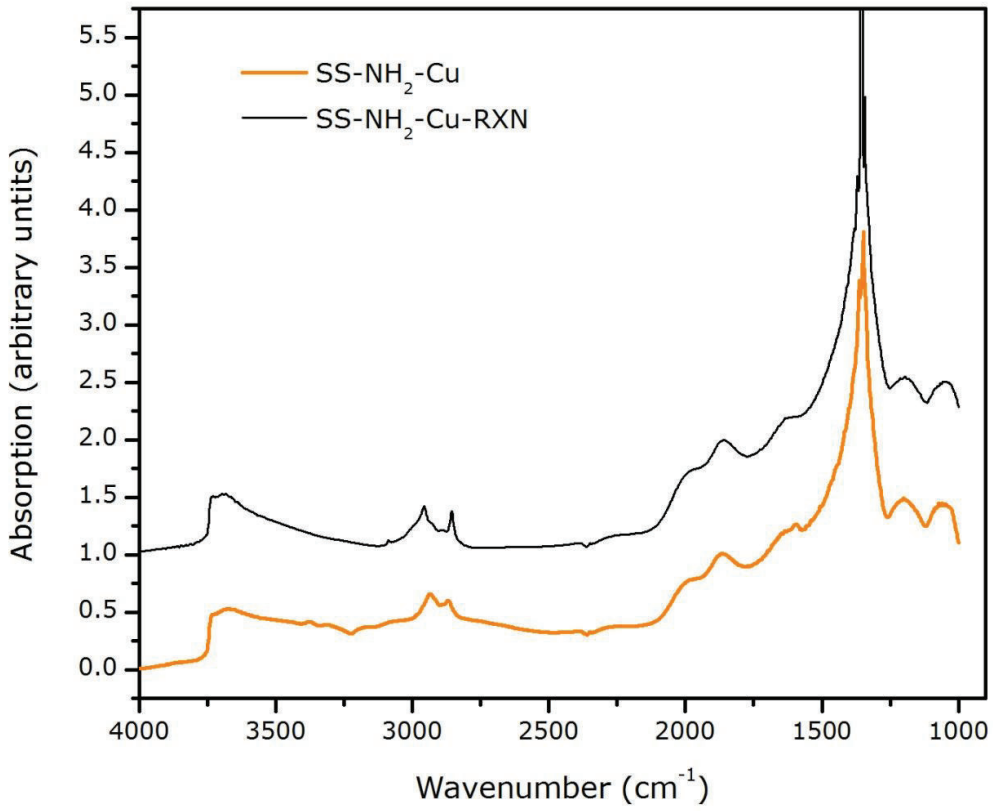

Figure 2.8 Infrared spectra of the amino functionalised catalyst before (orange) and after 230 hours of reaction (blue)

The overall shape of SS-NH_2-Cu-RXN (blue line) is quite similar to the line shape of the catalyst before reaction SS-NH_2-Cu (yellow line). The sharp peak at 3745 cm^{-1} caused by the OH stretching of free silanol is still absent after reaction. The characteristic CH vibrations of the propyl chain can be seen around 2940 cm^{-1} and 2875 cm^{-1}. In the catalyst after reaction there is a small peak visible next to those vibrations, at 3095 cm^{-1}. The origin of this peak is unknown. The NH vibrations of free amino groups, between 3300 cm^{-1} – 3400 cm^{-1} are not visible for the catalyst after reaction. Since those bands are normally very weak, the absence of these bands does not mean that the amino groups are not present any more.

The chemical composition of the catalyst after reaction was determined with ICP. In Table 2.4 the composition of the catalyst before and after reaction are compared.

Table 2.4 Chemical composition of the catalyst in several stages

Element[a] [wt %]	SS-NH_2[b]	SS-NH_2-Cu[c]	SS-NH_2-Cu-RXN[d]
C	1.4	1.1	1.2
N	0.3	0.2	0.2
N/C ratio	0.21	0.18	0.17

[a] percentages obtained from element analysis (ICP). [b] direct after functionalisation of the support. [c] after calcination of the catalyst at 350 ˚C in N_2 atmosphere. [d] after 230 hours of reaction for methanol synthesis.

One can see that the N/C ratio decreases a little bit after calcination. This value is not changed significantly after methanol synthesis reaction. Based on those results and the DRIFTS results showed above we conclude that the greater part of the amino groups are stable under reaction conditions. The extra peak in the DRIFTS spectra and the small decrease in activity while the particles have not grown could point towards partial decomposition of the amino groups. Decomposition of these groups could result in a decrease in active surface area by carbon deposition on the copper.

2.4 Conclusions

A liquid phase reaction with APTES and Stöber silica led to a decrease of the support surface area and pore volume. This indicates that there are functional groups present on the surface. DRIFTS results showed the presence of the CH_2 vibrations of the propyl chain, of the NH vibrations of the amino groups and the absence of free silanol groups. Hydrogen bonded silanol groups are still visible in the spectra of the functionalised support. The presence of carbon and nitrogen in the support was also shown by ICP and TGA.

Copper was deposited on the amino functionalised support by incipient wetness impregnation followed by calcination it either N_2 or NO. Calcination in NO led to the formation of 2 á 3 nm particles as determined by TEM whereas the particles size of the catalyst in N_2 could not be determined by either TEM or XRD, indicating particles < 2 nm. Intensive beam treatment of the in N_2 calcined catalyst while imaging the catalyst with TEM resulted in the formation of copper particles. This showed the presence of copper in the catalyst. It is possibly present in subnanometer particles or in atomic species. Functionalisation of the catalysts resulted in shifts of the reduction temperatures of copper towards higher temperatures.

Several functionalised catalysts show different deactivation behaviours when subjected to a catalytic test. The most interesting is the deactivation of the SS-NH_2-Cu(NO) catalyst, which contains 2 á 3 nm particles. It shows only very little deactivation after 10 days of testing. Compared to a non-functionalised catalysts, this catalyst deactivates only very little. This is attributed to the favourable interaction that the amino groups have with the copper particles and monomers, which are responsible for particle growth.

The stability of the amino groups was studied with DRIFTS and ICP. Their characteristic CH_2 vibrations are still observed after reaction and their carbon and nitrogen content remains same. There is however, an extra peak visible in the DRIFTS spectra and there is a small decrease in activity while the particles have not grown. This could point towards partial decomposition of the groups.

2.5 Outlook

The particle size of the SS-NH_2-Cu(N_2) catalyst could not be determined with TEM and XRD. In order to draw conclusions on the particle size dependence in a Cu/SiO_2 catalyst, the particle size in this catalyst should be determined. This could be done by Extended X-ray Absorption Fine Structure (EXAFS) spectroscopy measurements as is described in literature [20].

DRIFTS showed the presence of NH and CH_2 in the functionalised support. To get to know more about the way the functionalised groups, the support could be studied with NMR spectroscopy.

It was found that the SS-Cu-NH_2 catalyst exhibits a much lower activity then a non functionalised catalyst. This activity difference was attributed to the coverage of active copper phase by the amino groups. As described in the next chapter, similar results were found for a copper catalyst functionalised with methyl groups. With a heat treatment, in order to remove the methyl groups, the activity of the catalyst could not be increased to the activity of a non-functionalised catalyst. This is likely caused by the fact that there is still silica deposited on the copper. Copper surface area measurements could be used to verify the decrease in surface area.

In paragraph 2.3.3.3, a hypothesis is described on the stabilising effect of the amino groups. Calculations of the affinity of the amino groups for CuCO and CuCOOH would be interesting to support this hypothesis.

2.6 References

[1] S. Deng, R. Bai, J.P. Chen, Aminated Polyacrylonitrile Fibers for Lead and Copper Removal, (2003) 5058–5064.

[2] Y. Lin, H. Chen, K. Lin, B. Chen, C. Chiou, Application of magnetic particles modified with amino groups to adsorb copper ions in aqueous solution., J. Environ. Sci. (China). 23 (2011) 44–50.

[3] R. Ouyang, J.-X. Liu, W.-X. Li, Atomistic theory of Ostwald ripening and disintegration of supported metal particles under reaction conditions, J. Am. Chem. Soc. 135 (2013) 1760–71.

[4] C.T. Campbell, Catalyst-support interactions: Electronic perturbations, Nat. Chem. 4 (2012) 597–8.

[5] M. Behrens, F. Studt, I. Kasatkin, S. Kühl, M. Hävecker, F. Abild-Pedersen, et al., The active site of methanol synthesis over Cu/ZnO/Al2O3 industrial catalysts., Science (80-.). 336 (2012) 893–7.

[6] P. Munnik, M. Wolters, a. Gabrielsson, S.D. Pollington, G. Headdock, J.H. Bitter, et al., Copper Nitrate Redispersion To Arrive at Highly Active Silica-Supported Copper Catalysts, J. Phys. Chem. C. 115 (2011) 14698–14706.

[7] W. Stöber, A. Fink, Controlled Growth of Monodisperse Silica Spheres in the Micron Size Range 1, J. Colloid Interface Sci. 26 (1968) 62–69.

[8] M.J. Jacinto, P.K. Kiyohara, S.H. Masunaga, R.F. Jardim, L.M. Rossi, Recoverable rhodium nanoparticles: Synthesis, characterization and catalytic performance in hydrogenation reactions, Appl. Catal. A Gen. 338 (2008) 52–57.

[9] R.L. Oliveira, P.K. Kiyohara, L.M. Rossi, High performance magnetic separation of gold nanoparticles for catalytic oxidation of alcohols, Green Chem. 12 (2010) 144.

[10] D. Brühwiler, Postsynthetic functionalization of mesoporous silica., Nanoscale. 2 (2010) 887–92.

[11] T. Armaroli, T. Bécue, S. Gautier, Diffuse Reflection Infrared Spectroscopy (Drifts): Application to the in situ Analysis of Catalysts, Oil Gas Sci. Technol. 59 (2004) 215–237.

[12] Y. Chen, Z. Guo, T. Chen, Y. Yang, Surface-functionalized TUD-1 mesoporous molecular sieve supported palladium for solvent-free aerobic oxidation of benzyl alcohol, J. Catal. 275 (2010) 11–24.

[13] J. Pires, M. Pinto, J. Estella, J.C. Echeverría, Characterization of the hydrophobicity of mesoporous silicas and clays with silica pillars by water adsorption and DRIFT., J. Colloid Interface Sci. 317 (2008) 206–13.

[14] T. Seki, T. Ikariya, In situ diffuse reflectance infrared Fourier transform spectroscopy of MCM-41 mesoporous silica: mechanistic consideration on the chemical fixation of CO2 with N,N′-dimethylethylenediamine to 1,3-dimethyl-2-imidazolidinone, Phys. Chem. Chem. Phys. 11 (2009) 10073–9.

[15] V.N. Panchenko, V. a. Pozimenko, E. a. Paukshtis, V. a. Zakharov, IR spectroscopic study of the basicity of aminated silica gels, Russ. J. Inorg. Chem. 54 (2009) 1798–1803.

[16] T. Kovalchuk, H. Sfihi, L. Kostenko, V. Zaitsev, J. Fraissard, Preparation, structure and thermal stability of onium- and amino-functionalized silicas for the use as catalysts supports, J. Colloid Interface Sci. 302 (2006) 214–29.

[17] L.T. Zhuravlev, The surface chemistry of amorphous silica. Zhuravlev model, Colloids Surfaces A Physicochem. Eng. Asp. 173 (2000) 1–38.

[18] S.J. Gentry, P.T. Walsh, Influence of Silica and Alumina Supports on the Temperature-programmed Reduction of Copper (II) Oxide, J. Chem. Soc. Faraday Trans. 1. 78 (1982) 1515–1523.

[19] C.H. Bartholomew, Sintering kinetics of supported metals: new perspectives from a unifying GPLE treatment, Appl. Catal. A Gen. 107 (1993) 1–57.

[20] B.S. Clausen, L. Grabæk, H. Topsoe, L.B. Hansen, P. Stioltze, J.K. Norskov, et al., A new procedure for particle size determination by EXAFS based on molecular dynamics simulations, J. Catal. 141 (1993) 368–379.

3 The methylation of a catalysts surface and the influence on catalyst performance

3.1 Introduction

Functionalisation of silica with hydrophobic groups is widely used to change and study interactions between colloidal silica materials [1]. Hydrophobic silica materials are also used in the purification of water, they have the ability to absorb poorly soluble compounds such as benzene and toluene from aqueous solutions [2]. The influence of a hydrophobic support surface, made by methylation, on the stability the Cu/SiO_2 catalyst will be discussed in this chapter. As discussed earlier in paragraph 1.6.1.3, Rasmussen *et al*. suggested that the particles that are responsible for the copper transport in Oswald ripening during catalysis are mainly CuCO and Cu_2HCOO species [3]. The diffusion of these copper monomers can go via the surface of the support or via the vapour phase. For a Cu/SiO_2 catalysts it is likely that this diffusion goes over the surface as is explained in the introduction of previous chapter. It is expected that hydrophobic properties of the supports surface will influence the diffusion of such hydrophilic copper monomers over the support. In addition to influence on the monomer diffusion, the monomer formation and the attachment to larger particles will likely also be influenced by hydrophobic properties of the supports surface.

Hydrophobicity on the support surface was created by the introduction of methyl or trimethyl groups on the silica surface. This was done by a liquid phase reaction of methylmethoxysilane (MTMS) with the silanol groups on the silica surface or with a gas phase reaction with hexamethyldisilazan (HMDS). The liquid phase reaction theoretically results a methylated silica surface as can be seen in Figure 3.2. A gasphase reaction with HMDS theoretically results in a methylated silica surface as can be seen in Figure 3.3. Ammonia is released during this reaction. The degree of methylation of the supports was studied with TGA, ICP and DRIFTS.

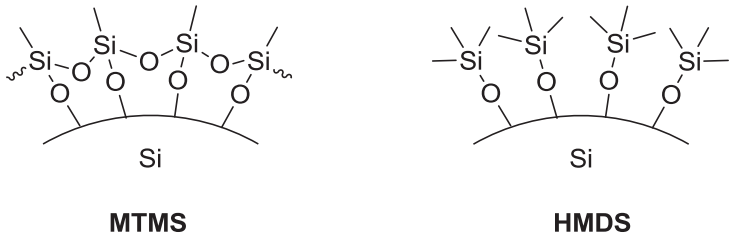

Figure 3.1 Schematic representation of the silica support methylated by MTMS (left) or HMDS (right)

Different catalysts were made. The methylated catalyst made by methylation with MTMS was made by methylation of a Cu/SiO_2 catalysts. The catalysts methylated with HMDS were made in two different ways. The first is the same as for the one made by MTMS, by methylation of the Cu/SiO_2. The second way is by first methylation of the surface and then an incipient wetness impregnation with a copper nitrate solution. Ethanol was used as solvent for the copper precursor in order to try to get a good copper dispersion.

The catalysts that are methylated after copper deposition, are subjected to a test on their catalytic performance for $\pm$230 hours.

3.2 Experimental

3.2.1 Synthesis of the Stöber silica support

The support was synthesised as described in paragraph 2.2.

3.2.2 Impregnation

Copper were deposited on the non-functionalised support as described in paragraph 2.2.3. Copper particles were deposited on a methylated support by impregnation of a copper nitrate solution (0.5 M) in ethanol. Ethanol was used since water did not wet the methylated support. The support was dried prior to impregnation under vacuum at a temperature of 120 °C for 1.5 hours. Subsequently, the support was cooled

down by an ice bath. This makes the impregnation easier. The support was then impregnated with the copper nitrate solution in ethanol to fill the complete pore volume, as measured with N_2-physisorption. After impregnation, the support was dried under vacuum for 12 hours. A thermal treatment at 350 ºC in a pure N_2 (750 mL/min) for 1 hour was used to decompose the copper precursor. Heating till 350 ºC occurred with 2ºC/min.

3.2.3 Functionalisation procedure

The introduction of methyl groups with MTMS as precursor was based on a procedure that is described by Fu *et al.* [4]. The Stöber silica supported copper catalyst (1.5 g) was put in a two necked round-bottomed flask. Toluene (59 mL) [Interchemica 100%] and demiwater (0.88 mL) were added to the round-bottemed flask. The addition of demiwater should result into crosslinking of the methyl groups on the surface. The mixture was heated to 111 ºC, stirred and allowed to reflux for 80 minutes after which MTMS (5.9 mL) [Acros Organics 97%] was added dropwise to the mixture and reluxing continued. After 4 hours, MTMS (3.0 mL) was again added to the mixture and refluxing was continued for 65 minutes. Heating was stopped and the mixture was allowed to cool down for 30 minutes after which the solvent was removed by centrifugation. The obtained solid was washed 2x with EtOH [Interchemica 100%] by means of centrifugation and dried over night at 60 ºC. A schematic representation of this methylation is given in Figure 3.2.

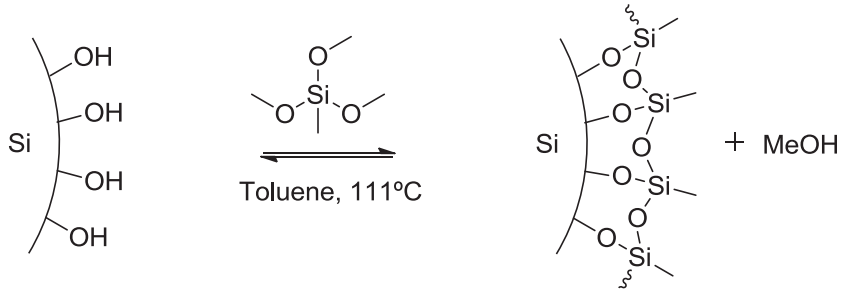

Figure 3.2 Schematic presentation of the of the methylation of the silica support with MTMS

The other methylation was done by a gas phase reaction with hexamethyldisilazan (HMDS). As described in paragraph 2.1, this catalyst was made by methylation before and after copper deposition. The method that was used for the catalyst that is methylated before copper deposition will be described first. The catalyst (0.8 g) was reduced and then re-oxidised prior to the functionalisation in order to try to clean the copper surface. Reduction took place at 250 ºC under a flow H_2/N_2 (20:80 vol. %) of 100 mL/min. After flushing the catalyst for 1 hour at room temperature with N_2, re-oxidation was started by flushing with a O_2/N_2 flow (5:95 vol. %) of 100 mL/min. The temperature was increased after 1 hour to 200 ºC with 2 ºC/min, where after the oxygen flow was changed to (15:85 vol. %). Subsequently the catalyst was allowed to cool down to room temperature.

A gas bubbler containing HMDS (approximately 14 g) [Acros organics 98%] was placed in between the reactor and the gas inlet. Temperature of the reactor was heated to 70 ºC with 2 ºC/min where after a N_2 flow of 40 mL/min was led through the gas bubbler over the catalyst. After approximately 48 hours the gas bubbler was empty and removed from the gas stream. Unreacted HMDS was removed from the catalyst by thermal treatment at 200 ºC for 3 hours under a N_2 flow (100 mL/min). The functionalisation reaction is schematically represented in Figure 3.3.

The catalyst that was made methylation of the surface before copper deposition didn't undergo the reduction and re-oxidation procedure. The support was dried prior to the methylation at 120 ºC after which the same methylation procedure as described above was used.

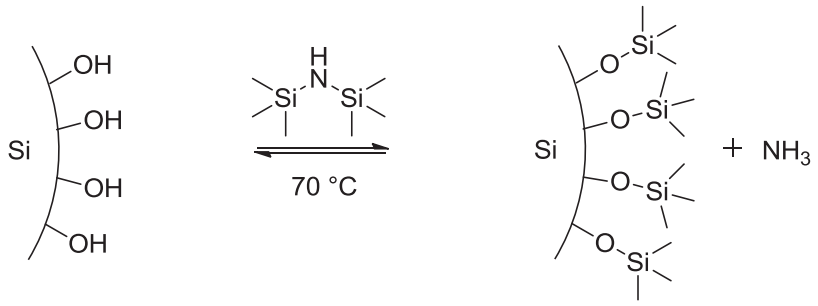

Figure 3.3 Schematic presentation of the methylation of the silica support with HMDS

3.2.4 Removal of methyl groups

Attempts to remove the methyl groups on the surface of the functionalised catalysts were done by thermal treatment in an oxygen atmosphere. The methylated catalyst (typically 0.8 g) was put in a calcination reactor and placed in an oven. The temperature was increased to 50 °C (2 °C/min) under a O_2/N_2 (10:90 vol. %) flow of 100 mL/min. Subsequently the temperature was raised to 100 °C under a O_2/N_2 (20:80 vol. %) with higher oxygen content. Then the temperature was raised to 150 °C under a O_2/N_2 (30:70 vol. %) and then to 200 °C under O_2/N_2 (40:60 vol. %). While keeping this atmosphere the temperature was further increased to 500 °C and was kept there for 3 hours. The catalyst was then cooled down.

Methyl groups were removed in between a catalytic test to see if the productivity of the catalyst increased after the removal. The reduced catalyst was first passivated by a small leakage in the testing reactor where after it was transferred to a calcination reactor.

3.2.5 N_2 physisorption

Nitrogen physisorption measurements were performed as described in paragraph 2.2.4.

3.2.6 TEM

TEM imaging was performed on a Tecnia 12 (FEI) transmission electron microscope as described in paragraph 2.2.5.

3.2.7 Catalytic testing

Catalytic testing was performed in a continuous fixed-bed stainless steel reactor from Autoclave Engineers as described in paragraph 2.2.6.

An attempt to make the copper surface free after functionalisation with HMDS was done by reduction and re-oxidation of the catalyst. Reduction of the methylated catalyst took place at 250 °C under a flow H_2/N_2 (20:80 vol. %) of 100 mL/min. After flushing the catalyst for 1 hour at room temperature with N_2, re-32oxidation was started by flushing with a O_2/N_2 flow (5:95 vol. %) of 100 mL/min. The temperature was increased after 1 hour to 200 °C with 2 °C/min, where after the oxygen flow was changed to (15:85 vol. %). The catalyst was then cooled down and tested in a catalytic testing experiment on its methanol productivity.

Methyl groups were removed during a catalytic test to see if the productivity of the catalyst increased after the removal. After 20 hours of reaction the test was stopped and apparatus was cooled down to room temperature. The reduced catalysts were first passivated by a small leakage in the testing reactor where after it was transferred to a calcination reactor and where it underwent a heat treatment in an oxygen atmosphere as described in paragraph 3.2.4. The reaction was then started again as described in 2.2.6.

3.2.8 ICP analysis

The chemical composition of the catalyst before and after reaction is determined by Inductively Coupled Plasma (ICP) analysis at the Mikroanalytisches Laboratorium Kolbe (Mülheim an der Ruhr, Germany). They make use of an ICP-OES Perkin Elmer spectrometer.

3.2.9 TPR

TPR measurements were performed as described in paragraph 2.2.8.

3.2.10 XRD

X-ray diffractograms are recorded as described in paragraph 2.2.9.

3.2.11 DRIFTS

The functionalised catalysts were studied with DRIFTS as described in paragraph 2.2.10.

3.3 Results and discussion

3.3.1 Introducing methyl groups on the silica support

Two different methylated supports were made, one with trimethyl groups on the surface by using HMDS as precursor and one with single methyl groups by using MTMS as precursor. These supports were made as described in paragraph 3.2.3. We further refer to the methylated support with trimethyl groups as SS-$(CH_3)_3$ and to the support with single methyl groups as SS-CH_3. The extent of methylation of these supports was studied with N_2-physisorption, DRIFTS, TGA and elemental analysis. Textural properties of the supports are summarised in Table 3.1.

Table 3.1 Textural properties Stöber silica and methylated Stöber silica catalysts

	$S^{[a]}$ [m^2/g]	$V_{meso}^{[b]}$ [cm^3/g]
SS	101	0.58
SS-$(CH_3)_3^{[c]}$	81	0.51
SS-$CH_3^{[d]}$	82	0.49

[a] Surface area. [b] Mesopore volume (2-50 nm pores). [c] methylated catalyst prepared with HMDS. [d] methylated catalyst prepared with MTMS

When comparing the methylated silica to the bare support one can see that the surface area and mesopore volume decreases upon functionalisation. This indicates that the functionalisations ware successful. The presence of methyl groups on the surface of the spheres cause a slight increase in effective diameter of the spheres that will decrease the mesopore volume and will decrease the effective diameter surface area per gram [5].

DRIFTS measurements also indicated the methylation of the supports was successful. The obtained spectra can be seen in Figure 3.4.

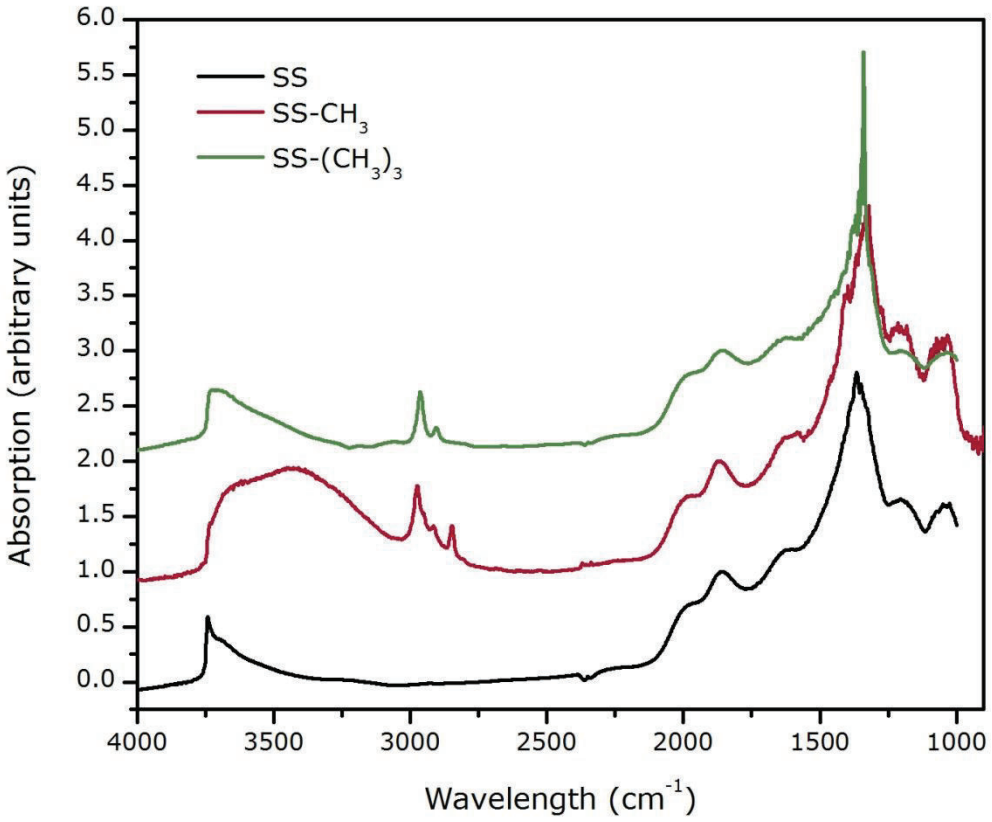

Figure 3.4 DRIFTS spectra of the bare support (SS) and the methylated supports (SS-CH_3, SS-$(CH_3)_3$)

All three spectra show characteristic vibrations of stretching modes of Si-O-Si and dangling modes of Si-O below 2000 cm^{-1} [6]. As explained in paragraph 2.3.1, free silanol groups can be seen with a sharp peak at 3745 cm^{-1} as is the case for the bare support [7,8]. Both the spectra of the functionalised catalysts do not contain this sharp peak, so the free silanol is absent in these supports as result of the functionalisation. However, in the spectrum of SS-$(CH_3)_3$ there is a broader peak visible around 3700 cm^{-1} due to hydrogen bonded silanol groups [7,8]. The spectrum of the SS-CH_3 looks different because it contains a broad peak ranging from 3700 cm^{-1} to 3200 cm^{-1}. This is resulting from OH vibrations from absorbed methanol that is formed during the functionalisation. This absorbed methanol also gives rice to the symmetric stretch vibration of C-H (νCH_{as}) of the methyl groups introduced during the functionalisation, at 2976 cm^{-1} and the symmetric stretch (νCH_s) around 2920 cm^{-1}. These peaks can be seen in both the spectra of the methylated sample.

Two extra peaks at 2954 cm^{-1} ($\nu_{as}CH_3$) and 2854 cm^{-1} (ν_sCH_3) can be distinguished in the spectra of SS-CH_3. These peaks and the broad peak between 3700 cm^{-1} to 3200 cm^{-1} are caused by absorption of methanol, that is formed during functionalisation [9,10]. In literature is described that methanol can be removed by evacuation at 200 ˚C, however, methanol can also form methoxy species on the silica surface and temperatures of 600 ˚C are needed to remove those species [10,11]. The presence of the broad band indicates that the SS-CH_3 contains methoxy species on the surface or that methanol is still present due to improper drying.

The chemical composition of the methylated supports was determined with elemental analysis and TGA. Results for the SS-$(CH_3)_3$ support is given in Table 3.2 and for the SS-CH_3 support is given in Table 3.3. The theoretical values are calculated with the Kiselev-Zhuravlev constant (4.6 OH/nm^2) and the assumptions that one HMDS molecule as well as one MTMS molecule reacts with one free silanol group on the silica surface.

Table 3.2 Chemical composition of the SS-$(CH_3)_3$ support

Element [wt %]	Theoretical monolayer[a]	ICP	TGA
C	2.7	0.7	0.8
H	0.7	0.5	0.2
N	-	0.1	-

[a] number based on the Kiselev-Zhuravlev constant (4.6 OH/nm^2) [12] and the assumption that one HMDS molecule reacts with one free silanol group

Table 3.3 Chemical composition of the SS-CH_3 support

Element [wt %]	Theoretical monolayer[a]	TGA
C	0.9	2.0
H	0.2	0.5

[a] number based on the Kiselev-Zhuravlev constant (4.6 OH/nm^2) [12] and the assumption that one MTMS molecule reacts with 1 free silanol groups.

From Table 3.2 can be seen that the carbon content in the support determined by element analysis and by TGA is much lower than the theoretical value. This can be attributed to the incomplete coverage of the surface due to steric hindrance of the methyl groups [13]. Since the DRIFTS spectrum of SS-$(CH_3)_3$ showed no vibrations of free silanol, we assume that all free silanols have reacted and that the surface still contains unreacted hydrogen bonded silanol groups.

The theoretical carbon and hydrogen contents of the SS-CH_3 are lower than the values determined with TGA. This can be caused by the fact that the MTMS molecules are cross linked with each other but not every molecule is bound a silanol group on the silica surface.

The methylated supports have a different behaviour in contact with water or ethanol than the non-functionalised Stöber silica spheres. This can be seen in Figure D 1 in appendix D. When non-functionalised silica spheres are brought into contact with water, they sink to the bottom. Methylated silica, on the other hand, stays on the water-air interface. Also the TEM images of methylated silica look different then non-functionalised silica spheres. The spheres are not directly in contact with each other and form an almost hexagonal packed structure.

3.3.2 The influence of the methyl groups on catalyst properties

3.3.2.1 The reduction temperature of copper

The influence of the methyl groups on the surface on the reduction temperature of the copper is studied with TPR. A catalyst that was made by copper deposition before methylation with HMDS as described in 3.2.3 is studied with TPR. The TPR profile of this catalyst and the TPR profile of a non-functionalised catalyst can be seen in Figure 3.5.

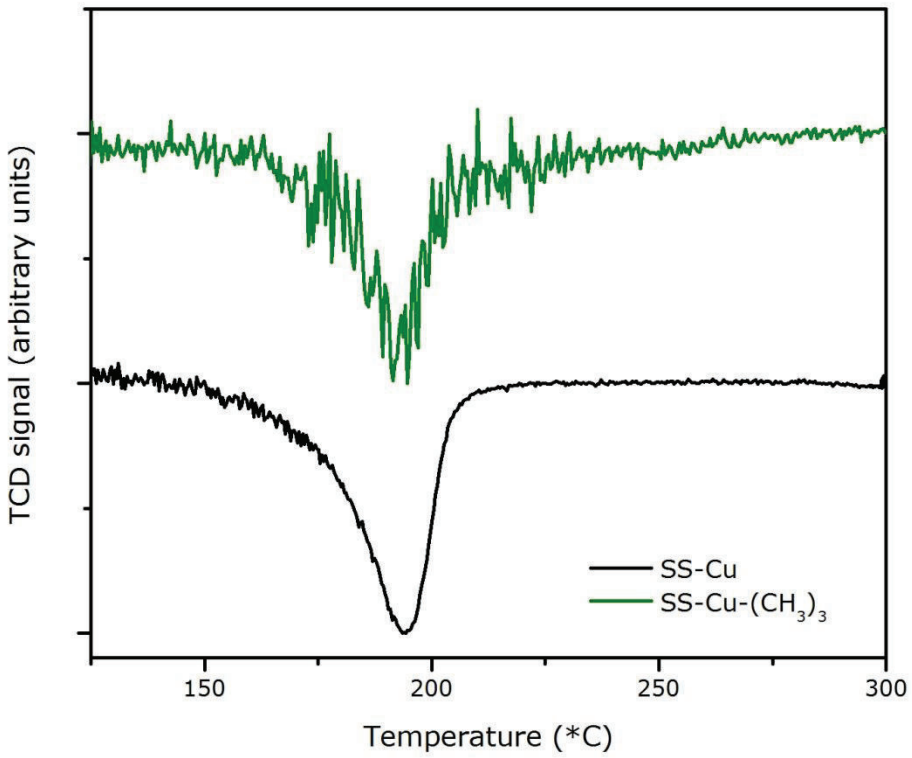

Figure 3.5 TPR profile of the SS-$(CH_3)_3$ support and the bare catalyst.

Both the profiles show a minimum at 190 ˚C, this shows that the presence of methyl groups on the support by functionalisation with HMDS did not influence the reduction temperature of the catalyst. Subsequently the catalyst was subjected to a catalytic test to study the influence of methylation on the catalytic performance.

3.3.2.2 The activity of the methylated catalyst

The catalytic performance for methanol synthesis of methylated catalysts was tested in a deactivation test of ±230 hours. The coming paragraphs will focus on the activity of the catalysts and in a later paragraph the deactivation of the catalysts will be discussed. An overview of catalyst properties such as loading and the initial methanol productivity during a catalytic test is given in Table 3.4. From these data one can see that the methylated catalyst, SS-Cu(N_2)-$(CH_3)_3$, has a very low initial productivity that is about $^1/_3$ of the activity of the bare catalyst, SS-Cu. There are several hypotheses on the reason of the differences in activity. For instance, it could be possible that active copper surface area is blocked due to overlap or coverage of methyl groups. Other reasons could be poisoning of copper by the ammonia that is released during functionalisation or that the silica support is assisting in the catalysis but is not able to do this anymore because of the functionalisation. The latter reason is likely not the reason since the amino functionalised catalyst, SS-NH_2-Cu(NO), was found to have an activity comparable to the non-functionalised catalyst.

The above described hypotheses on the lower catalysts activities were tested in different experiments. To test if the lower activity can be described to blockage or covering of copper surface area, a catalyst with bigger copper particles was made and tested and there was tried to make a catalyst in which the copper was deposited after methylation. A catalysts support was methylated in absence of the evolution of ammonia to test if ammonia could have a poisoning effect. And in the last experiment was tried create an empty copper surface by a thermal treatment in an oxygen atmosphere. The results of these experiments will be discussed now.

Table 3.4 Catalytic properties of several catalysts

Catalyst	Cu[a] [wt%]	Cu[b] ICP [wt %]	Cu[c] TPR [wt %]	d Cu[d] TEM [nm]	Methanol yield[e] [mol kg_{Cu}^{-1} h^{-1}]
SS-Cu	1.8	1.7	-	2.0	58
SS-Cu(N_2)-(CH_3)$_3$	1.8	1.7	1.2	2.4	22
SS-Cu(N_2)-(CH_3)$_3$-red-ox	1.8	-	-	-	14
SS-Cu(N_2)-CH_3	1.8	-	-	2.5	22
SS-Cu(NO)-(CH_3)$_3$	1.8	1.7	1.2	6.2	29
SS-Cu(NO)	1.8	-	1.2	6.2	37

a] based on amount of impregnation. [b] from ICP results [c] based on hydrogen consumption during TPR measurements [d] mean diameter of non reduced copper particles by TEM. [e] initial productivity of the catalysts.

Coverage or blockage of copper active surface area could be a reason for the lower activity of the catalyst. Methyl groups attached to the support surface could block some copper surface or methyl groups could be deposited on the copper itself. If methyl groups that are attached to the support block the copper surface, this would have a smaller effect on big copper particles than on smaller ones. Therefore a methylated catalysts with 6 nm copper particles (SS-Cu(NO)-(CH_3)$_3$) was prepared and its performance was compared to a non-methylated catalysts with 6 nm particles (SS-Cu(NO)). The catalysts with 6 nm particles were prepared by calcining the catalyst in NO instead of N_2. As is described in paragraph 2.3.2.1, the copper precursor decomposes via a different copper phase depending on the calcination atmosphere. This results in differences in particles sizes in different calcination atmospheres. The activity of the methylated and non-methylated catalyst with 6 nm copper particles are given in Table 3.4. One can see that the activity is 29 and 37 mol kg_{Cu}^{-1} h^{-1} respectively. So the methylated catalyst with larger copper particles is also less active than a non-methylated catalyst. This indicates that the lower activity can't be ascribed to blockage of active copper surface area by methyl groups that are present on the support.

The catalysts in Table 3.4 are made by depositing copper on the support surface prior to the methylation. It is therefore possible that methyl groups are deposited on the copper particles and block active surface area. This could make the catalyst less active. Therefore, preparing the catalyst the other way around, first by functionalisation and then copper deposition, as described in paragraph 2.2.3, is also tried. However, these methylated supports are not very wettable by water and that makes incipient wetness impregnation with the aqueous solution difficult. These catalyst supports were impregnation with a solution of copper nitrate in ethanol. A good copper dispersion of 2 á 3 nm particles copper particles was not obtained. Copper particles of with several sizes ranging from 2 nm to very large clumps of 20 nm were found.

An attempt to make the copper surface clean was done by reducing and oxidising the catalyst before it was tested. This is described in 3.2.7. The initial productivity of this catalyst, SS-Cu(N_2)-(CH_3)$_3$-redox, didn't improved in respect to the SS-Cu(N_2)-(CH_3)$_3$ catalyst.

In literature it was reported once that ammonia can be poisoning for copper nanoparticles. Therefore a catalyst support was methylated with MTMS since there is no ammonia evolution during functionalisation [14]. This catalyst, SS-Cu(N_2)-CH_3, has a similar initial methanol productivity as the SS-Cu(N_2)-(CH_3)$_3$ catalyst. Next to this elemental analysis of the SS-Cu(N_2)-(CH_3)$_3$ catalyst showed that there is almost no nitrogen present in the sample (Table 3.2). Because of these indications it is assumed that poisoning by ammonia is not the reason for the low productivity of methylated catalysts.

The last approach tried to regain the activity of the catalyst was by removing the methyl groups by a thermal treatment in an oxygen atmosphere. A methylated catalyst was tested on its initial activity, where after the reaction was stopped and the catalyst was subjected to a removal treatment in a O_2 atmosphere at 500 ˚C as described in paragraph 3.2.4. After this treatment the catalyst was tested again for its productivity. A reference catalyst that was not methylated was tested in the second reactor and was subjected to exactly the same treatment.

A DRIFTS spectrum was taken from the methylated catalyst that underwent a heat treated in an oxygen atmosphere, this spectrum can be seen in Figure 3.6. One can see that the sharp peak at 3745 cm-^{1} attributed to free silanol groups has appeared again and the intensity of the peak caused by CH_3 stretching vibrations around 2950 cm^{-1} has decreased drastically. However, since this vibration is still there, there will be some carbon left in the sample. This is also confirmed with TGA-MS, those results can be found in the appendix D Figure D 4.

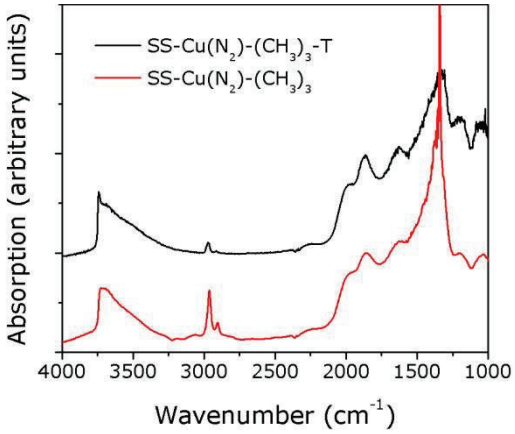

Figure 3.6 DRIFTS spectra of a metylated support [SS-CU(N_2)-(CH_3)$_3$] and the support after heat treatment at 500 ˚C in an oxygen atmosphere [SS-CU(N_2)-(CH_3)$_3$-T]

The behaviour of the heat treated methylated catalyst when it is brought on a water/air interface can be seen in Figure D 1 in the appendix. A non-functionalised catalyst has sunk to the bottom of the flask while a methylated catalyst stays on the water/air surface. The heat treated methylated catalyst sinks for the greatest part to the bottom and a small part is still on the water surface. Based on these observations and the DRIFTS spectra it is assumed the largest part of the methyl groups is removed by the heat treatment.

The productivities of the catalysts before and after the treatment are given in Table 3.5. The original productivity of the methylated catalyst, SS-Cu(N_2)-(CH_3)$_3$, is not even half of the activity of the bare catalyst, SS-Cu(N_2). After the heat treatment the productivity has not increased compared to the non-functionalised catalyst.

Table 3.5 Performance of the methylated and bare catalyst in methanol synthesis before and after thermal treatment

Methanol yield[a] [mol kg_{Cu}^{-1} h^{-1}]	SS-Cu(N_2)[b]	SS-Cu(N_2)-(CH_3)$_3$[c]
Original	54	29
After thermal treatment	59	34

[a] initial productivity of the catalyst. [b], [c] catalyst made from the same batch, functionalisation is the only difference.

Removal of the largest part of the methyl groups does not influence the productivity of the catalysts and DRIFTS results showed that there are still some methyl groups after heat treatment. It is possible that the copper surface is still decorated with those methyl groups or that the methyl groups are removed but silica, left over from the removed methyl groups, is decorating the surface.

3.3.2.3 Deactivation in methylated catalysts

The catalytic performance for methanol synthesis of methylated catalysts was tested in a deactivation test of ±230 hours. Data is plotted as the productivity normalised by the initial productivity versus the time-on-stream (TOS) in Figure 3.7. The original data points show a lot of scatter since the methylated catalyst is not so active, therefore a smoothed line is shown so that the deactivation trend is clearly visible.

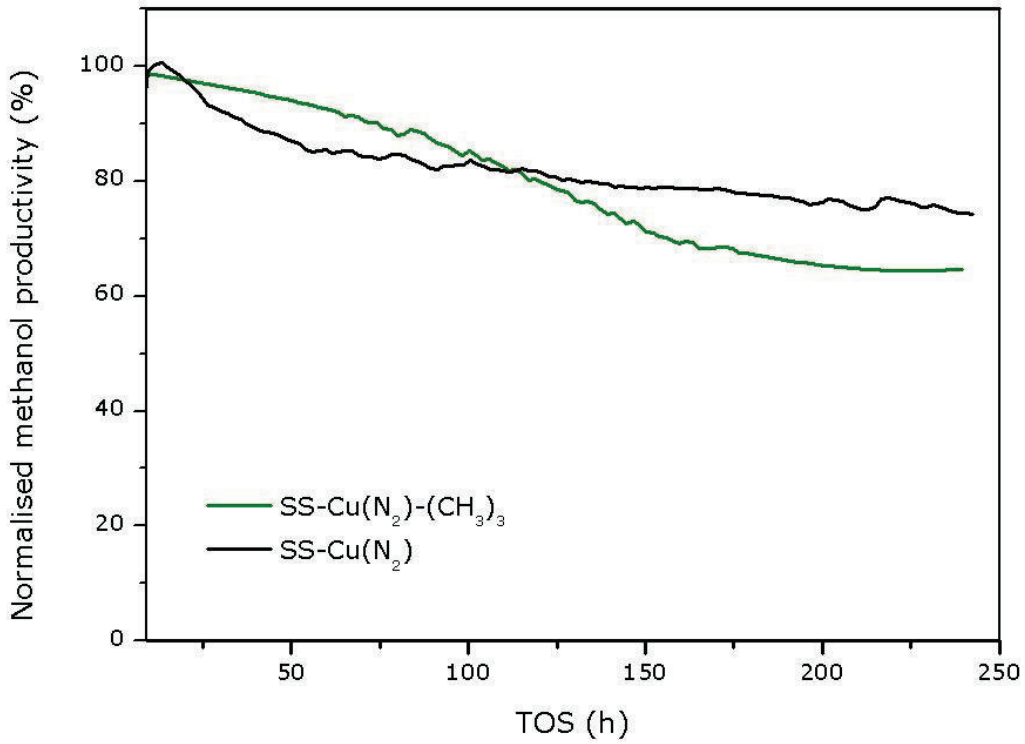

Figure 3.7 Results from deactivation tests a methylated catalyst plotted as normalised methanol productivity versus the time-on-stream.

A non-functionalised silica supported copper methanol synthesis catalyst typically deactivates with a fast decrease in productivity in the beginning that stabilises over time, as the SS-Cu(N_2) (black) does in Figure 3.7 [15]. The deactivation curve of the methylated catalyst (SS-Cu(N_2)-(CH_3)$_3$ (green) has a different shape than the curve a (SS-Cu(N_2) catalyst. There is only little productivity loss in the beginning but after 75 hours of operation the catalyst starts to lose productivity rapidly until it seems to stabilise again after 175 hours.

The drop in productivity of the catalysts is attributed to particle growth. Figure 3.8 shows the particle size distribution of the bare catalyst (b) and methylated catalyst (a) before and after the catalytic test. One can see that the copper particles in the methylated catalyst have grown a bit more than in a non-functionalised catalyst during reaction. As described above, the shape of the deactivation curve of the methylated catalyst is different than that of a bare Cu/SiO_2 catalyst. So the methyl groups seem to influence the Ostwald ripening process. As explained in paragraph 1.6.1.2, one can consider two different equilibriums in Ostwald ripening, that is the detachment of monomers from small particles and the attachment of the monomers to the larger particle (**A)** and the second equilibrium is the diffusion of monomers towards larger particles (**B**). The presence of the methyl groups seems to influence the rate of these steps. We can now, however, only speculate which steps are favoured or disfavoured. Possibly diffusion of hydrophilic copper monomers over the supports surface is favoured by the hydrophobic character of the support; the diffusion of these species can therefore go very quick. The formation of the monomers can also be influenced by the hydrophobic character off the support. Since it is thought that these monomers are hydrophilic it is likely that the formation is disfavoured by the hydrophobic character. However, the way the hydrophobic character of the support influences the particle growth exactly remains unknown.

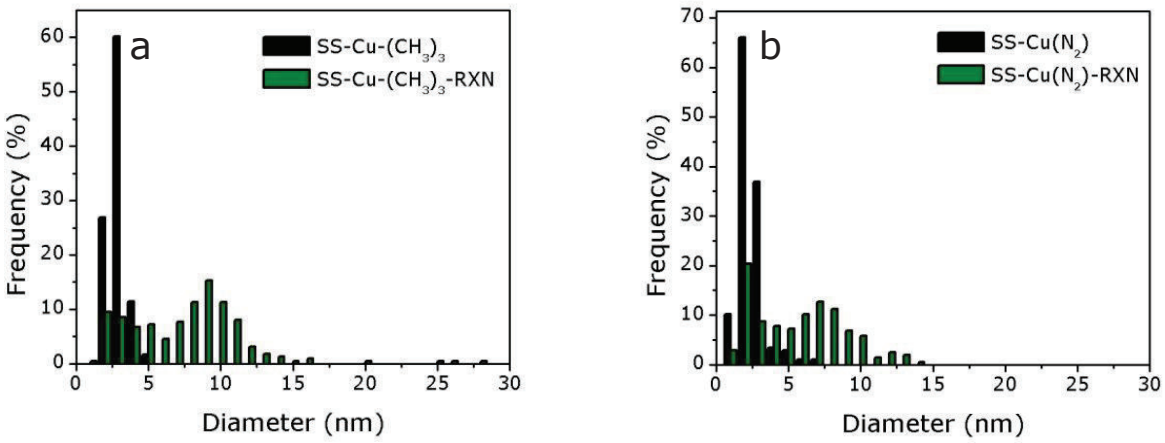

Figure 3.8 Comparison of copper particles sizes of the fresh and the spent catalyst derived from TEM images from [a] the SS-Cu-$(CH_3)_3$ catalyst and [b] the SS-Cu(N_2) catalyst.

3.3.2.4 Stability of the methyl groups during reaction

The methyl groups are organic groups. In the previous chapter the stability of the amino groups present on the support, was questioned. It could also be possible that the methylgroups can decompose during the methanol synthesis reaction since it takes place at 260 ˚C, 40 bar pressure and involves the generation of water in the reverse water gas shift reaction. Therefore DRIFTS, TGA-MS and elemental analysis were used to study the stability of the functionalised groups during reaction. The DRIFTS spectra of the methylated catalyst after reaction can be seen in Figure 3.9.

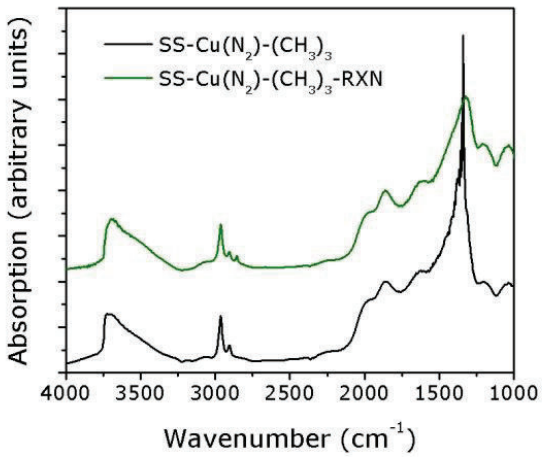

Figure 3.9 DRFITS spectra of the methylated catalyst before and after reaction

One can see that the DRIFTS spectra of the methylated catalyst before (black) and after (green) reaction look quite similar. They both show the characteristic broad peak of hydrogen bonded silanol around 3600 cm^{-1} and the methyl vibrations around 2950 cm^{-1}. However, the spectrum of the methylated catalyst after reaction exhibits three peaks around 2950 cm^{-1} and where the spectrum before reaction contains just two. Vibrations of absorbed or methoxy species are normally visible in that region but those species cause also a broad peak between 3700 cm^{-1} and 3200 cm^{-1} that is absent in the spectrum [9,11]. The extra peak can therefore not be attributed to absorbed methoxy species and the origin of the peak remains unclear. The spectrum of the catalyst after reaction does not contain the peak at 3745 cm^{-1} attributed to free silanol.

Elemental analysis shows no difference in the C/H ratio before and after reaction, as can be seen in Table 3.6. Although it should be mentioned that the SS-Cu-$(CH_3)_3$ is from a different batch than the catalyst that is tested. This explains why the catalyst before reaction has lower weight percentages then after. Likely this catalyst has a different degree of functionalisation. However, that the ratio between C and H does not change upon reaction indicates that the methyl groups are not decomposed. This is supported by the absence of the free silanol peak in the DRIFTS spectrum of the catalyst after reaction.

Table 3.6 Chemical composition of a methylated catalyst before and after reaction

Element[a] [wt %]	SS-Cu-$(CH_3)_3$[b]	SS-Cu-$(CH_3)_3$-RXN[c]
C	0.7	1.1
H	0.5	0.8
C/H ratio	1.4	1.4

[a] percentages obtained from element analysis (ICP). [b] direct after functionalisation of the catalyst. [c] after 230 hours of reaction for methanol synthesis. Note that the two catalysts come from a different batch, this explains the higher weight percentages after reaction

3.4 Conclusions

Methylation of the Stöber silica surface by a gas phase reaction with HMDS or a liquid phase reaction with MTMS led to a decrease in surface area of the support and pore volume. This indicates that these methylations were successful. Methylated supports were studied with DRIFTS, which showed the presence of CH_3 vibrations in both supports. Vibrations of the free silanol groups cannot be seen in the spectra, which indicate that the free silanol groups have reacted with the silane precursor. Hydrogen bonded silanol groups are on the other hand, still visible in the spectra. Probably these have not reacted. Methoxy species were found to be absorbed in the methylated catalyst made by liquid phase reaction with MTMS. ICP showed that the coverage of methyl groups in the support methylated with HMDS is lower than a theoretical monolayer, likely this is caused by the fact that hydrogen bonded silanol groups have not reacted with the silane.

Methylation of a Cu/SiO_2 catalyst does not change the reduction temperature of the copper but does change its deactivation profile when it is subjected to a catalytic test for $\pm$230 hours. Methyl groups seem to influence the steps involved in the deactivation process. The deactivation curve of methylated catalysts has a different shape than the deactivation curve of non-methylated catalysts. Methylated catalysts made by methylation after copper deposition are found to be less active than non–methylated catalysts. This is most likely caused by coverage of the active copper surface by the methyl groups.

The amount of carbon and hydrogen present in the catalysts does not change significantly during reaction and CH_3 vibrations are still visible in the DRIFTS spectrum, therefore is concluded that the methyl groups remain stable during reaction.

3.5 Outlook

The methylated catalyst, which is made by methylation of the silica surface after copper deposition, was found to be less active than non-methylated catalysts. This is attributed to a decrease in active surface area by coverage by the methyl groups. Copper surface area measurements are necessary to confirm this.

A deactivation curve with a very different shape than normal Cu/SiO_2 catalysts was obtained from a deactivation test of this catalyst, this is likely caused by favouring/disfavouring of steps involved in Ostwald ripening. An attempt to restore the activity of this catalyst is done by removing the methyl groups by thermal treatment in an oxygen atmosphere. The catalytic test was stopped when it turned out that removal of the methyl groups did not result in an increased activity. It would, however, be interesting to see if the same deactivation shape will be obtained. The same is true for the methylated sample made by a liquid phase reaction with MTMS. Only the initial activity was measured for this catalyst, it would, however, be interesting to

extend the test to see if the shape of the deactivation curve of this catalyst also deviates from that of a typical Cu/SiO_2 catalyst.

NRM spectroscopy could be useful to get to know more about the degree and way of binding of the methyl groups to the silica support.

3.6 References

[1] Z. Li, R.-H. Yoon, Thermodynamics of hydrophobic interaction between silica surfaces coated with octadecyltrichlorosilane., J. Colloid Interface Sci. 392 (2013) 369–75.

[2] M.L.N. Perdigoto, R.C. Martins, N. Rocha, M.J. Quina, L. Gando-Ferreira, R. Patrício, et al., Application of hydrophobic silica based aerogels and xerogels for removal of toxic organic compounds from aqueous solutions., J. Colloid Interface Sci. 380 (2012) 134–40.

[3] D.B. Rasmussen, T.V.W. Janssens, B. Temel, T. Bligaard, B. Hinnemann, S. Helveg, et al., The energies of formation and mobilities of Cu surface species on Cu and ZnO in methanol and water gas shift atmospheres studied by DFT, J. Catal. 293 (2012) 205–214.

[4] J. Fu, Q. He, R. Wang, B. Liu, B. Hu, Comparative study of phenol compounds adsorption on mesoporous sieves with different degrees of modification, Colloids Surfaces A Physicochem. Eng. Asp. 375 (2011) 136–140.

[5] M.C. Capel-Sanchez, L. Barrio, J.M. Campos-Martin, J.L.G. Fierro, Silylation and surface properties of chemically grafted hydrophobic silica., J. Colloid Interface Sci. 277 (2004) 146–53.

[6] J. Pires, M. Pinto, J. Estella, J.C. Echeverría, Characterization of the hydrophobicity of mesoporous silicas and clays with silica pillars by water adsorption and DRIFT, J. Colloid Interface Sci. 317 (2008) 206–13.

[7] V.N. Panchenko, V. a. Pozimenko, E. a. Paukshtis, V. a. Zakharov, IR spectroscopic study of the basicity of aminated silica gels, Russ. J. Inorg. Chem. 54 (2009) 1798–1803.

[8] T. Kovalchuk, H. Sfihi, L. Kostenko, V. Zaitsev, J. Fraissard, Preparation, structure and thermal stability of onium- and amino-functionalized silicas for the use as catalysts supports, J. Colloid Interface Sci. 302 (2006) 214–29.

[9] R.R. Sever, R. Alcala, J. a Dumesic, T.W. Root, Vapor-phase silylation of MCM-41 and Ti-MCM-41, Microporous Mesoporous Mater. 66 (2003) 53–67.

[10] M.A. Natal-Santiago, J.A. Dumesic, Microcalorimetric , FTIR , and DFT Studies of the Adsorption of Methanol , Ethanol , and 2 , 2 , 2-Trifluoroethanol on Silica, J. Catal. 175 (1998) 252–268.

[11] C. Morterra, M.J.D. Low, Collapse of the methoxy groups of methylated aerosil, J. Phys. Chem. 73 (1969) 321–326.

[12] L.T. Zhuravlev, The surface chemistry of amorphous silica. Zhuravlev model, Colloids Surfaces A Physicochem. Eng. Asp. 173 (2000) 1–38.

[13] S. Haukka, A. Roots, The Reaction of Hexamethyldisilazane and Subsequent Oxidation of Trimethylsilyl Groups on Silica Studied, (1994) 1695–1703.

[14] J.B. Hansen, P.E.H. Nielsen, Methanol synthesis, in: Handb. Heterog. Catal., 2008: pp. 2920–2948.

[15] G. Prieto, J. Zečević, H. Friedrich, K.P. de Jong, P.E. de Jongh, Towards stable catalysts by controlling collective properties of supported metal nanoparticles, Nat. Mater. (2012) 1–6.

4 The grafting of metal oxides on a silica support and its influence on catalysts properties

4.1 Introduction

Supports that are used in heterogeneous catalyst are often metal oxides. One of the roles of these supports is to stabilise the metal nanoparticles and prevent them from growing. Interaction that the metal has with the support (MSI) plays therein a pivotal role and is unique for each system [1]. The main goal of this part of the study is to determine the stability of copper particles on different supports while maintaining the same supports morphology. This will be done by grafting a layer of different metal oxides namely alumina, zinc oxide or titania on the surface of a Cu/SiO_2 methanol synthesis catalyst. Grafting a layer of metal oxides on the silica support will change the interaction of the copper particles with the support.

The $Cu/ZnO/Al_2O_3$ catalyst that is used in industrial operations contains between 10-30% zinc oxide and 5–10% alumina as is discussed in paragraph 1.5. Since the commercial catalyst contains zinc oxide and alumina, grafting with these oxides is interesting. Alumina is referred to as the structural promoter in the catalyst [2,3]. However, the actual nature of this promotion effect is only poorly understood. Alumina is also known to exhibit Brønsted acidity, a grafted layer of alumina on silica will therefore raise the acidic properties of the support [4,5].

Zinc oxide in known to improve the life time by acting as a physical barrier between the copper nanoparticle keeping the particles in a dispersed state [5–9]. In addition to this, the presence of zinc oxide results in an increase in activity of the industrial applied catalyst. Some reseachgroups attribute this promoting effect to a synergy between copper and zinc [7–10]. It is interesting to see if such promotion or stabilising effects are also present in a Cu/SiO_2 catalyst with a grafted layer of zinc oxide.

Grafting titania on silica surfaces is found to affect the catalytic behaviour of a Rh/SiO_2 catalyst significantly [11]. This was attributed to the capability of titania to keep the rhodium particles in a highly reduced and dispersed state. That can probably be explained by the strong metal-support interaction (SMSI) titania exhibits [4]. Titania is also more acidic then silica and a grafting layer of titania will also raise the acidity of the supports surface. The SMSI effect of titiania can also be present in a monolayer of titania and this could be able to influence the stability of the copper particles.

Metal oxides can be introduced on a silica support material by using different methods. It can be done by the use of metal-acetate ($M\text{-}(O_2CMe)_2$) precursors, metal alkoxides or metalchlorides [12–17]. Since chlorides are poisons for copper based catalysts, the method involving chlorides is avoided. Alumnia and titania are introduced by using metal alkoxides (aluminium isopropoxide and titania *tert*-butoxide) and zinc oxide is introduced by using zinc acetate as precursor. The degree of metal oxides introduced was studied with energy dispersive x-ray (EDX) analysis performed on an electron microscope. Textural properties were studied with N_2-physisoportion, the reduction behaviour with TPR and the catalytic performance and deactivation of the catalyst in a test for methanol synthesis for 230 hours. TEM and XRD were used to study the copper particle size.

4.2 Experimental

4.2.1 Synthesis of the Stöber silica support

The Stöber silica support is synthesised as described in paragraph 2.2.1.

4.2.2 Grafting procedures

The grafting procedures are performed under an inert nitrogen atmosphere by using standard Schlenk techniques to prevent the presence of water. The precursor will undergo self hydrolysis upon contact with water and this will result in metal oxide particles which will lead to a non uniform metal oxide distribution. The different grafting procedures used are described below.

Grafting with alumina- This procedure is based on a method that is described by Mokaya *et al.* [13]. Stöber silica (1 g) was dried in a Schlenk under vacuum at 120 ˚C for 120 minutes. An aluminum isopropoxide (Al(O-iPr)$_3$) [Acros Organics, 99.99% for analysis] solution of 0.356g Al(O-iPr)$_3$ in dry hexane (40 mL) (dried 3 days over activated molsieves of size 5) was prepared. The entire solution was added to the Schlenk with dried Stöber silica and this was stirred continuously at 70 rpm. Stirring was stopped after 75 minutes and the mixture was filtered over a Schlenk filter. The filtrate was washed with dry hexane. Ethanol [Interchemica 100 %] was used to remove the powder from the filter, where after the ethanol was removed with the rotary evaporator.

The obtained support was dried at 120 ºC under a N_2 flow (40 mL/min). The alumina precursor was then decomposed by heat treatment at 550 ºC for 1 hour under a N_2 flow (40 mL/min). The heating rate used was 2 ºC/min.

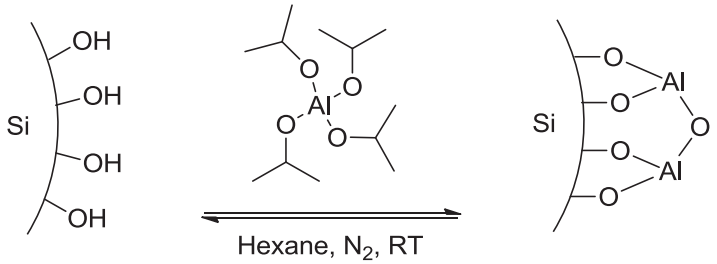

Figure 4.1 Schematic presentation of the grafting of silica with aluminium isopropoxide

Grafting with titania- This procedure is based on a method that is described by Srinivasan *et al.* [14,15]. Prior to the grafting The silica support (1g) was dried in a Schlenk under vacuum at 120 ºC for 120 minutes. Dry THF (30 mL) (column dried at a mBraun MB SPS-80) was added to the Schlenk containing the silica. This was stirred continuously. Titanium tertbutoxide (0.45 mL) [Acros Organics, 99%] was taken from a glovebox and quickly transferred in a syringe, this was then dropwise added to the silica mixture. The mixture was stirred for 25 minutes where after it was filtered using a Schlenk filter. It was washed 3x with THF [Interchemica 100 %], subsequently the silica was removed from the filter with EtOH. The EtOH was subsequently removed with the rotary evaporator.

The obtained support was dried at 120 ºC under a N_2 flow (40 mL/min). The titania precursor was then decomposed by heat treatment at 500 ºC for 1 hour under a O_2/N_2 flow (25 vol. %) (40 mL/min). The heating rate used was 2 ºC/min.

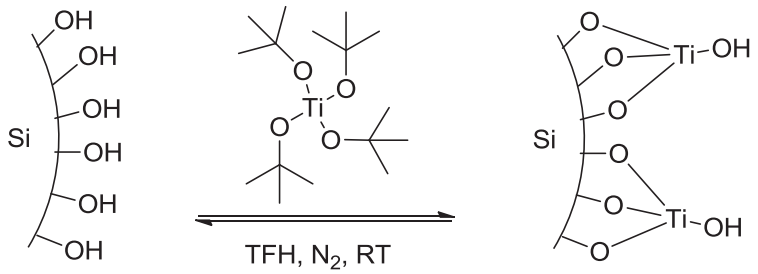

Figure 4.2 Schematic presentation of the grafting of silica with titanium tert-butoxide

Grafting with zinc- This procedure is based on a method that is described by Ryoo *et al*. [12]. The silica support (1g) was dried in a dried in a Schlenk under vacuum at 120 ºC for 120 minutes prior to the grafting. Zinc acetate (0.339 g) [Aldrich, 99.99%] was put in a Schlenk and brought under vacuum. Dry EtOH (20 mL) (dried 3 days over activated molsieves 5) was added both to the Schlenk with the silica support as well as to the Schlenk with the zinc precursor. The mixed zinc precursor suspension was dropwise added to the stirring silica support with a syringe and this was stirred for 75 minutes. The mixture was then filtered over a Schlenk filter and washed 2x with dry EtOH. EtOH was used to remove the powder from the filter and was then removed again with the rotary evaporator.

The obtained support was dried at 120 ºC under a N_2 flow (40 mL/min). The zinc precursor was then decomposed by heat treatment at 500 ºC for 1 hour under a O_2/N_2 flow (25 vol. %) (40 mL/min). The heating rate used was 2 ºC/min.

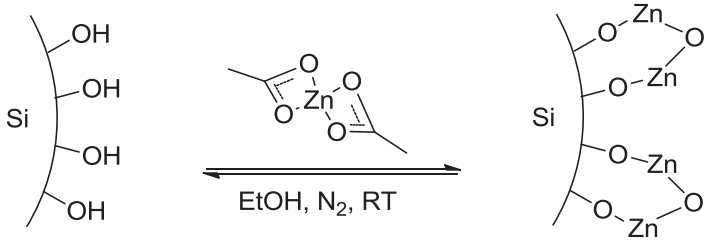

Figure 4.3 Schematic presentation of the grafting of silica with zinc acetate

4.2.3 Impregnation

The grafted supports were impregnated as described in paragraph 2.2.3. The pore volumes that were used were measured with N_2-physisorption.

4.2.4 N_2 physisorption

Nitrogen physisorption measurements were performed as described in paragraph 2.2.4.

4.2.5 TEM

The catalysts were studied with electron microscopy as described in paragraph 2.2.5.

4.2.6 EDX spectroscopy

EDX spectroscopy was performed on a Technai 20FEG (FEI) electron microscope equipped with a field emission gun with an EDAX Super Ultra Thin Window (SUTW) EDS detector and processed with a Tecnai Imaging and Analysis software (TIA). HAADF images were also recorded using this equipment. Samples were prepared by crushing followed by sonification in ethanol. A few droplets were supplied on a carbon coated Ni TEM grid (Agar 162 200 Mesh Ni). The results, given in Table 4.1 are based on a single EDX measurement.

4.2.7 Catalytic testing

Deactivation of the catalyst was tested in a catalytic test as described in paragraph 2.2.6. During catalytic testing of the three catalysts there were issues with the setup which resulted in a pressure drop in the reactor. Therefore there are sometimes gaps of several hours in the deactivation curves of these catalysts.

4.2.8 ICP analysis

The chemical compositions of the grafted catalysts were determined as described in paragraph 2.2.7.

4.2.9 TPR

TPR measurements were performed as described in paragraph 2.2.8.

4.2.10 XRD

Diffractrograms were recorded as described in paragraph 2.2.9

4.3 Results and discussion

4.3.1 Extent of grafting on the silica support

Alumina, titania and zinc oxide were introduced on the surface of the Stöber silica support as described in paragraph 4.2.2. The extent of grafting of metal oxides on the Stöber silica support was investigated with EDX spectroscopy, element analysis and nitrogen physisorption. The EDX analysis and element analysis results are summarised in Table 4.1. The value for the theoretical monolayer of metal oxides is based on the Kiselev-Zhuravlev constant (4.6 OH/nm^2) [18] and the assumption that one aluminium isopropoxide molecule, one titanium-*tert*butoxide molecule and one molecule of zinc acetate reacts with respectively 2, 3 and 2 silanol groups on the silica surface. TEM images made from the different grafted supports can be seen in Figure 4.4. The alumina grafted support is further referred to as SS-Al_2O_3, the titania grafted support as SS-TiO_2 and the zinc oxide grafted supports as SS-ZnO.

Table 4.1 Chemical composition of the with metal oxides grafted silica spheres in wt % metal

	Theoretical monolayer [wt %][a,b]	ICP [wt %][b]	EDX analysis [wt %][b,c]
SS-Al_2O_3	0.9	1.7	3.1
SS-TiO_2	1.0	1.4	1.0
SS-ZnO	4.2	0.4	-

[a] number based on the Kiselev-Zhuravlev constant (4.6 OH/nm^2) [18] and the assumption that one alumium isopropoxide molecule, one titanium *tert*-butoxide molecule and one molecule zinc acetate reacts with respectively 2, 3 and 2 silanol groups. [b] weight percentage of the metal itself [c] 'bulk' value determined on a very large amount of spheres as can be seen in appendix D Figure D 3.

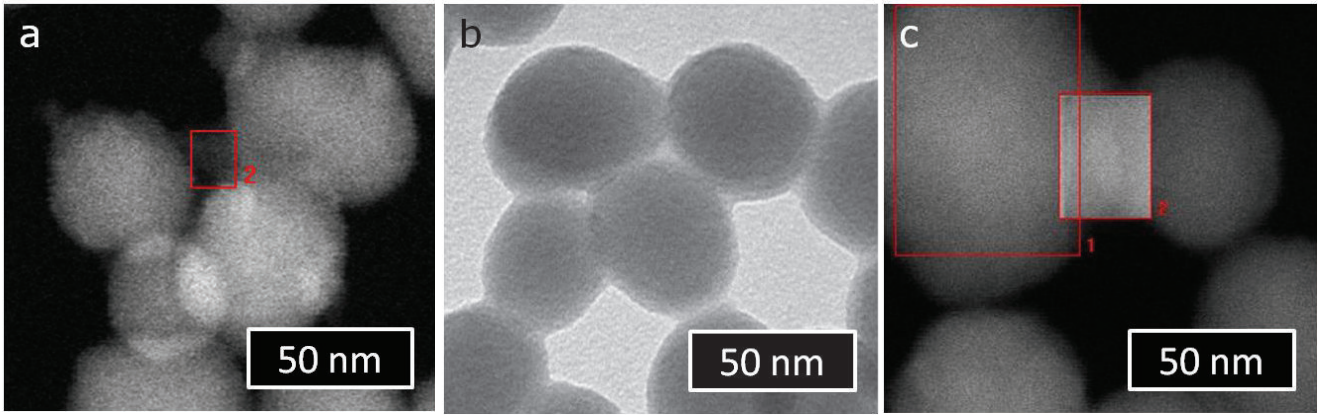

Figure 4.4 [a] HAADF image of SS-Al_2O_3. Section 2 contains a typical lump that is connected to a silica sphere that consists of aluminium. [b] BF TEM image of SS-TiO_2. Titanium is found to be equally present on all the spheres [c] HAADF image of SS-ZnO. In either section 1 and 2 is no zinc present. Some spheres have grown as the upper left one have grown during the grafting procedure.

From Table 4.1 one can see that the aluminia grafted catalyst has higher aluminium content than a theoretical monolayer according to ICP as well as EDX analysis. TEM studies showed that most of the alumina was present as lumps connected to the support, as can be seen in Figure 4.4a. This explains the higher aluminum content than in a theoretical monolayer. Aluminium was not detected on the silica spheres itself, however it could be possible that it is present on the spheres but in such a low amount that it could not be detected.

The amount of titanium determined with ICP and EDX analysis is comparable to the value of a theoretical monolayer. EDX spectroscopy showed that the amount of titanium on in a 'bulk' analysis on a very large amount of spheres is similar to the value on single spheres. Therefore it is assumed that titanium is present as a monolayer on the silica support.

Zinc was not detected with EDX spectroscopy in the zinc grafted sample. However, ICP showed that there is a small amount of zinc present in the sample. This amount is smaller than a theoretical monolayer. It is possible that zinc is present in small zinc oxide particles which could not be located and detected with EDX. Another possibility is that zinc is present in very small amounts on the surface and could not be detected. The grafted support did contain some larger silica spheres, as can be seen in the upper left corner of Figure 4.4c, which probably have grown during the grafting procedure. The zinc oxide precursor was not fully soluble in dried ethanol and formed a suspension. This could be the reason why formation of a monolayer of zinc oxide was not successful.

Nitrogen physisorption was used to study textural properties of grafted supports, results are summarised in Table 4.2.

Table 4.2 Textural properties of the SS support and the metal oxide grafted SS support

	$S^{[a]}$ [m^2/g]	$V_{meso}^{[b]}$ [cm^3/g]
SS	101	0.58
SS-Al_2O_3	84	0.57
SS-TiO_2	103	0.60
SS-ZnO	91	0.59

[a] Surface area. [b] Mesopore volume

The mesopore volumes of the grafted support are similar to the volume of the normal support. The surface area of the titania grafted catalyst is quite the same as for the normal support. Textural properties did this not change much by the titania grafting. A monolayer of titania would increase the size of the spheres only with a few Angström. Monolayer coverage is therefore possible although the textural properties didn't change much. The surface areas of the alumina and zinc oxide grafted catalyst decreased with respect to the normal catalyst, the pore volume stayed however, almost the same. The change in surface area shows that things have changed upon grafting. It could be possible that the surface becomes less rough upon functionalisation and that this caused the decrease in surface area. Some of the silica spheres in the zinc grafted sample had grown after the grafting procedure. This will also result in different textural properties.

The grafted supports were synthesised in larger amounts and they were impregnated with a copper nitrate solution for the deposition copper on the supports. The location of the copper particles on the supports was studied with EDX spectroscopy. We further refer to the copper containing alumina grafted catalyst as SS-Al_2O_3-Cu, to the copper containing titania grafted catalyst as SS-TiO_2-Cu and to the copper containing zinc oxide grafted catalyst as SS-ZnO-Cu.

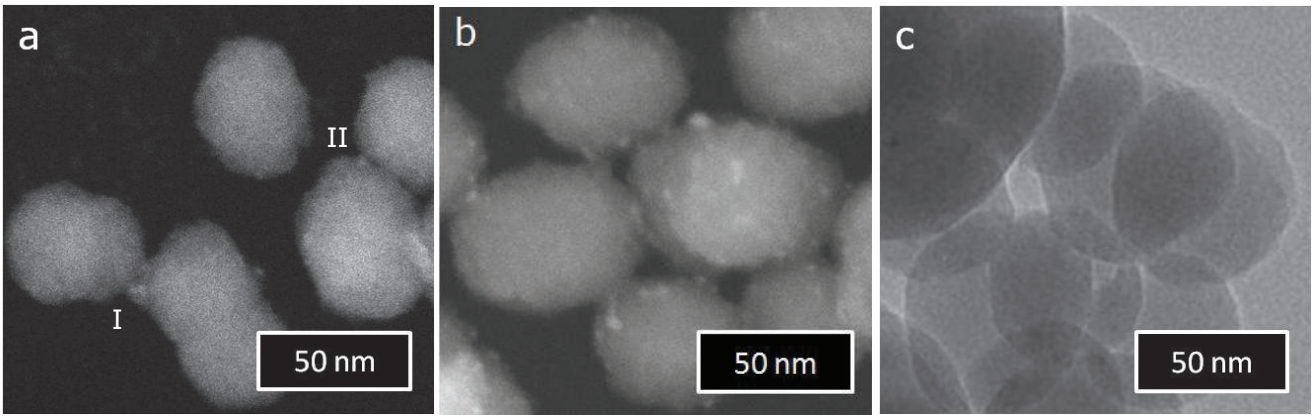

Figure 4.5 [a] HAADF TEM image of SS-Al_2O_3-Cu. The copper particles are located on the support itself (II) as well as on the aluminum containing lumps next to the spheres as is the case at I. [b] HAADF TEM image of SS-TiO_2-Cu. The copper particles seem to be well distributed over the support. [c} BF TEM image of SS-ZnO-Cu. Copper particles are visible on the support but note that it is more difficult to see in BF mode.

Copper particles on the alumina grafted support were found on the bare silica as well as on the alumina lumps next to the spheres. This can be seen in Figure 4.5a, a copper particle is located on an alumina lump at I and on the silica spheres at II. So, it seems like the copper particles have remarkably no preference for either one of the oxides. Perhaps this is caused by the presence of very small amounts of alumina on the bare support. The copper particle sizes were comparable to the size of copper particles on a bare silica support. A bare support contains copper particles of 2 á 3 nm. Particles around this size were also found on the titania grafted support, as can be seen in Figure 4.5b. The zinc oxide grafted support, Figure 4.5c, contains also copper particle of 2 á 3 nm in size. This is what was expected since no zinc was detected on the spheres with EDX spectroscopy. The TEM image of the zinc grafted support includes a silica sphere that is larger than 30 nm. More of such large spheres are seen in the sample. Growth of the spheres has happened during the grafting procedure.

4.3.2 Influences of the metal oxides on the properties of the catalyst

4.3.2.1 The reduction temperature of copper

The influence of the presence of the different metal oxides on the surface of the catalyst on the reduction behaviour of the catalyst was studied with TPR. These results can be seen in Figure 4.6. To the bare non-grafted catalysts is referred to as SS-Cu.

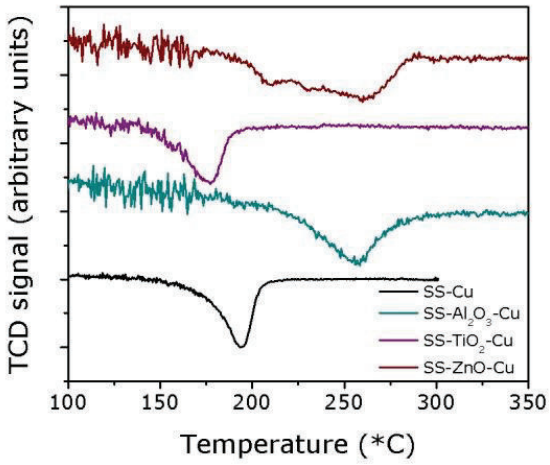

Figure 4.6 TPR profiles of the with metal oxides grafted catalyst and the bare catalyst

The peak in the profile of the SS-Al_2O_3-Cu has shifted to higher temperature compared to the bare catalyst. So the presence of alumina influences the reduction behaviour of the catalyst. EDX spectroscopy showed that copper particles are present on the bare support as well as on the alumina lumps, as described in paragraph 4.3.1. Therefore there were two reduction peaks expected, one from copper on bare silica and one from copper on alumina. However the profile contains, only one reduction peak. It is possible that a very low amount of alumina present on the silica and that this influences the reduction behaviour of the copper particles that are located on the silica.

Reduction in the titania grafted catalyst takes place at lower temperatures than the bare catalyst, the presence of titania clearly influence the reduction behaviour. When the reduction behaviour of a Cu/SiO_2 catalyst is compared to a Cu/TiO_2 catalyst one sees also a shift towards lower temperatures [19]. This can be explained by the strong metal-support interaction properties of titania.

The TPR profile of the zinc oxide grafted catalyst shows a very different reduction pattern compared to the other catalysts. Reduction starts at higher temperatures than the bare catalyst but the pattern seems to contain multiple peaks resulting in a very broad reduction profile. Multiple peaks cannot be explained by reduction of zinc oxide itself since that takes place at higher temperatures [20]. It is possible that the zinc oxide itself takes up some hydrogen, without being reduced or that there are several classes of copper with a different environment, each class reducing at a slightly different temperature.

The shift in reduction temperature for each grafted catalyst indicates a difference in metal-support interaction between the grafted catalysts. Reduction of the titania grafted catalyst takes place at lower temperatures, attributed to the stronger metal support interaction of copper with the titania grafted support. Reduction in the alumina and zinc oxide grafted catalysts takes place at higher temperature. This indicates a smaller metal-support interaction of the copper with the grafted supports. A difference is the metal-support interaction is expected to lead to a difference in catalysts activity and in deactivation of the catalyst.

4.3.2.2 The activity of the grafted catalysts

In order to test the catalytic performance of the grafted catalysts and the stability of copper, the catalysts were subjected to a catalytic test to test their productivity in methanol synthesis for $\pm$ 230 hours. Results are given in Table 4.3. The activity and the selectivity of the catalysts will be discussed first. The deactivation of the catalysts will be discussed in the next paragraph.

Table 4.3 Catalytic properties of the with metal oxides grafted catalysts

Catalyst	Cu[a] [wt%]	Cu[b] ICP [wt %]	Cu[c] TPR [wt %]	d Cu[d] TEM [nm]	CO + CO_2 conversion[e] [mol kg_{Cu}^{-1} h^{-1}]	Selectivity [f] [MeOH:DME]	$k_{D,2}$[g] [10^{-3} h^{-1}]
SS-Cu	1.8	-	-	2.0	58	100 : 0	15.4± 0.7
SS-Al_2O_3-Cu	1.6	1.6	1.1	2.1	48	70 : 30	20.7±5.1
SS-TiO_2-Cu	1.8	1.8	1.7	3.1	38	90 : 10	20.2±1.6[h] 12.6± 0.5[i]
SS-ZnO-Cu	1.9	1.3	1.1	2.2	61	100 : 0	21.0±0.4

[a] based on amount of impregnation. [b] from ICP results [c] based on hydrogen consumption during TPR measurements [d] mean diameter of non reduced copper particles by TEM. [e] initial CO + CO_2 conversion of the catalyst. [f] Selectivity of the catalysts for methanol and DME. [g] deactivation rate constant defined by fitting a second order general power law equation. [h] initial deactivation rate of the first 40 hours. [i] deactivation constant after 30 hours of operation.

In Table 4.3 can be seen that the initial productivity of the alumina grafted catalyst SS-Al_2O_3-Cu is a little bit lower than the bare catalyst SS-Cu. This could be caused by partial coverage of copper by alumina resulting from a strong interaction of copper with alumina. Copper surface area measurements are needed to verify this. Next to methanol, also dimethyl ether (DME) was generated in the catalytic test by the dehydration of methanol. The dehydration is caused by the acidic properties of the alumina present [21]. The ratio between methanol and DME is 70:30. That is lower than typical one-pot copper based DME synthesis catalysts [22].

The activity of the titanium grafted catalysts is also lower than that of the bare catalysts. This could be a result of coverage of the copper particles by titania die to the strong SMI properties of titania. The deactivation curve of this catalysts hints that coverage of copper with titania also takes place during the catalytic test. This will be discussed more detailed in the next paragraph. DME is also produced in the test of the titania grafted catalyst, This is caused by acidic properties of titania but since titania is less acidic then alumina, the methanol:DME ratio is lower, 90:10.

The initial productivity of the zinc oxide grafted sample, SS-ZnO-Cu, is comparable to the bare catalyst. So there is probably no promoting effect of zinc present in this catalyst. This could be caused by the very low amount of zinc oxide present in the catalyst. However, the presence of zinc oxide did have its influence on the reduction temperature.

4.3.2.3 Deactivation of the grafted catalysts

The data obtained from the catalytic test plotted as the normalised productivity versus the time on stream can be seen in Figure 4.7.

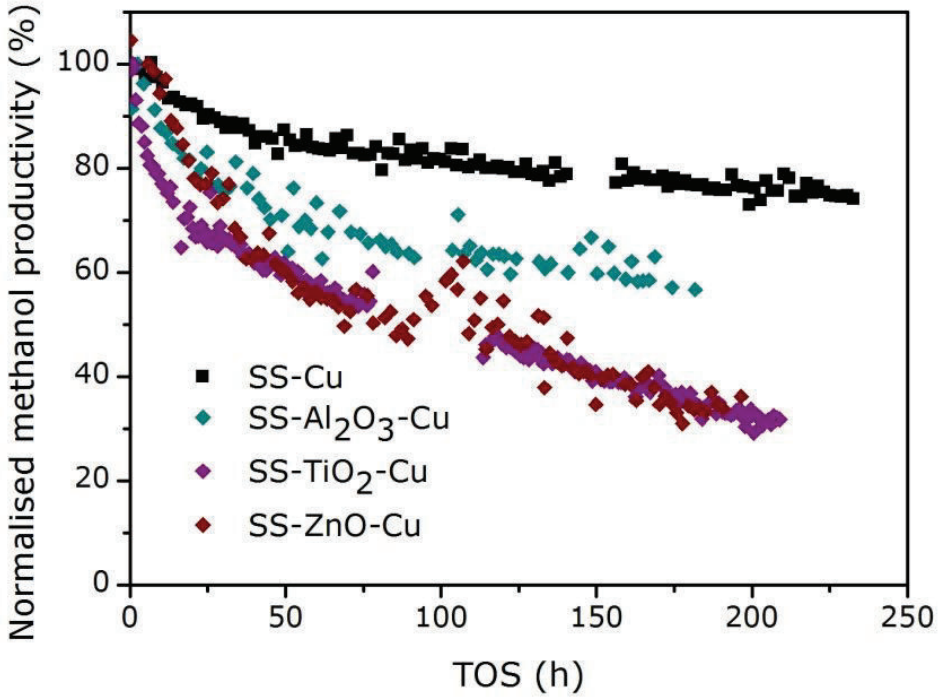

Figure 4.7 Results from deactivation tests of the metal oxide grafted catalysts plotted as normalised methanol productivity versus the time on stream

If one compares the deactivation curves of all three the metal oxide grafted catalyst with the non-grafted catalysts, one can see that the grafted catalysts show all a much faster drop in productivity than the bare catalyst. Catalyst deactivation constants are derived from these curves using a general power law equation as described in paragraph 2.3.3, this and other catalyst properties are summarised in Table 4.3. The linear deactivation fits can be found in appendix Error! Reference source not found..

The bare catalyst, SS-Cu, has a deactivation behaviour as found before for a copper supported on silica catalyst [23]. Its deactivation constant is defined as $15.4 \pm 0.7\ 10^{-3}\ h^{-1}$. In Table 4.3 one can see that the metal oxide grafted catalysts have a higher deactivation rate constant and deactivate faster. The deactivation rate of the alumina grafted catalyst is $20.7 \pm 5.1\ 10^{-3}\ h^{-1}$. The deactivation is most likely caused by particle growth since the particles have grown after reaction, as can be seen in Figure 4.8b. It is not clear what specifically causes the decrease in stability of this grafted support compared to the non-grafted support.

The deactivation rate constant of the titania grafted catalyst in the first ~30 hours is different and higher than after 40 hours, as can be seen in appendix Figure B 2. This indicates that there is a fast and initial productivity loss where after the catalyst becomes more stable and deactivates with a much lower rate. A common problem in titania supported catalysts is the metal coverage by titania caused by the SMSI properties of titania [24]. The fast productivity loss in the catalyst is likely an SMSI effect, so titania partially covers the copper particles and thereby decreases the active surface area. The deactivation rate constant after the fast initial deactivation is smaller than for the bare catalyst and in Figure 4.8c one can see that the particles have not grown much during catalysis. Therefore it seems like that the titania, when it is present on the copper particles, provides some stabilisation to the particles. The initial activity of the catalyst is lower than the bare catalyst; this is attributed to blockage of active surface area by titania already before reaction.

The zinc oxide grafted catalyst exhibited a similar as the bare catalyst. A promoting effect of zinc oxide was not found. The deactivation behaviour of the catalyst is different than the bare catalyst. The catalyst deactivates faster and has a higher deactivation constant. This could have something to do with the increased size of some

Stöber silica spheres in the zinc oxide grafted catalyst as can be seen in Figure 4.5c. Zinc oxide is known to have stabilising effect in the industrial applied catalysts. It would therefore be unlikely that the presence of zinc oxide in the catalyst decreases the stability of the catalysts.

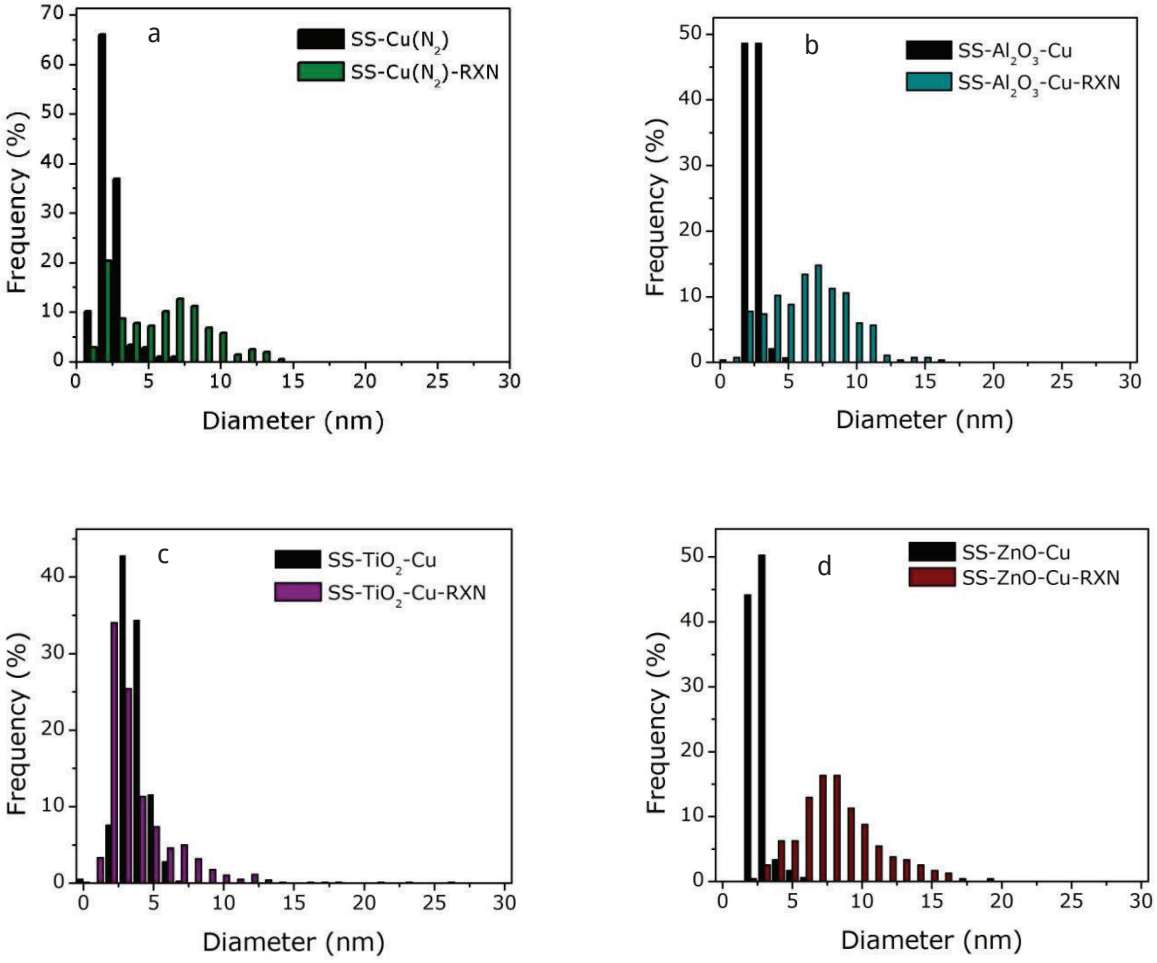

Figure 4.8 Comparison of copper particles sizes of the fresh and the spent catalyst derived from TEM images from [a] the bare catalyst SS-Cu, [b] the with alumina grafted catalyst, [c] the with titania grafted catalyst and [d] with the zinc oxide grafted catalyst.

4.4 Conclusions

The interaction that the support has with the metal particles is important in providing the particles stability. Grafting of metal oxides on a support will change the support properties and can influence the stability of the metal particles. Grafting of Stöber silica spheres with titanium *tert*-butoxide has successfully led to the formation of a titania monolayer as determined by EDX spectroscopy and N_2 physisorption. Grafting with aluminium isopropoxide resulted in lumps of alumina next to the silica spheres as shown by EDX spectroscopy. The zinc acetate grafted support contained some zinc as shown by elemental analysis but could not be located in the sample.

Copper deposited by incipient wetness impregnation on the grafted supports led to the formation of 2 á 3 nm copper particles equally distributed over the support. Remarkable is that the copper particles seem to have no preference for the alumina lumps or the bare silica spheres in with alumina grafted sample. TPR measurement showed that the reduction temperature of copper is influenced by the presence of alumina. Since there is only one reduction peak of copper visible in the profile, it is suggested that there is also some alumina present on

the bare silica spheres, although this could not be detected with EDX spectroscopy. The reduction temperature of the titania grafted catalysts has shifted to lower temperatures, which can be explained by the SMSI effects of titania. Also the reduction temperature of the zinc oxide grafted catalyst shows a shift. This profile consists, however, not of a single reduction peak but of a broad peak with three peaks in it.

The alumina and titania grafted catalysts are, due to the acidic properties of the grafting layer, single step DME synthesis catalyst with methanol:DME ratio of 70:30 and 90:10 respectively. Both were less active than a non functionalised catalyst. This difference in activity for the titania grafted catalyst is attributed to coverage of copper by titania caused by the SMSI effect of titania which occurs in the first 40 hours in a catalytic test. Coverage of titania provides stability to the copper particles and the particles do not grow during the test. The zinc grafted sample exhibits an initial productivity that is comparable to a bare catalyst, so there is no promoting effect of zinc oxide present. The catalyst does deactivate faster than a bare catalyst, this could be caused by textural changes of the support upon grafting. The alumina grafted catalyst shows also faster deactivation than the bare catalyst.

4.5 Outlook

Monolayer formation of alumina and zinc oxide on Stöber silica spheres has not been successful yet. A different way of grafting should be found, by for example using different reaction temperatures, time or precursors. The formation of alumina lumps is likely caused by the presence of water in the reaction mixture. The alumina and the zinc oxide precursors that were used were not stored in the glovebox. Storing these chemicals in the glovebox and transferring without exposure to air to a Schlenk could be tried to optimise the grafting procedures. Performing the grafting reaction in a glovebox could also be a good option to prevent the formation of metal oxide lumps that are formed by self hydrolysis of the precursor.

Binding of the metal oxides with the support could be studied with DRIFTS. This is not done in this study because the windows of the DRIFTS cell should be replaced by different ones when measuring below 1000 cm^{-1}, where Si-O-M vibrations can be found [25].

TPR measurements showed that grafting with different metal oxides changes the temperature of reduction of the copper particles. It was suggested that alumina and zinc oxide were present in very small amounts on the supports surface and could therefore influenced the reduction temperature of copper. Since EDX spectroscopy was not sensitive enough to detect very low amounts of metal oxides on the silica surface, a different method should be used to investigate if these oxides are present. Another interesting topic is to investigate how the presence of other metal oxides can influence the reduction temperature of copper.

The titania grafted catalyst showed very fast deactivation in the first 40 hours of reaction, this was attributed to the coverage of the copper particles with titania because of its strong SMSI effect. Copper surface area measurements are necessary to verify this conclusion. These measurements are recommended for all the grafted supports, before and after grafting and after the catalytic test.

4.6 References

[1] R. Ouyang, J.-X. Liu, W.-X. Li, Atomistic theory of Ostwald ripening and disintegration of supported metal particles under reaction conditions, J. Am. Chem. Soc. 135 (2013) 1760–71.

[2] M. Behrens, S. Zander, P. Kurr, N. Jacobsen, J. Senker, G. Koch, et al., Performance improvement of nanocatalysts by promoter-induced defects in the support material: methanol synthesis over Cu/ZnO:Al., J. Am. Chem. Soc. 135 (2013) 6061–8.

[3] M. V Twigg, M.S. Spencer, Deactivation of copper metal catalysts for methanol decomposition , methanol steam reforming and methanol synthesis, Top. Catal. 22 (2003) 191–203.

[4] H. Rojas, G. Borda, P. Reyes, J.J. Martínez, J. Valencia, J.L.G. Fierro, Citral hydrogenation over Ir/TiO2 and Ir/TiO2/SiO2 catalysts, Catal. Today. 133-135 (2008) 699–705.

[5] M.S. Spencer, The role of zinc oxide in Cu / ZnO catalysts for methanol synthesis and the water – gas shift reaction, Top. Catal. 8 (1999) 259–266.

[6] M. Behrens, F. Studt, I. Kasatkin, S. Kühl, M. Hävecker, F. Abild-Pedersen, et al., The active site of methanol synthesis over Cu/ZnO/Al2O3 industrial catalysts., Science (80-.). 336 (2012) 893–7.

[7] T. Fujitani, J. Nakamura, The effect of ZnO in methanol synthesis catalysts on Cu dispersion and the specific activity, Catal. Letters. 56 (1998) 119–124.

[8] J.B. Hansen, P.E.H. Nielsen, Methanol synthesis, in: Handb. Heterog. Catal., 2008: pp. 2920–2948.

[9] S. Zander, E.L. Kunkes, M.E. Schuster, J. Schumann, G. Weinberg, D. Teschner, et al., The role of the oxide component in the development of copper composite catalysts for methanol synthesis, Angew. Chemie (International Ed.). 52 (2013) 6536–40.

[10] Y. Kanai, T. Watanabe, T. Fujitani, T. Uchijima, J. Nakamura, The synergy between Cu and ZnO in methanol synthesis catalysts, Catal. Letters. 38 (1996) 157–163.

[11] C. Mateospedrero, C. Cellier, P. Ruiz, Rh/Ti–SiO2 catalysts prepared by organic grafting: A novel class of catalysts towards hydrogen production by partial oxidation of methane, Catal. Today. 117 (2006) 362–368.

[12] R. Ryoo, S. Jun, J.M. Kim, M.J. Kim, Generalised route to the preparation of mesoporous metallosilicates via post-synthetic metal implantation, 41 (1997) 2225–2226.

[13] R. Mokaya, Ultrastable Mesoporous Aluminosilicates by Grafting Routes., Angew. Chem. Int. Ed. Engl. 38 (1999) 2930–2934.

[14] S. Srinivasan, A. Datye, M. Hampden-Smith, I.E. Wachs, G. Deo, J.M. Jehng, et al., The formation of titanium oxide monolayer coatings on silica surfaces, J. Catal. 131 (1991) 260–275.

[15] a. Hanprasopwattana, S. Srinivasan, a. G. Sault, a. K. Datye, Titania Coatings on Monodisperse Silica Spheres (Characterization Using 2-Propanol Dehydration and TEM), Langmuir. 12 (1996) 3173–3179.

[16] K. Schrijnemakers, N.R.E.N. Impens, E.F. Vansant, Deposition of a Titania Coating on Silica by Means of the Chemical Surface Coating †, Langmuir. 15 (1999) 5807–5813.

[17] A. Zukal, H. Siklova, J. Cejka, Grafting of Alumina on SBA-15: Effect of Surface Roughness, Langmuir. (2008) 9837–9842.

[18] L.T. Zhuravlev, The surface chemistry of amorphous silica. Zhuravlev model, Colloids Surfaces A Physicochem. Eng. Asp. 173 (2000) 1–38.

[19] F.S. Delk, A. Vavere, Anomalous Metal-Support Interactions in Cu / TiOs Catalysts, J. Catal. 85 (1984) 380–388.

[20] M. Liang, W. Kang, K. Xie, Comparison of reduction behavior of Fe2O3, ZnO and ZnFe2O4 by TPR technique, J. Nat. Gas Chem. 18 (2009) 110–113.

[21] S.-M. Kim, Y.-J. Lee, J.W. Bae, H.S. Potdar, K.-W. Jun, Synthesis and characterization of a highly active alumina catalyst for methanol dehydration to dimethyl ether, Appl. Catal. A Gen. 348 (2008) 113–120.

[22] G. Qi, J. Fei, X. Zheng, Z. Hou, DME SYNTHESIS FROM CO/H 2 OVER Cu-Mn/γ-Al 2 O 3 CATALYST Go, 73 (2001) 245–256.

[23] G. Prieto, J. Zečević, H. Friedrich, K.P. de Jong, P.E. de Jongh, Towards stable catalysts by controlling collective properties of supported metal nanoparticles, Nat. Mater. (2012) 1–6.

[24] M. Cargnello, P. Fornasiero, R.J. Gorte, Opportunities for Tailoring Catalytic Properties Through Metal-Support Interactions, Catal. Letters. 142 (2012) 1043–1048.

[25] M. Cozzolino, M. Di Serio, R. Tesser, E. Santacesaria, Grafting of titanium alkoxides on high-surface SiO2 support: An advanced technique for the preparation of nanostructured TiO2/SiO2 catalysts, Appl. Catal. A Gen. 325 (2007) 256–262.

5 Conclusions & outlook

World's crude oil resources are depleting due to the ever growing demand for crude oil based fuels. Therefore one should look for alternative fuels and use the oil that is left in the world as efficient as possible. The use and productions of methanol can play an important role herein. Natural gas which is released during oil drilling processes is often flared. It can, however, also be used for the generation of methanol, which can in its turn be used as a fuel and can be used as feedstock to replace all crude oil based feedstock now used. Catalysis plays a pivotal role in the generation of methanol. To make methanol generation as efficient as possible we should keep optimising these catalysts to find the most active and sustainable as possible. The life time of the $Cu/ZnO/Al_2O_3$ catalyst used in methanol synthesis is limited by growth of the copper particles, which is the active phase in this catalyst. The interaction of the copper with the support material plays an important role in this growth. This study has focussed on the influence of the chemical nature of the support on the growth of copper particles in a methanol synthesis catalyst. A model Cu/SiO_2 catalyst was used for this study. The chemical nature of the support was changed by the introduction of amino or methyl groups and alumina, titania or zinc oxide on the silica surface.

Amino groups act as anchoring sites for the copper precursor and can thereby facilitate the formation of very tiny copper particles or atomic copper species on the supports surface. This was observed when the functionalised support was impregnated by an aqueous copper nitrate solution and was then calcined in N_2. The catalyst was found to be not very active and has a very low deactivation over time. To investigate size dependence activity of this catalyst it would be interesting to determine the copper particle size by for example EXAFS.

A copper catalyst made by incipient wetness impregnation of an amino groups functionalised support followed by calcination in NO, was found to deactivate only very little compared to a non-functionalised catalyst. Likely this is caused by the favourable interaction between the amino groups and the copper particles and copper monomers that will suppress the diffusion of these monomers towards larger particles. DRIFTS and ICP measurement pointed out that the amino groups remain stable during methanol synthesis reaction at least for $\pm$230 hours of reaction. The use of amino groups to stabilise copper particles has not been reported in literature before and could play a potential role in increasing the life time of catalysts.

Functionalised catalysts made by introduction of the amino or methyl groups after copper deposition were found to be a lot less active than non-functionalised catalyst. This is attributed to coverage of active surface area by the amino or methyl groups. Even after removal of functional groups the activity is not restored because the silica of the functional group is still present on the copper surface. However, copper surface area measurements should be carried out to verify this.

The presence of methyl groups on the surface did not change the reduction temperature of the copper particles. On the other hand the deactivation curve obtained in a catalytic test differs a lot from that obtained from a non-functionalised catalyst. Therefore, it seems like the presence of methyl groups influences the steps the deactivation mechanism in the catalyst.

Introduction of alumina, titania or zinc oxide on the silica surface changes the reduction temperature of the copper particles, when deposited on the support after grafting. The alumina grafted sample consisted of the silica spheres with aluminium containing lumps next to these spheres. Since copper seemed to have no preference for the silica spheres or the alumina lumps and only one reduction peak is observed in TPR measurements, it is assumed that there is also alumina present on the 'bare' silica spheres although this could not be detected with EDX spectroscopy. An equal loading of titanium was found on the silica spheres as in the bulk in the with titania grafted catalyst by making use of EDX spectroscopy. Based on these results and ICP results it is assumed that monolayer formation of titania was successful. The titania grafting resulted in a reduction temperature shift of copper towards lower temperature, which can be explained by the strong metal-support interaction that titania exhibits. EDX spectroscopy and ICP showed the presence of zinc in the zinc oxide grafted sample, the location of the zinc oxide could, however, not be determined. The TPR profile of the with zinc oxide grafted catalyst consisted of multiple peaks that form one broad one. It remains unclear

why multiple peaks appear, possibly zinc oxide takes up some hydrogen itself or the there are several classes of copper present with a different environment, each class reducing at a slightly different temperature.

The alumina and titania grafted catalysts are, due to the acidic properties of the grafting layer, single step DME synthesis catalyst with methanol: DME ratio of 70:30 and 90:10 respectively. The activity of the titania grafted catalyst is significantly lower that the non-functionalised catalyst. This is attributed to the strong metal support interaction of titania which results in coverage of the copper particles and therefore the active surface area decreases. To proof this, copper surface area measurements would again be very useful. The titania does stabilise the copper during reaction since the particles have not grown. Deactivation is than not caused by particle growth but by a decrease in active surface area by migration of titania on the copper. The zinc grafted sample exhibits an initial productivity that is comparable to a bare catalyst, so there is no promoting effect of zinc oxide present. The catalyst does deactivate faster than a bare catalyst which could be caused morphological changes during grafting. The alumina grafted catalyst shows also faster deactivation than the bare catalyst.

Overall we can conclude that changing the chemical nature of the support surface causes significant changes in the stability of catalysts. The effect is unique for each modified system and no trend is observed in this. The use of alkoxy silanes to introduce organic functional groups on the silica surface was found to be very effective. Whereas grafting of metal oxides with metal alkoxides or metal acetate precursors is found to be difficult since the precursors tend to undergo self hydrolysis in the presence of water.

6 Acknowledgements

I would like to thank all the people who contributed to the work that was done for this research. First of all and foremost I would like to thank Roy! I have definitely made a really good choice by deciding to do my master thesis under your supervision. You're always willing to offer all the help that is needed, I could ask you all my questions, you gave me the freedom to make decisions for the project, you involved me in the group and you're always in for a 'gezellig kletspraatje'! Thanks a lot! ☺

I'm very glad I could perform my master's thesis in this researchgroup, I would like to thank Krijn de Jong for offering me this opportunity! The discussions with you and Roy always resulted in new ideas and gave the right direction to the project. Thanks a lot for your interest and input in the project.

Hans Meeldijk performed the EDX measurements of the grafted samples for me. I really enjoyed these microscopy sessions! Peter taught me how to use the DRIFTS setup, Fouad helped me with the outcome of these measurements. Thanks! Also I want to thank Fernando, thank you for sharing your knowledge about functionalisation with aminogroups with me.

I would also like to thank Gonzalo and Selvedin for N_2-physisorption measurements and Korneel and Thomas E. for TPR measurements. Further I would like all the people within the synthesis gas team, Petra de Jong, Gonzalo, Peter, Arjan and all the others. Thank you for your interest in my project and the advice you gave me in the groupmeetings.

At last I would like to thank everybody in the research group! Thank you all for including me in the group, I really enjoyed my time here and the chats with you all in the lab or during lunch.

Appendix

A

Particle growth in Cu/SiO_2 catalysts

Earlier studies in this researchgroup on the deactivation behaviour of Cu/SiO_2 catalysts strongly suggest that particle growth in Cu/SiO_2 catalysts takes place via Ostwald ripening. These results are obtained by and copied from Roy van den Berg. Some of the results that indicate this mechanism of particle growth will be discussed underneath.

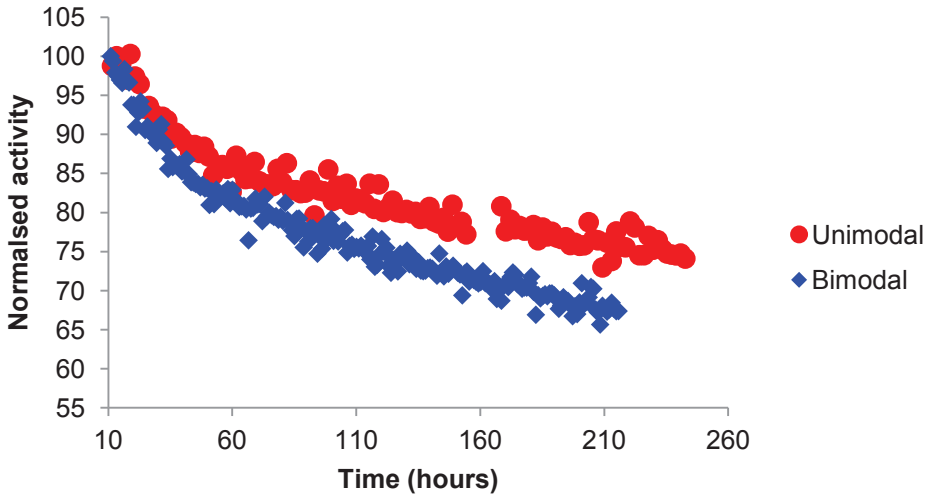

Figure A 1 Deactivation plot of two Cu/SiO_2 catalysts with a unimodal (red) and a bimodal (blue) size distribution of the copper particles.

In Figure A 1 one can see the deactivation plot of two Cu/SiO_2 catalysts with a unimodal (red) or bimodal (blue) copper particle size distribution. The catalyst with bimodal copper particles loses more activity than the catalysts with unimodal copper particles while on stream. This is an indication that particle growth happens via Ostwald ripening, a bimodal size distribution would result in a big monomer concentration differences around the particles, which would lead to a higher monomer flux towards larger particles.

Next to this, the decrease in activity of the catalysts was found to be independent on the inter particle spacing. In Figure A 2 is a deactivation plot visible of two Cu/SiO_2 catalysts with a different particle loading. The catalyst with the lower copper loading, 0.9 wt% (red), has a larger interparticle spacing than the higher loaded catalyst, 1.8 wt% (blue). The catalysts lose a similar amount of activity in the deactivation test so interparticle spacing seems not to influence that deactivation of the catalysts. This supports the idea that deactivation takes place via Ostwald ripening and not via sintering.

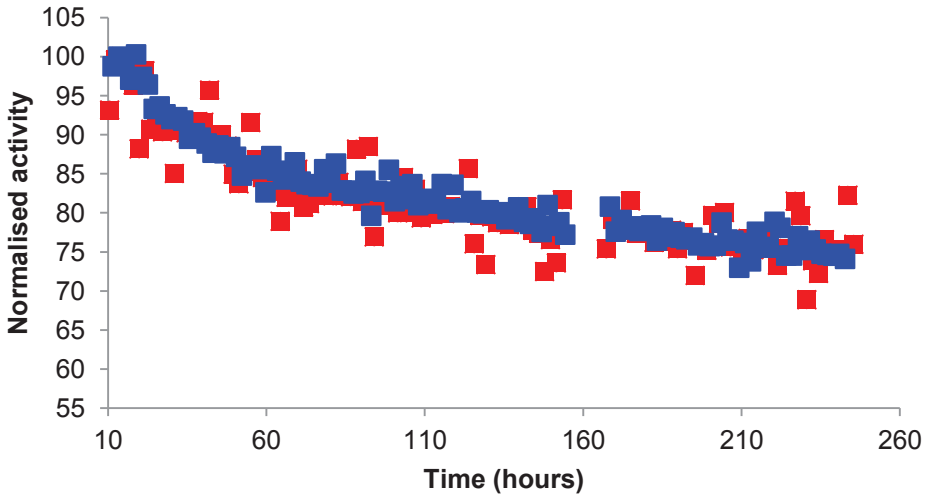

Figure A 2 Deactivation plot of two Cu/SiO_2 catalysts with a copper loading of 0.9 wt% (red) and of 1.7 wt% (blue)

There is also a difference in deactivation observed when silica supports are used with different morphological properties. In Figure A 3 once can see the deactivation plots of copper supported on Stöber silica spheres (red) and on SBA15 (blue). The copper particle size and surface coverage is the same for both catalysts.

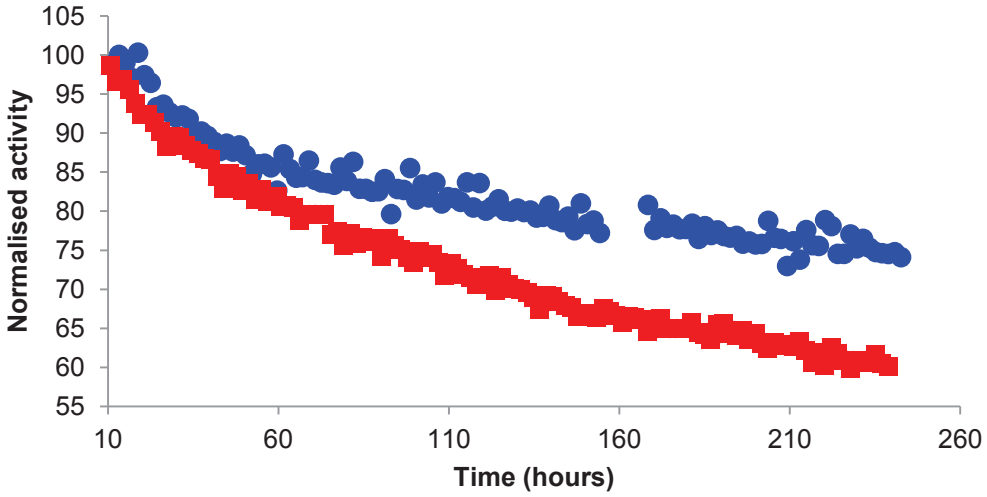

Figure A 3 Deactivation plot of two Cu/SiO_2 catalyst on different supports. One catalyst consists of copper particles supported on Stöber silica (blue) and the other one on SBA15 (blue).

The clear difference in deactivation behavior indicates that the deactivation mechanism is influenced by the structure of the support. If deactivation takes place via Ostwald ripening, it is likely that diffusion therefore takes place over the surface of the support.

Also comparison of the particle size distribution of the fresh and spent catalysts indicates that Ostwald ripening takes place. The bigger particles will grow in the expense of smaller once during Ostwald ripening and that is also what is observed for these catalysts as can be seen in Figure A 4.

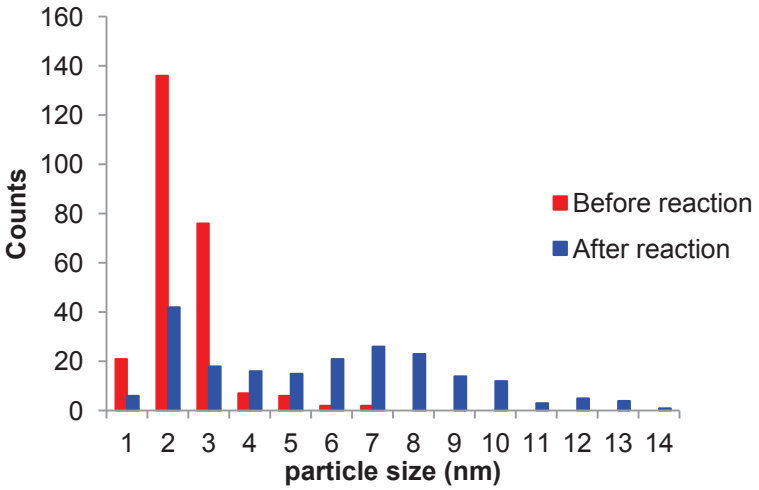

Figure A 4 The particle size distribution of a fresh (red) and spent (blue) Cu/SiO_2 catalyst.

B

Deactivation fits for the different catalysts

For determination of the deactivation constants of the catalysts, the productivity was fitted as a function of time on stream to a general power law equation. The obtained plots for the amino functionalized catalysts and the metal oxide grafted catalysts are shown in Figure B 1 and Figure B 2. The fits were made by Origin but unfortunately it is not possible to show the fit in the graphs. An overview of the determined deactivation constants are given in Table B 1. Two deactivation constants are determined for the SS-TiO_2-Cu catalyst since the slope of the fit during the first 30 hours is much steeper than after this time.

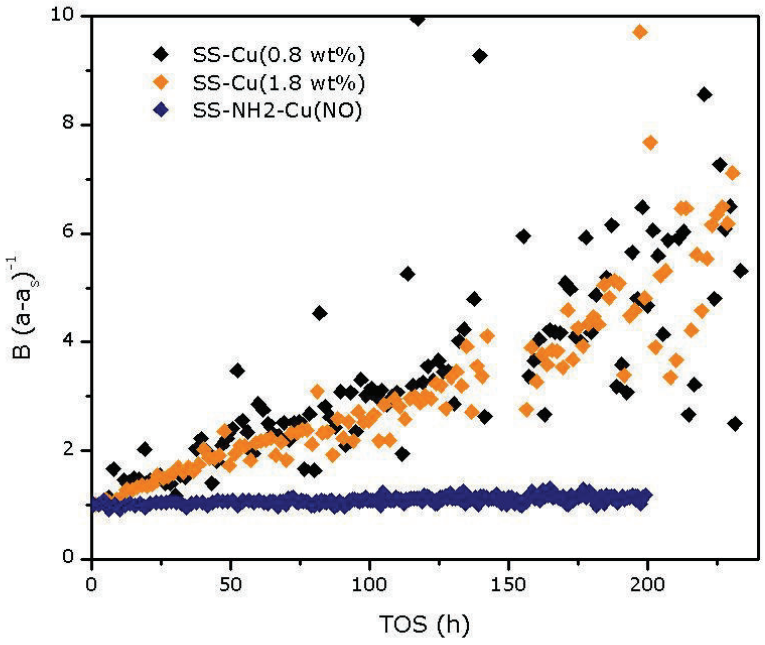

Figure B 1 Results from deactivation tests of several catalyst plotted as a linear form of a second order (*n*=2) general power law equation. The deactivation constants k_D are determined by the slope of the fits.

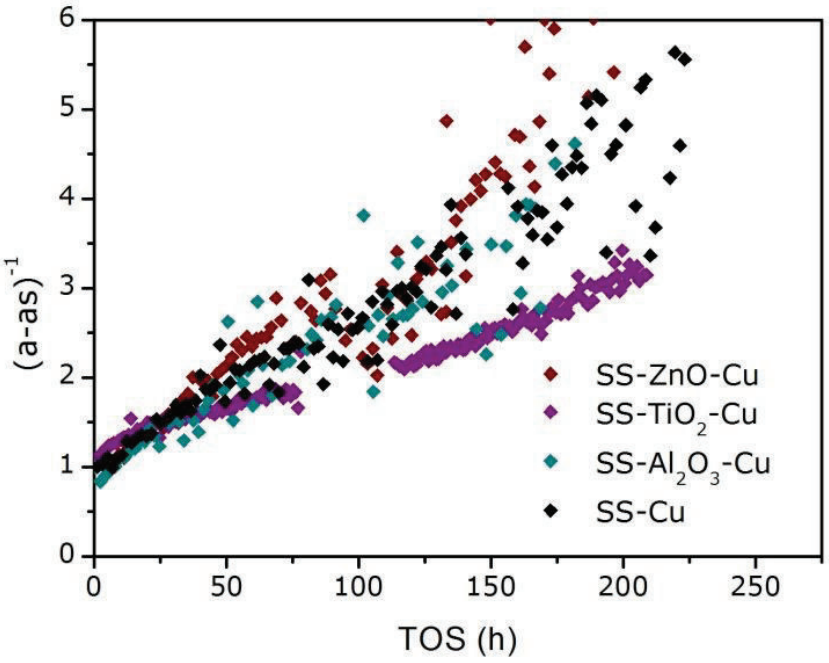

Figure B 2 Results from deactivation tests of several catalyst plotted as a linear form of a second order (*n*=2) general power law equation. The deactivation constants k_D are determined by the slope of the fits.

Table B 1 Overview of catalyst properties and the determined deactivation constants.

Catalyst	Cu[a] [wt%]	Cu[b] ICP [wt %]	Cu[c] TPR [wt %]	d Cu[d] TEM [nm]	CO + CO_2 conversion[e] [mol kg_{Cu}^{-1} h^{-1}]	$k_{D,2}$[g] [10^{-3} h^{-1}]
SS-Cu	0.8	-	-	1.9	70	19.8±0.4
SS-Cu	1.8	-	-	2.0	58	15.4± 0.7
SS-NH_2-Cu(NO)	0.8	-	0.83	2.6	68	1.1±0.3
SS-Al_2O_3-Cu	1.6	1.6	1.1	2.1	48	20.7±5.1
SS-TiO_2-Cu	1.8	1.8	1.7	3.1	38	20.2±1.6[h] 12.6± 0.5[i]
SS-ZnO-Cu	1.9	1.3	1.1	2.2	61	21.0±0.4

C
TGA results

TGA was used to determine the amount of functional groups present on the catalysts. The spectra obtained for the amino functionalised support (SS-NH_2) and the methylated support (only SS-$(CH_3)_3$) can be seen in Figure C 1 and Figure C 2. Note that there is a weight the curve of the bare support and the methylated support. Therefore the results aren't too reliable.

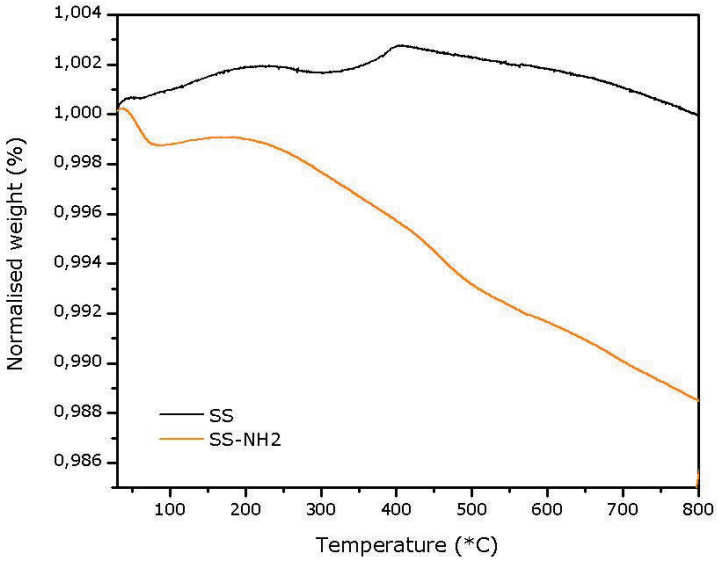

Figure C 1 TGA curve of the amino functionalised support (SS-NH_2)

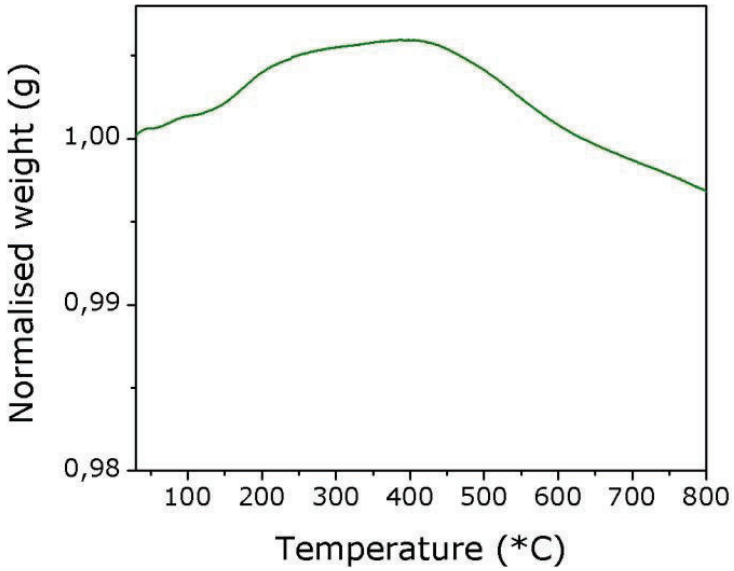

Figure C 2 TGA curve of the support methylated by HMDS (SS-$(CH_3)_3$.

D
(TEM) images

An heat treatment in an oxygen atmosphere was used to remove the methyl groups from the methylated catalysts. By interalia the wetting behavior of the catalyst in water, was studied if the removal was successful. In Figure D 1 one can see a bare Cu/SiO2 catalyst, these silica particles sunk to the bottom of the flask. On the other hand, the methylated catalyst (middle) stays on the water-air interface. After this catalyst went a heat treatment in oxygen atmosphere the catalysts sinks for the largest part to the bottom of the flask, very little stays on the water surface.

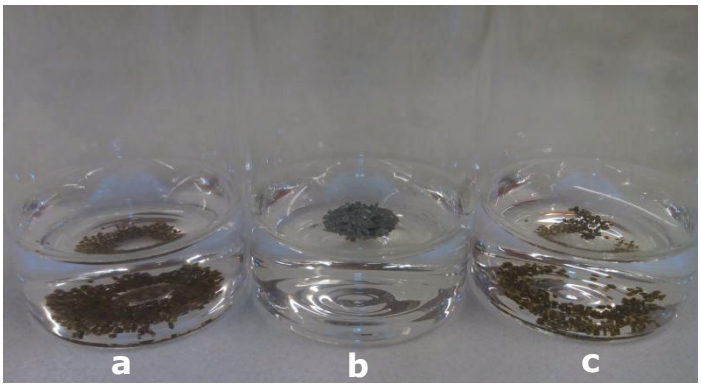

Figure D 1 [a] SS-Cu(N_2) [b] SS-Cu(N_2)-$(CH_3)_3$ [c] SS-Cu(N_2)-$(CH_3)_3$-T

A methylated support does not only have a different behaviour than a non-methylated support in contact with water, also the TEM images are quite different. In Figure D 3 one can see a TEM image of a methylated support (SS-$(CH_3)_3$). Theses silica spheres are not connected to each other, there is always some empty space between them. This is caused by the increased hydrophobicity of the support.

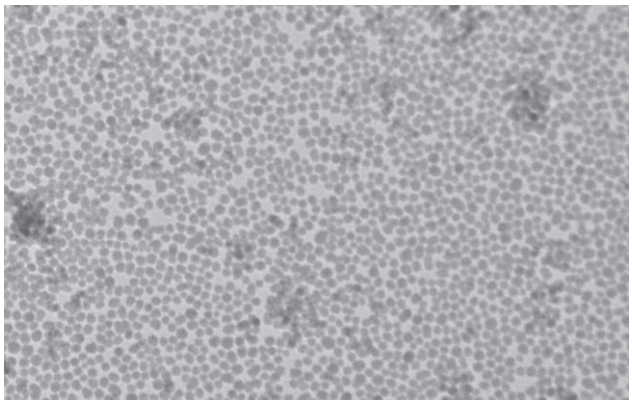

Figure D 2 A image of the methylated support (SS-$CH_3)_3$. Different then a non-methylated support is that the spheres don't tough each other.

The amount of metal of the metal oxide grafted catalysts were inter alia determined by EDX spectroscopy. The bulk loading of metal in these catalysts were determined on an amount of sample as can be seen in Figure D 3.

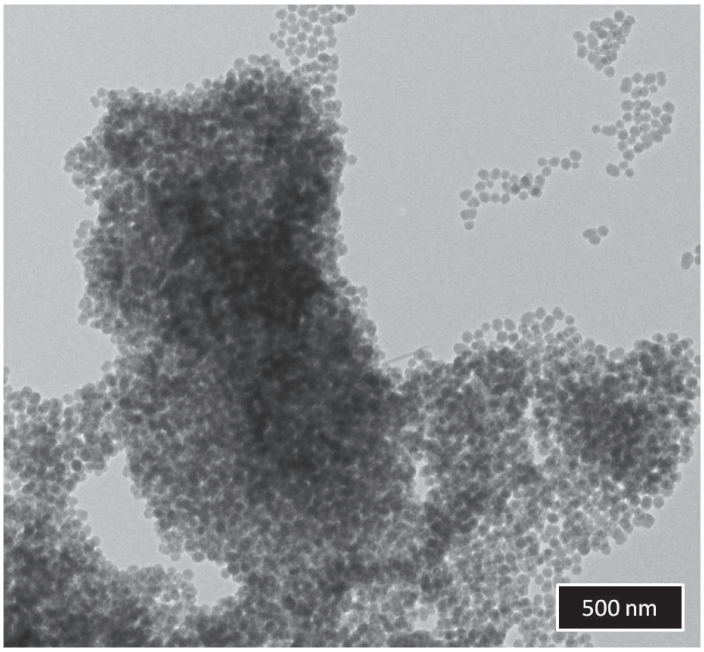

Figure D 3 A TEM image of a typical amount of spheres on which the bulk loading aluminium or titanium is determined with EDX spectroscopy

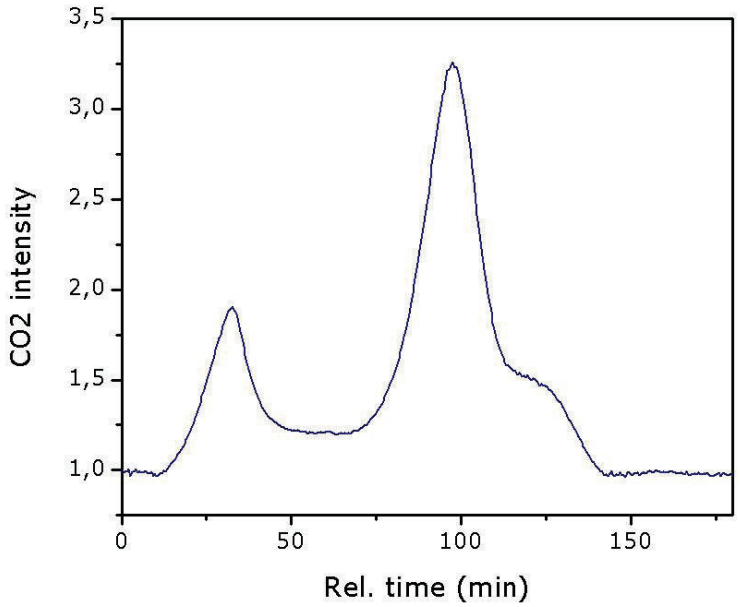

Figure D 4 CO_2 signal over time during a TGA-MS measurement.